PLASTIDY

Jsou plastidy tím, co dělá rostlinu rostlinou?

Klíčový význam přechodu života na souš pro pochopení přisedlosti rostlin.

ATP a NADPH vzniklé při fotosyntéze se využívají k „redukci CO2“ a syntéze cukrů.

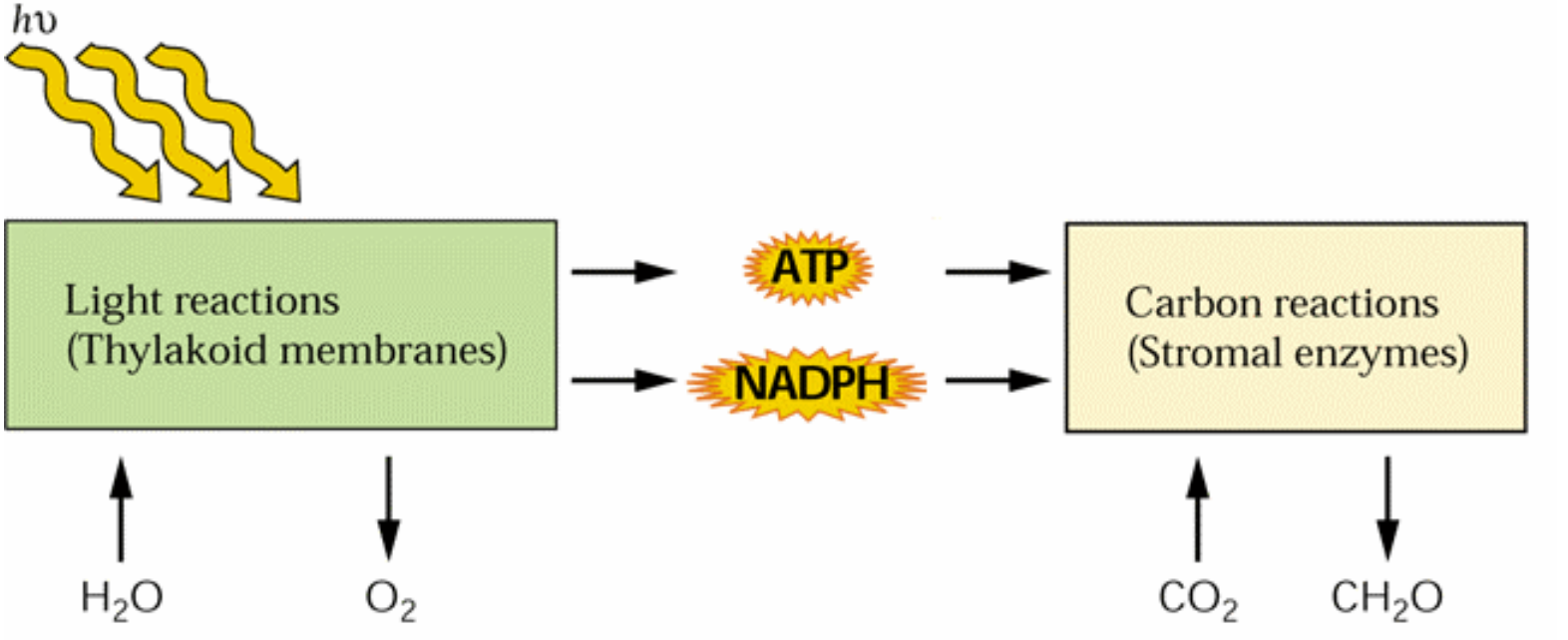

v plastidech se toho ovšem děje víc

- syntéza aminokyselin (př. glutamin Gln, glutamát Glu, aromatické aminokys =,Phe,Trp,Tyr;; dále lysin, threonin….)
- syntéza mastných kyselin a lipidů
- syntéza a modifikace fytohormonů (př. ABA, cytokininy...)

Nás zde zajímá biogenese a biologie pastidů

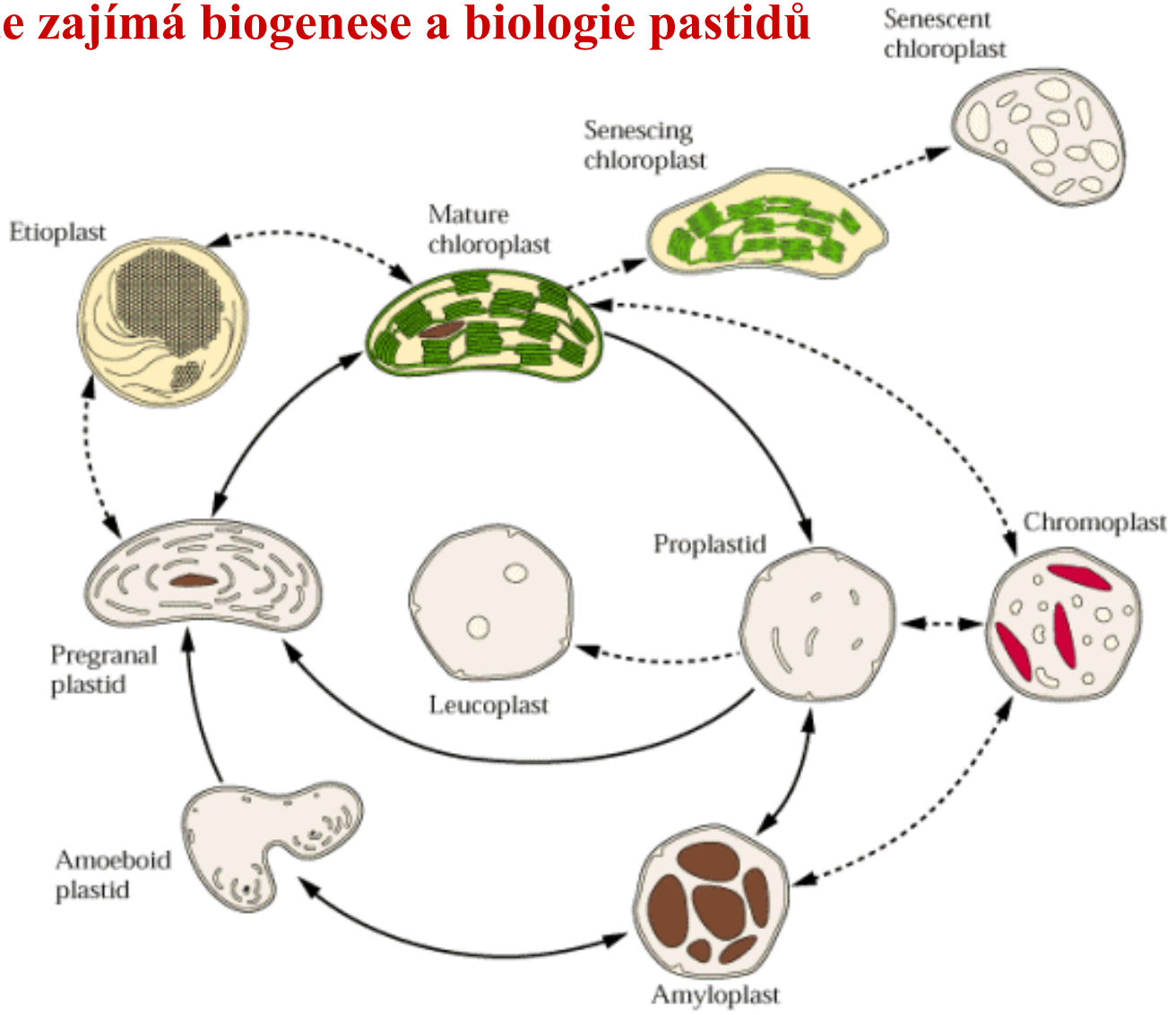

TYPY PLASTIDŮ

JSOU REVERSIBILNÍ

Proplastid s bílkovinným tělískem a krůpějemi tuků.
Ribozómy plastidu i mitochondrie jsou menší než „eukaryotické“ v cytoplasmě.

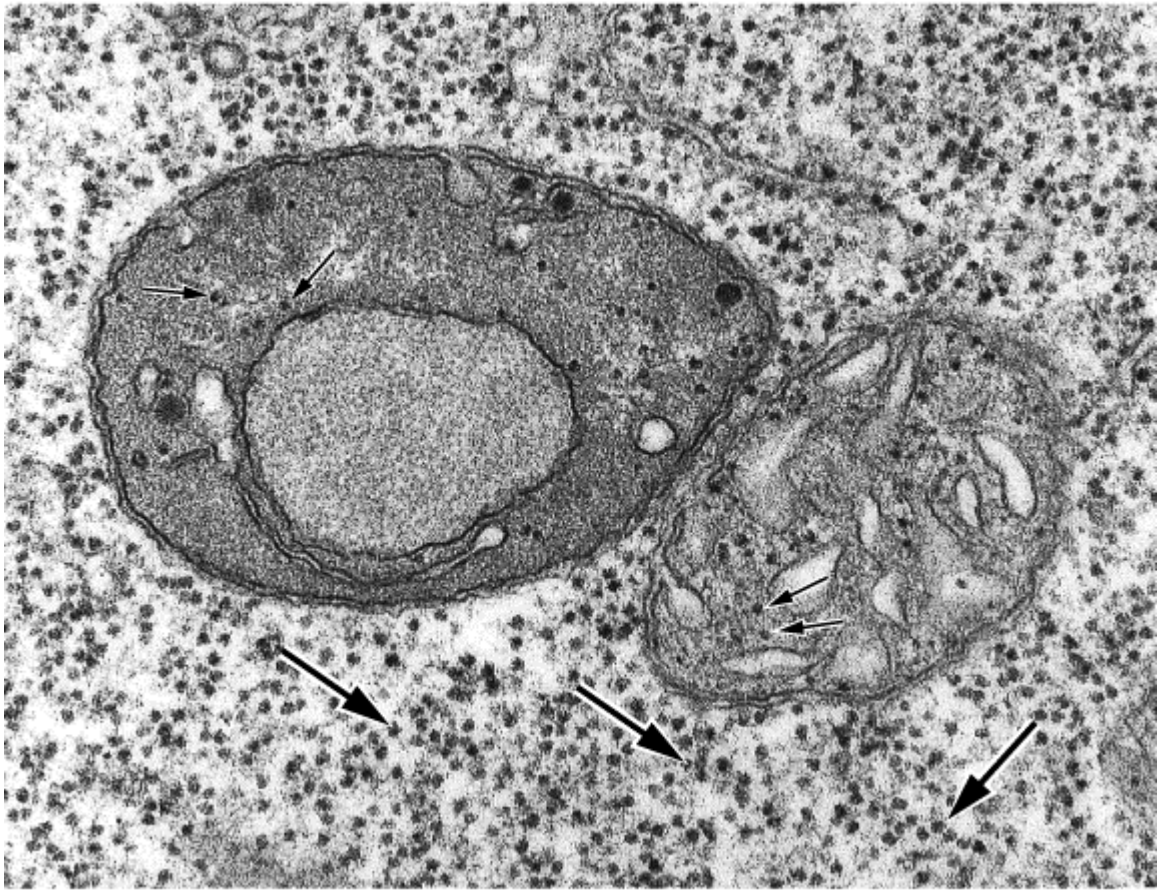

Proplastid s agregátem fytoferritinu.

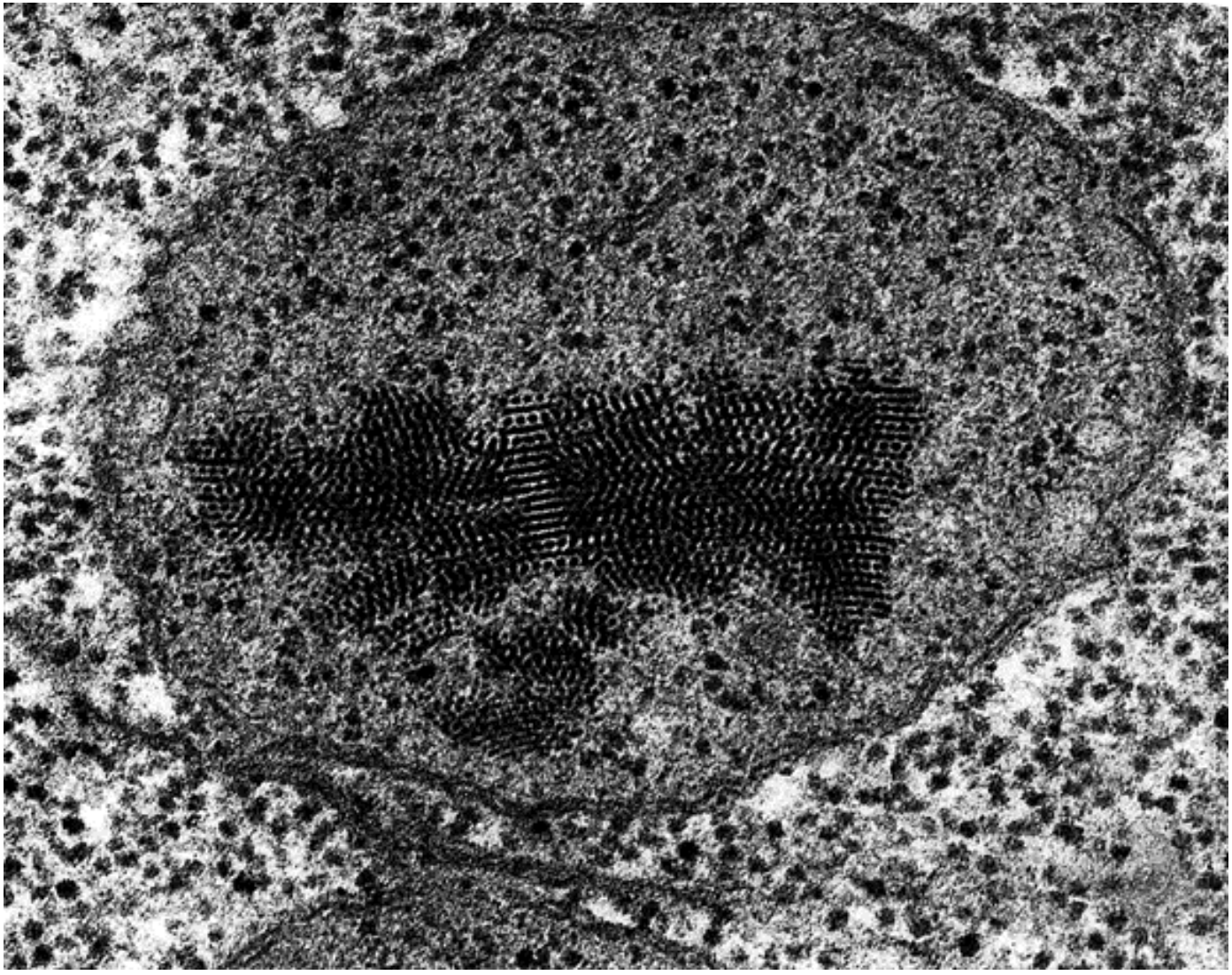

Amyloplast kořenové čepičky-kolumely;
funguje jako statolit, ale také jako zásobárna škrobu

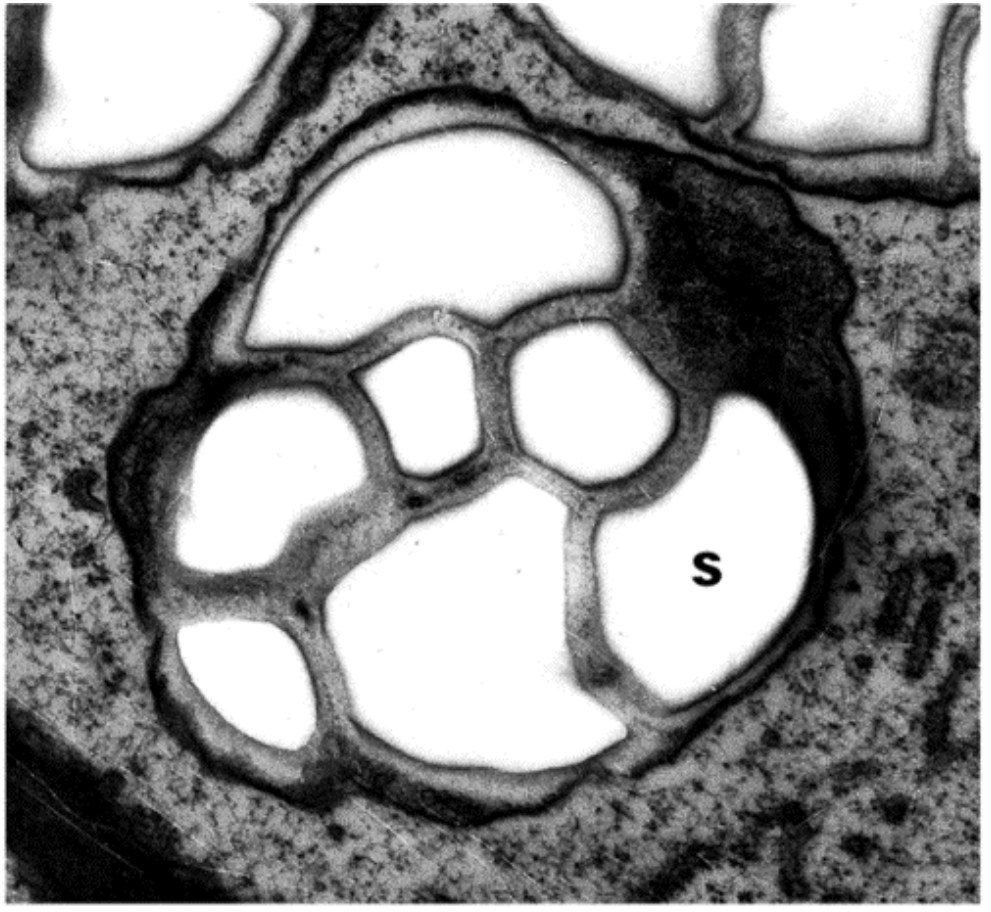

V plastidech řady řasových taxonů je dobře viditelný světlolomný pyrenoid (karboxysom) tvořený agregací Rubiska.

Leukoplast žlaznatého trichomu máty; scházejí vnitřní membrány, hromadí tukové krůpěje a je obklopen ER (SER – smooth…)

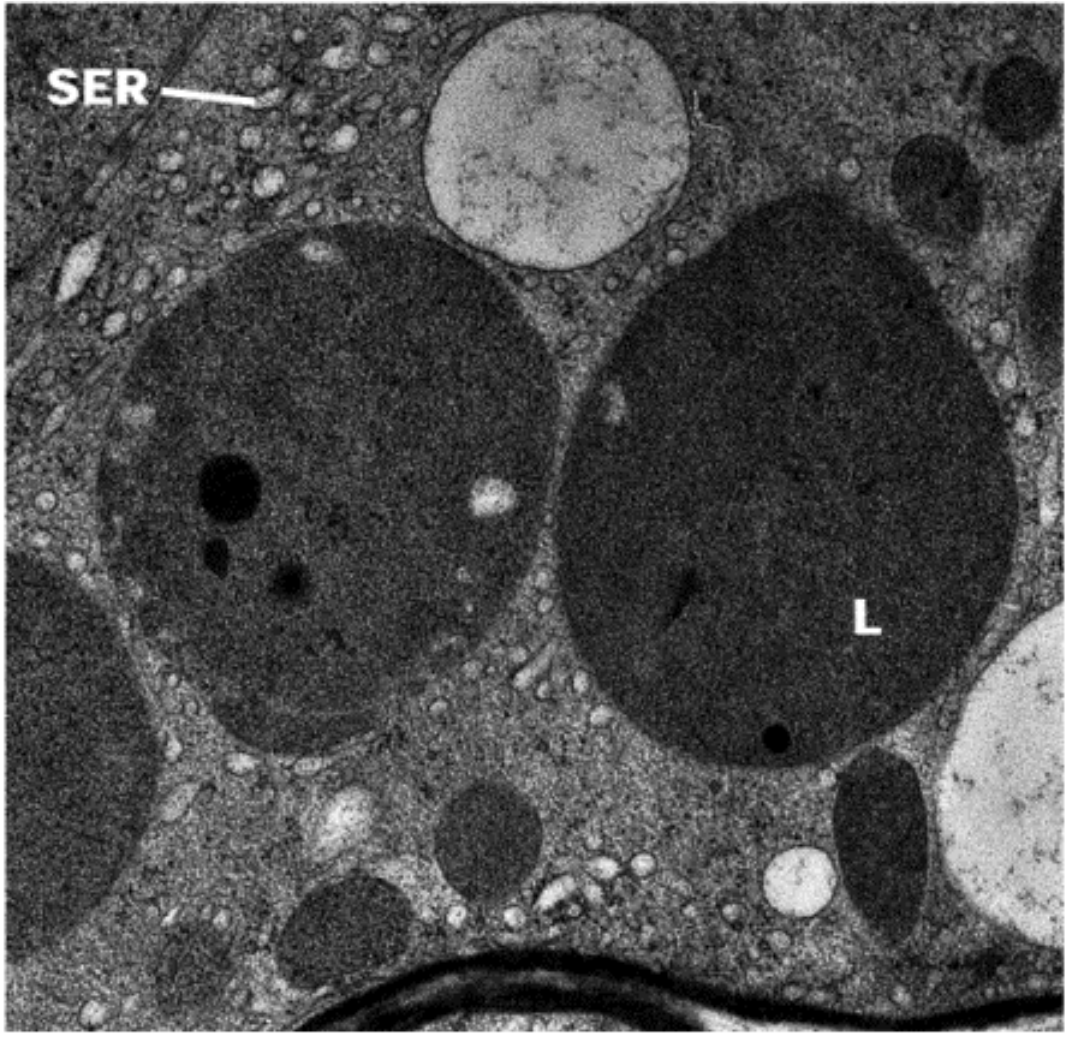

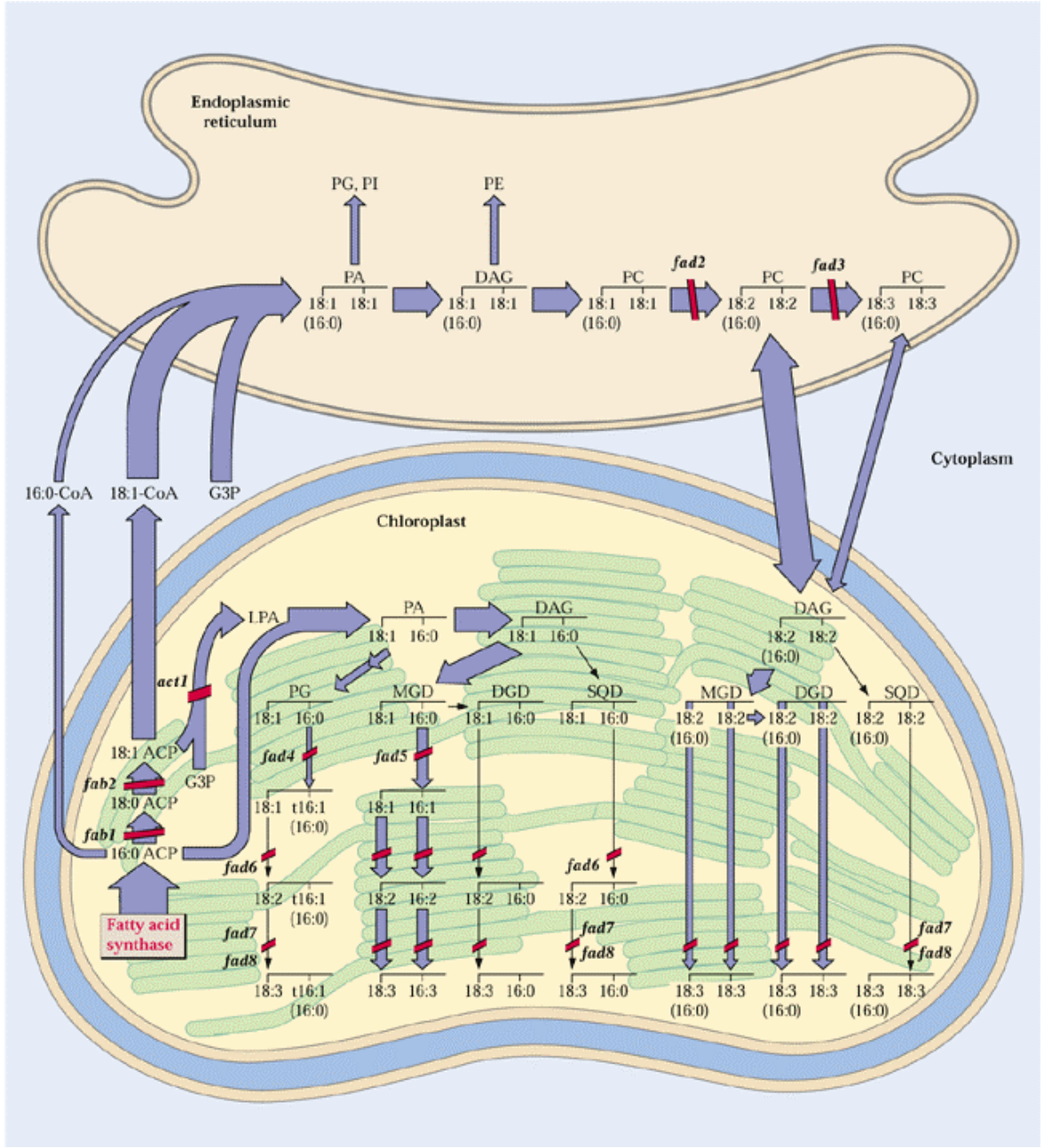
Endoplasmic reticulum
PG, PI
PE
PA
DAG
PC
fad2
PC
fad3
PC
18:1 18:1 (16:0)
18:1 18:1 (16:0)
18:1 18:1 (16:0)
18:2 18:2 (16:0)
18:3 18:3 (16:0)
Cytoplasm
16:0-CoA
18:1-CoA
G3P
Chloroplast
LPA
PA
DAG
DAG
18:1 16:0
18:1 16:0
18:2 18:2 (16:0)
acl1
PG
MGD
DGD
SQD
MGD
DGD
SQD
18:1 16:0
18:1 16:0
18:1 16:0
18:1 16:0
18:2 (16:0)
18:2 18:2 (16:0)
18:2 18:2 (16:0)
18:2 18:2 (16:0)
18:1 ACP
fad4
fad5
G3P
fab2
18:0 ACP
18:1 t16:1 (16:0)
18:1 16:1
fab1
16:0 ACP
fad6
fad6
18:2 t16:1 (16:0)
18:2 16:2
18:2 16:0
18:2 16:0
Fatty acid synthase
fad7
fad8
fad7
fad8
fad7
fad8
18:3 t16:1 (16:0)
18:3 16:3
18:3 16:0
18:3 16:0
18:3 18:3 (16:0)
18:3 18:3 (16:0)
18:3 18:3 (16:0)

Chromoplast s nahromaděnými karotenoidy.

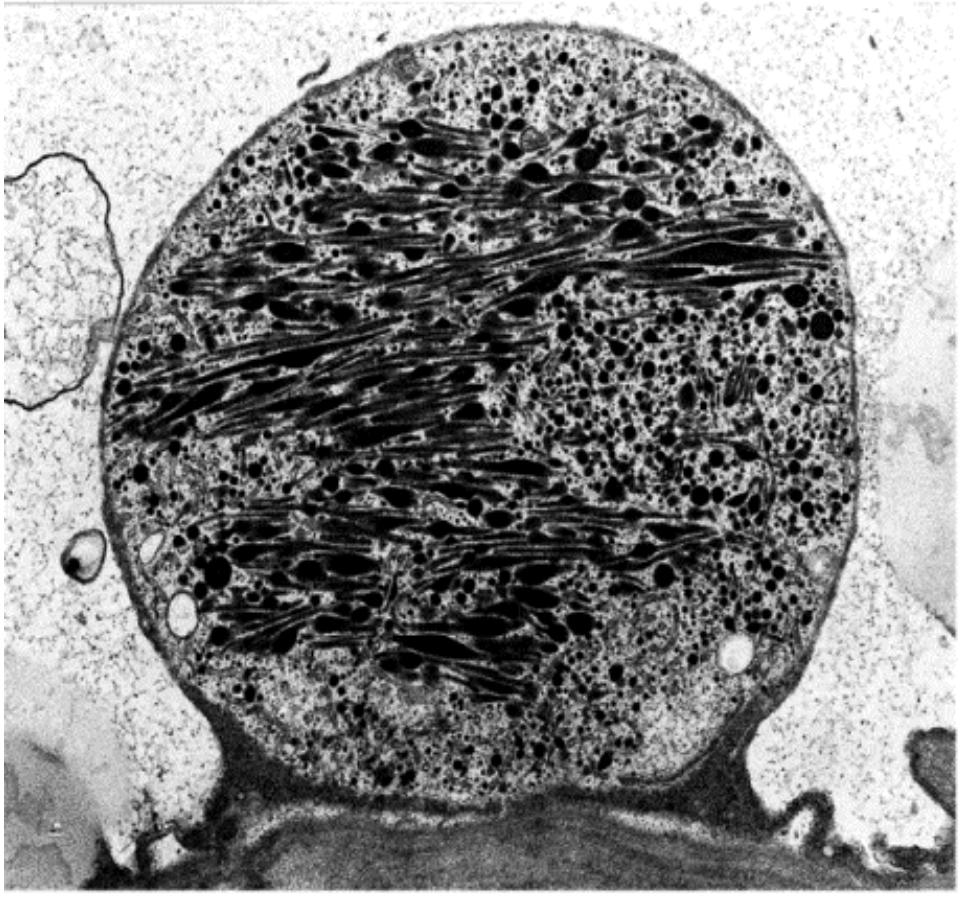

Etioplast kukuřice, s volnými thylakoidy a prolamelárním tělískem (B-D model prolamelárního tělíska)

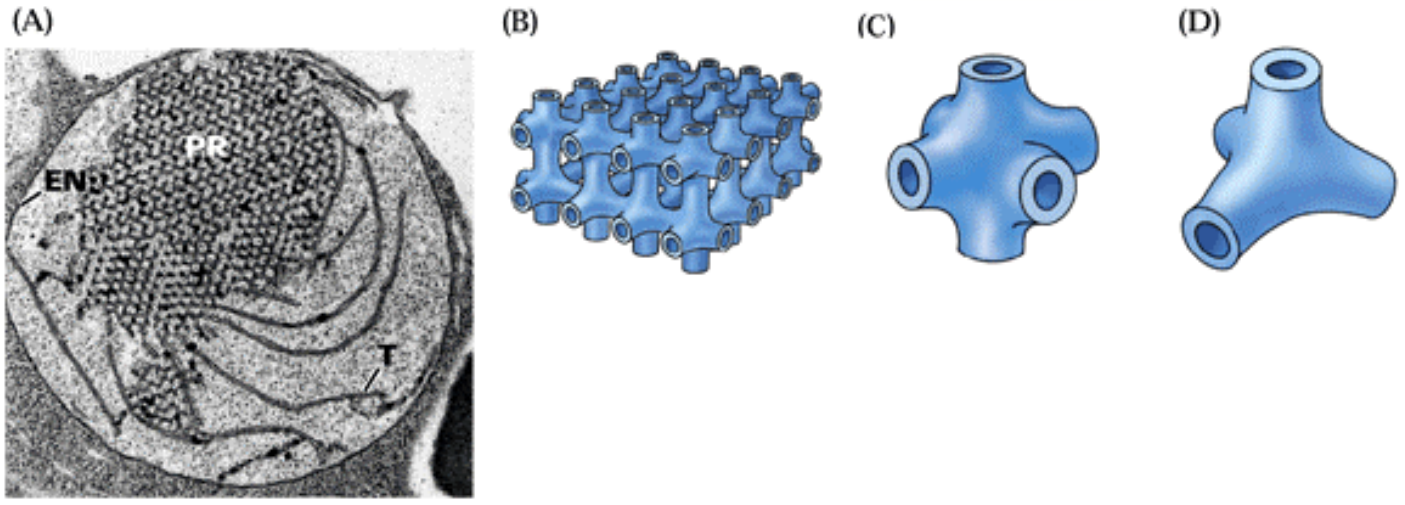

Časná fáze vývoje thylakoidů v zelenajících etioplastech se zbytkem prolamelárního tělíska.

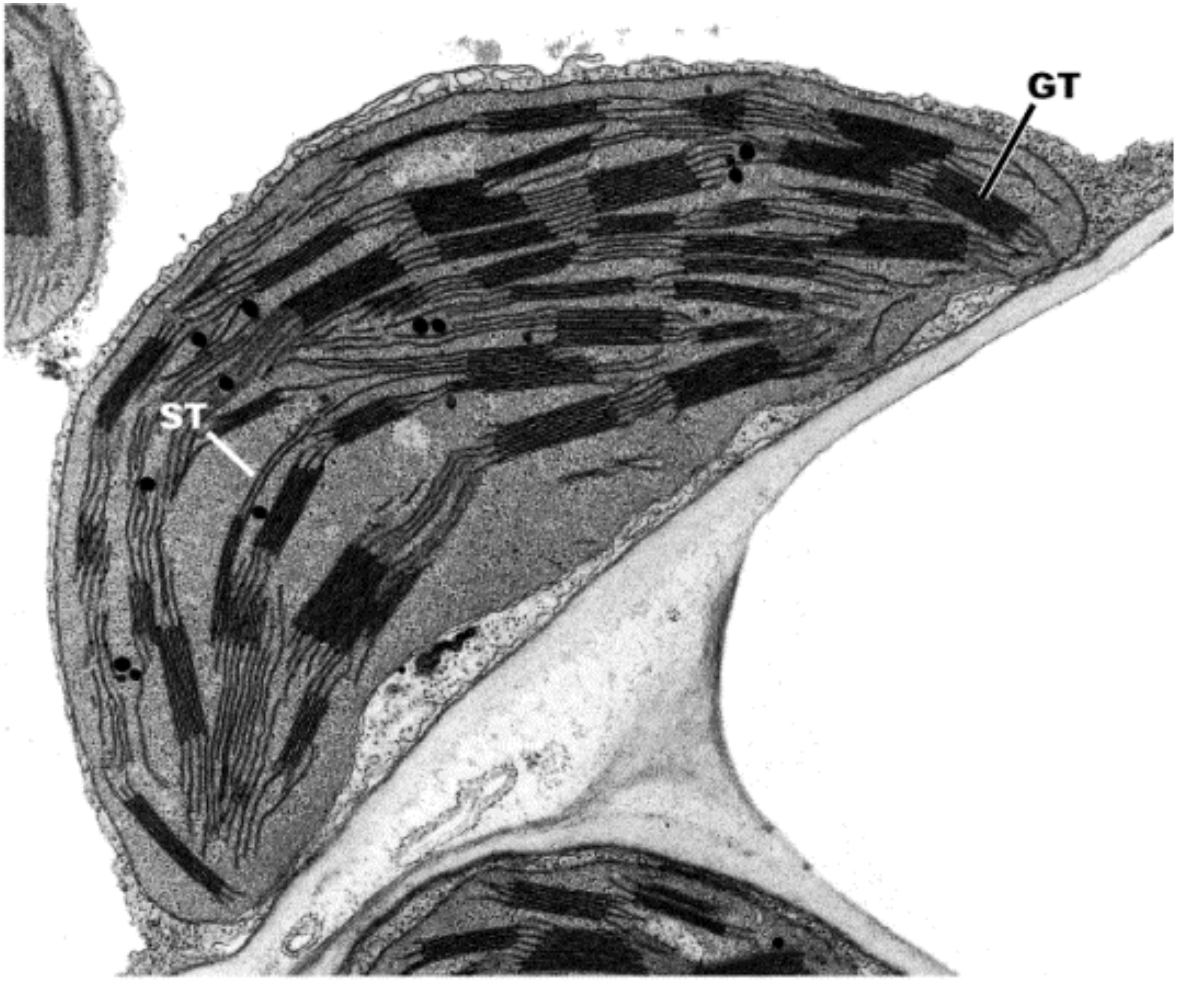

Funkční chloroplast s granálními a stromatálními thylakoidy. Tuková tělíska – plastoglobuly.

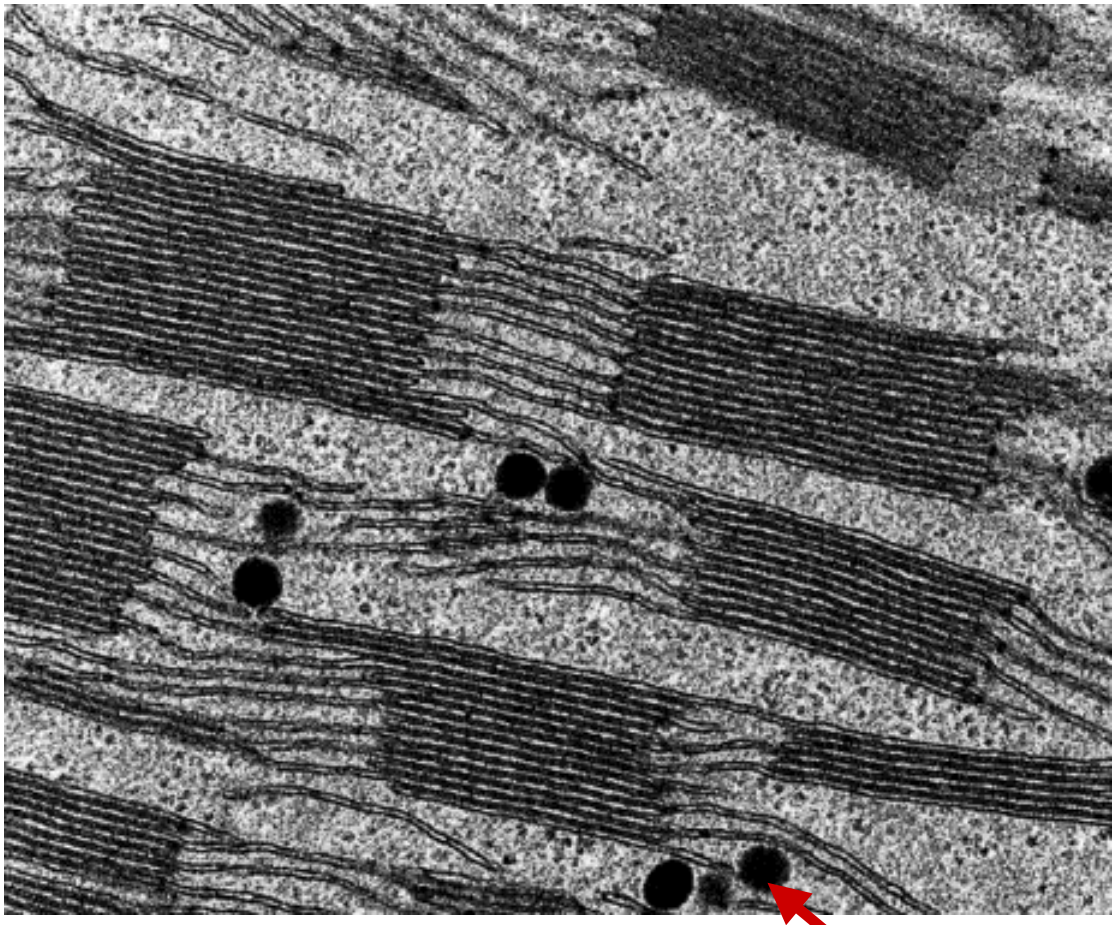

Thylakoidy, grana a lipidové **plastoglobuly**

Mrazově „leptaný“ zlom grana

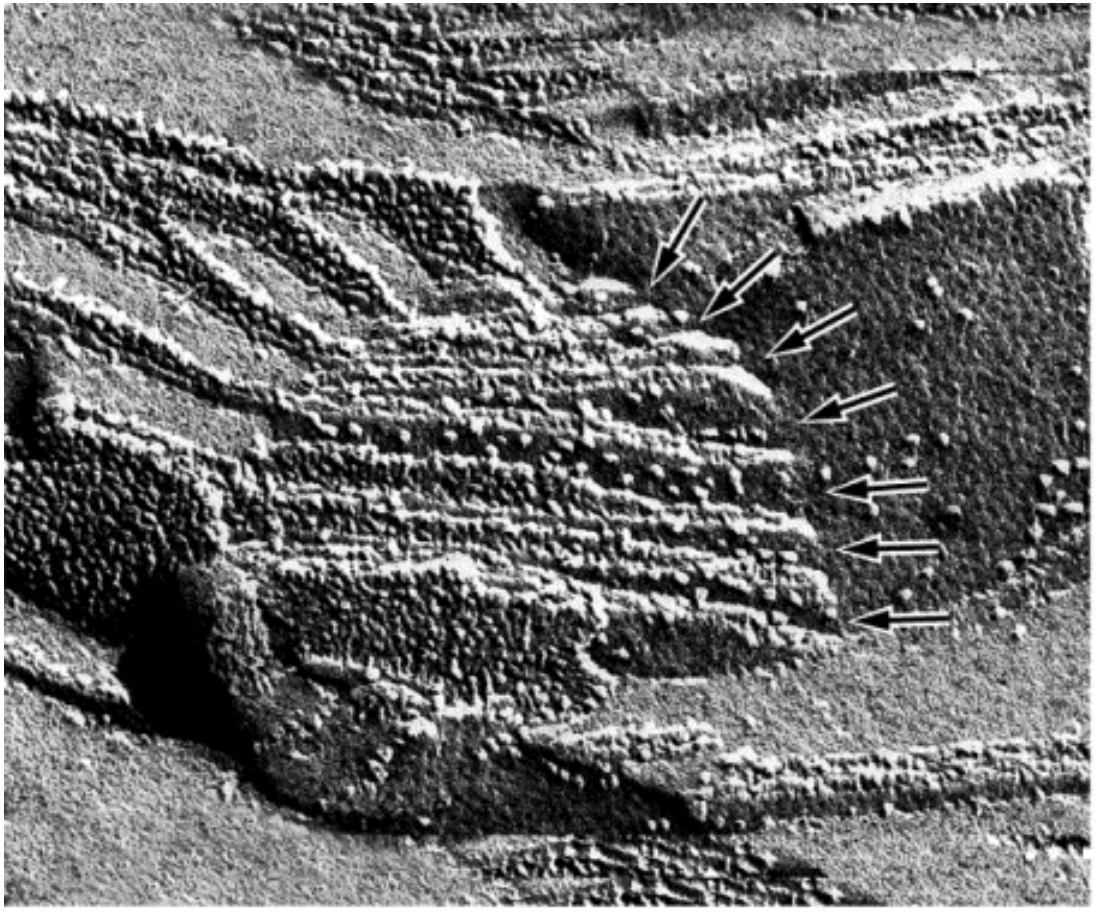

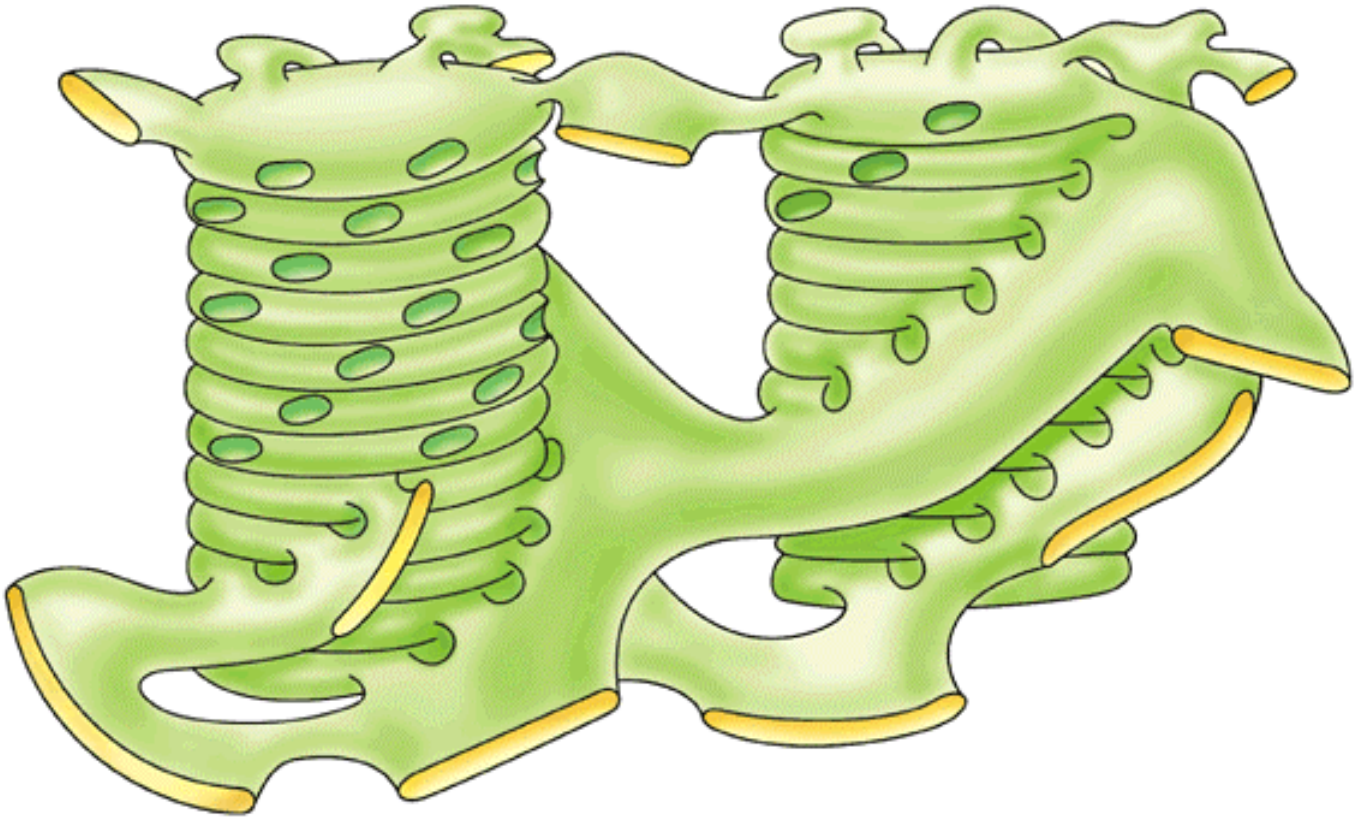

Rozdíl mezi granálními (GT) a stromatálními (ST) thylakoidy. „Zrna“ na GT jsou PSII

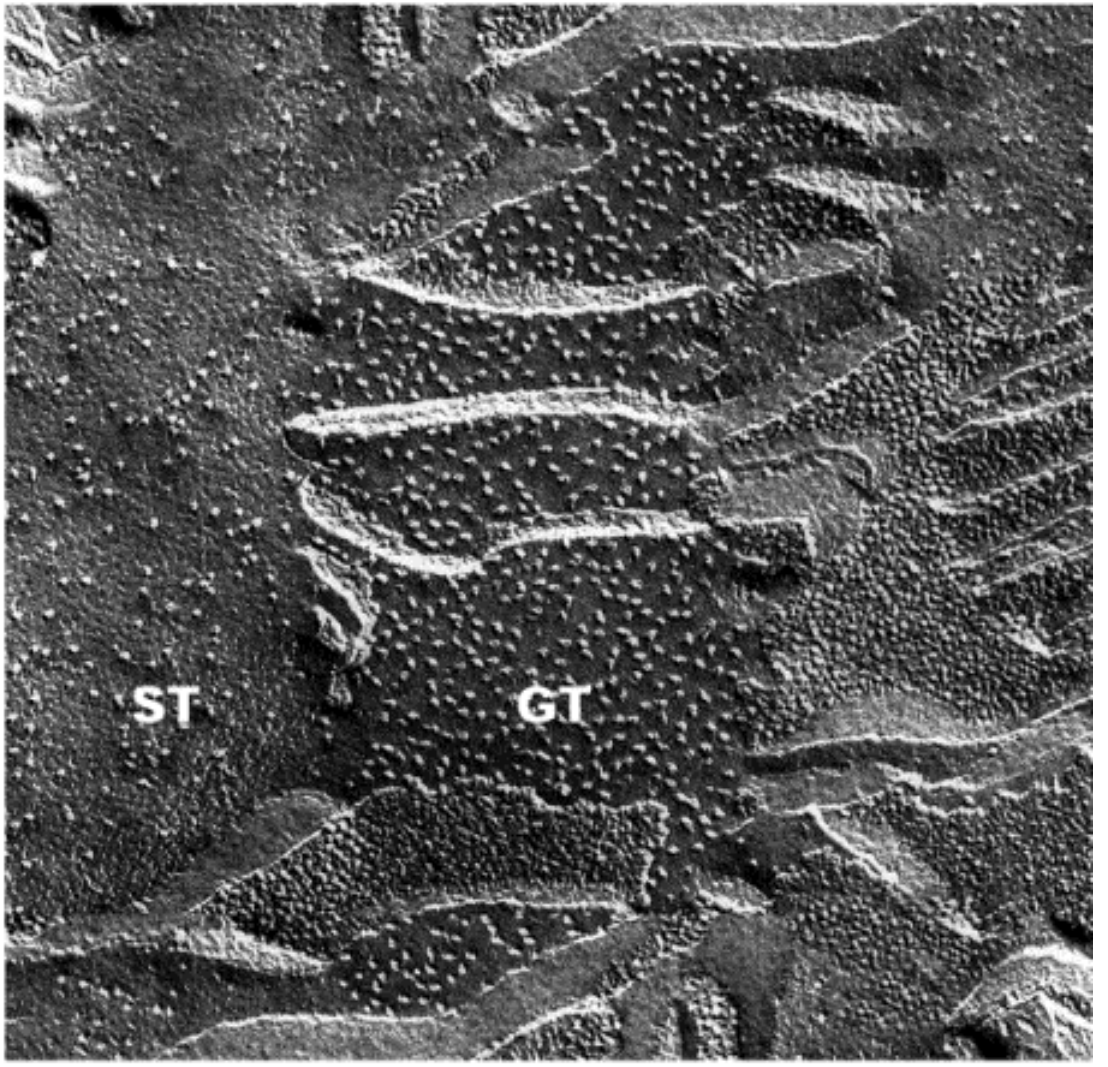

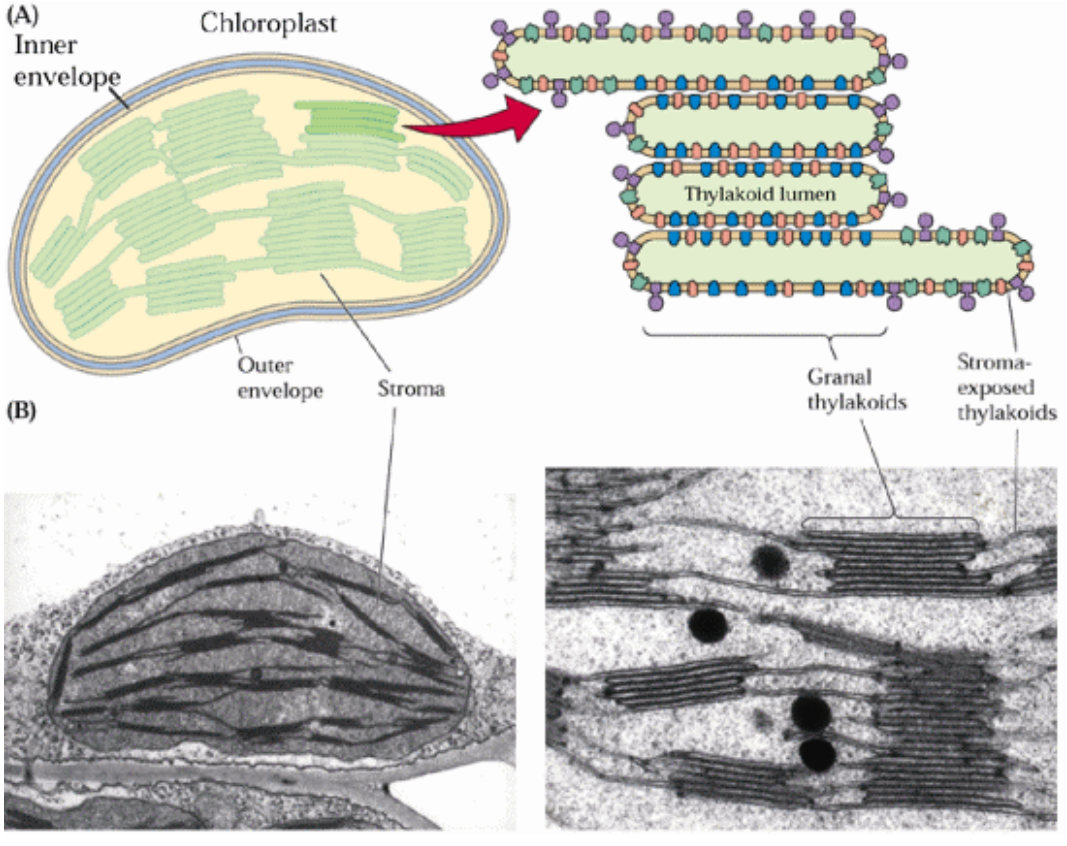

Laterální nehomogenita v distribuci komplexů.

PSII je přednostně lokalizován do "vrstvených" oblastí granálních tylakoidů, zatímco PSI a ATPsyntáza jsou mimo tuto oblast. Cytochromový komplex b6f je rovnoměrně všude. Separace PSII a PSI implikuje fci mobilních nosičů elektronů - plastochinonu (v membráně) plastokyanu (v roztoku).

STROMA

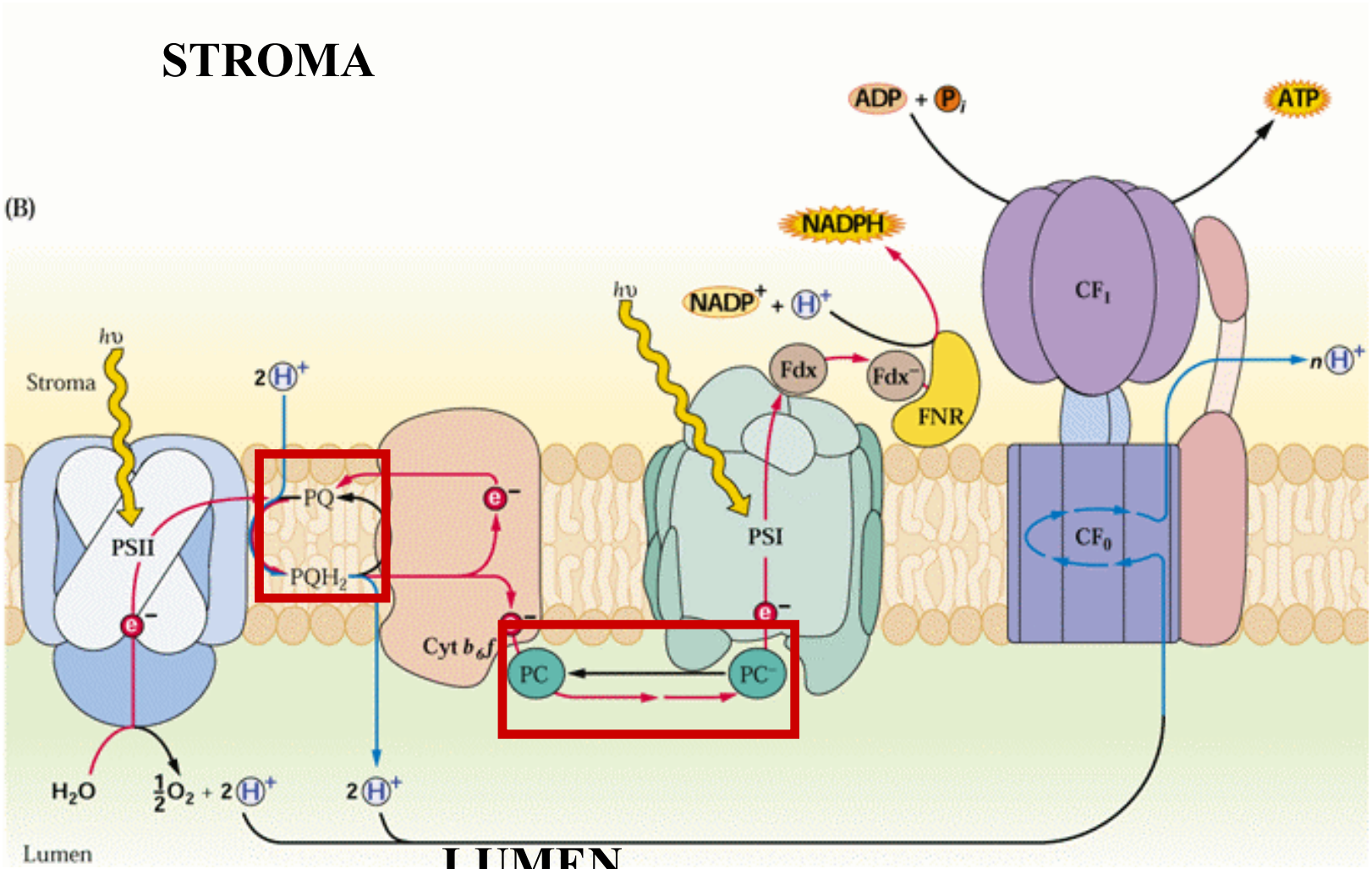

LUMEN

Čtyři thyl. komplexy – elektrony uvolněné fotolýzou vody jsou přenášeny na NADP; Vzniklý protonový gradient je spotřebován na syntézu ATP.

Membrány plastidů

Jsou bohaté na galaktolipidy.

Vnější membrána snadno prostupná až do 10kDa (poriny)

Vnitřní prostupná jen pro nízkomol. látky (O2, NH4, nedis. monokarbox. kyseliny) – bohatá na specifické přenašeče (e.g. Pi vs. triosa-fosfátový přenašeč)

Thylakoidní membrána je samostatná (prolam. těl.) – bočná heterogenita bílk. komplexů (viz. výše).

Stromuly spojující plastidy

jsou velmi dynamické (plastidy exprimují GFP ve stromatu)

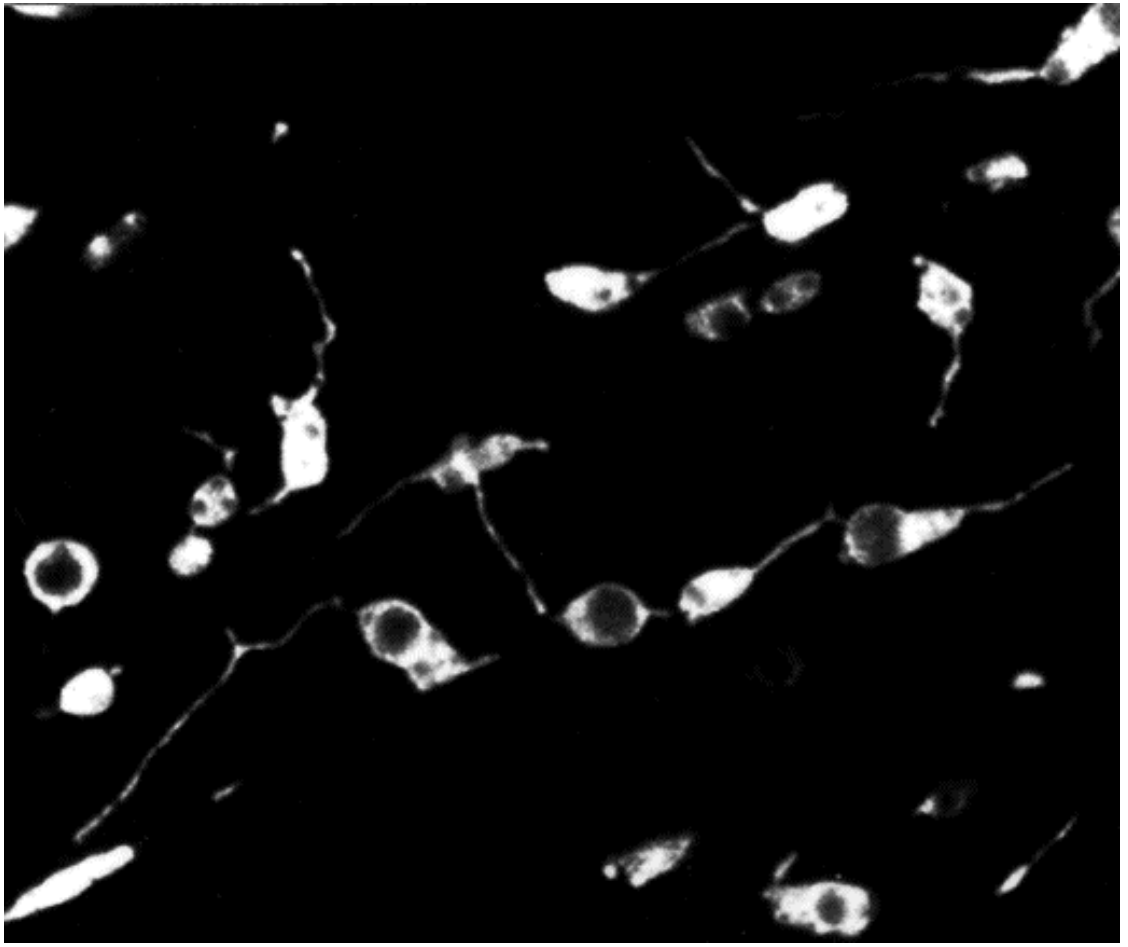

Stromuly se rozvijeji zvláště u nezelených plastidů – čím je v buňce
Méně plastidů, tím vice spojení se vytváří. Vzniká extenzí plastidových membr.obalů.

ATP a NADPH vzniklé při fotosyntéze se využívají k „redukci CO2“ a syntéze cukrů.

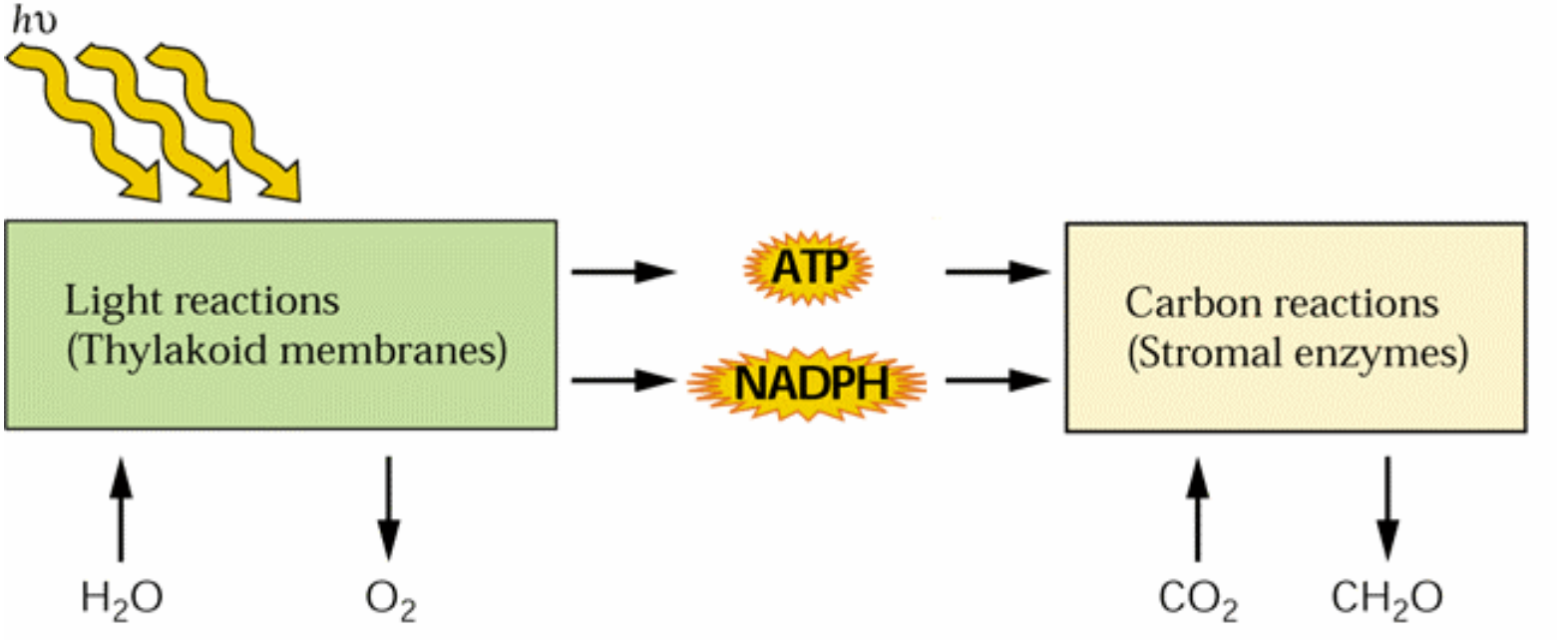

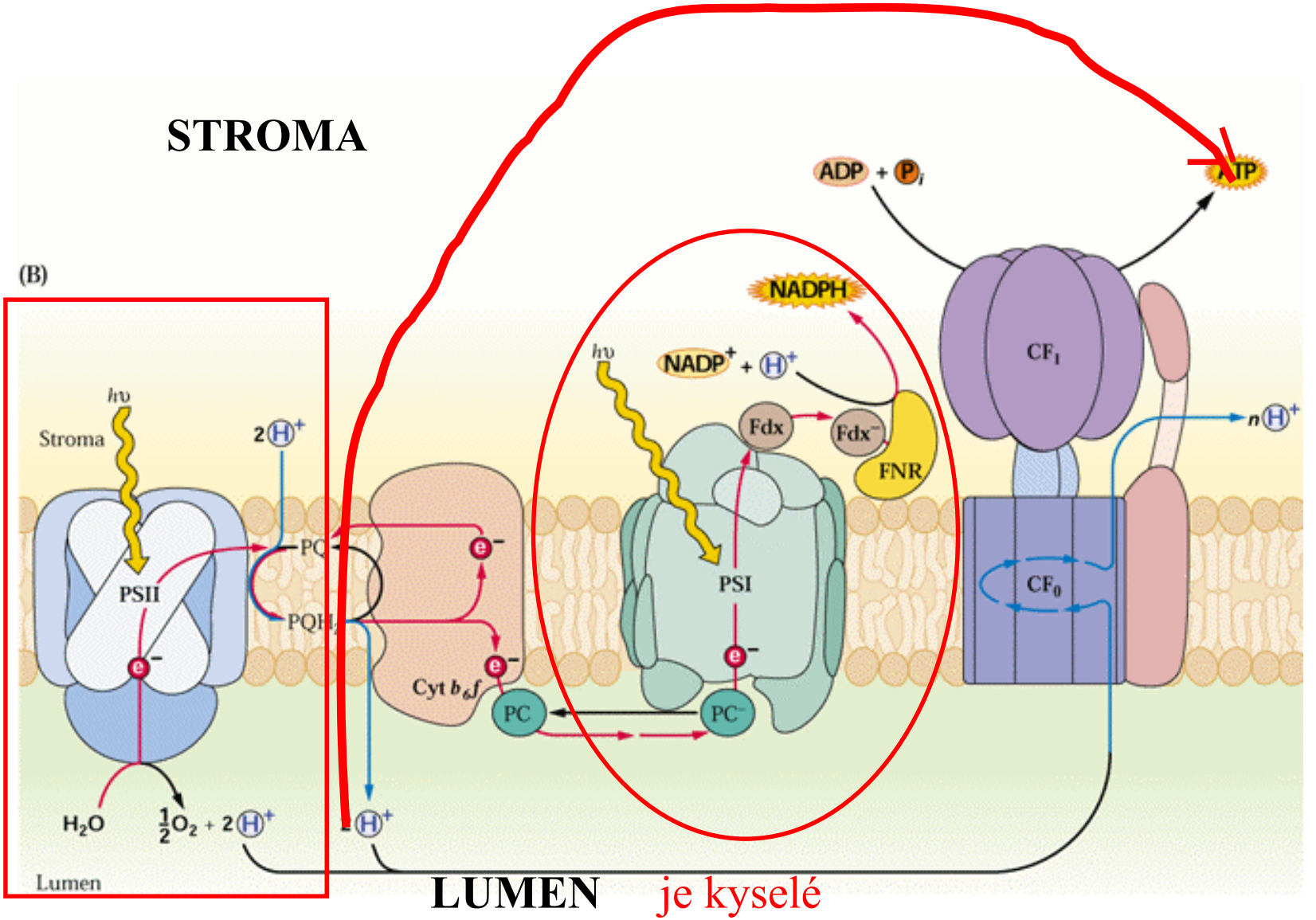

LUMEN je kyselé

Čtyři thyl. komplexy – elektrony uvolněné fotolýzou vody jsou přenášeny na NADP; Vzniklý protonový gradient je spotřebován na syntézu ATP.

Do cytoplasmy se produkty fotosyntézy transportují jako cukr-fosfáty (dihydroxyacetonfosfát či glukosa-6-fosfát) antiportem - přenašečem vnitřní membrány plastidu výměnou za anorg. fosfát.

V cytoplasmě jsou užity k syntéze sacharosy, či se metabolizují za vzniku ATP a NADPH.

(tj. ATP syntetizovaný v plastidech není přímo exportován!!)

Základy regulace syntézy škrobu

Jak ve fotosyntetických tak heterotrofních pletivech je ADP-glukoso pyrofosforyláza aktivována 3-fosfoglycerátem a inhibována anorganickým fosfátem Pi.

Regulace syntézy škrobu v chloroplastech

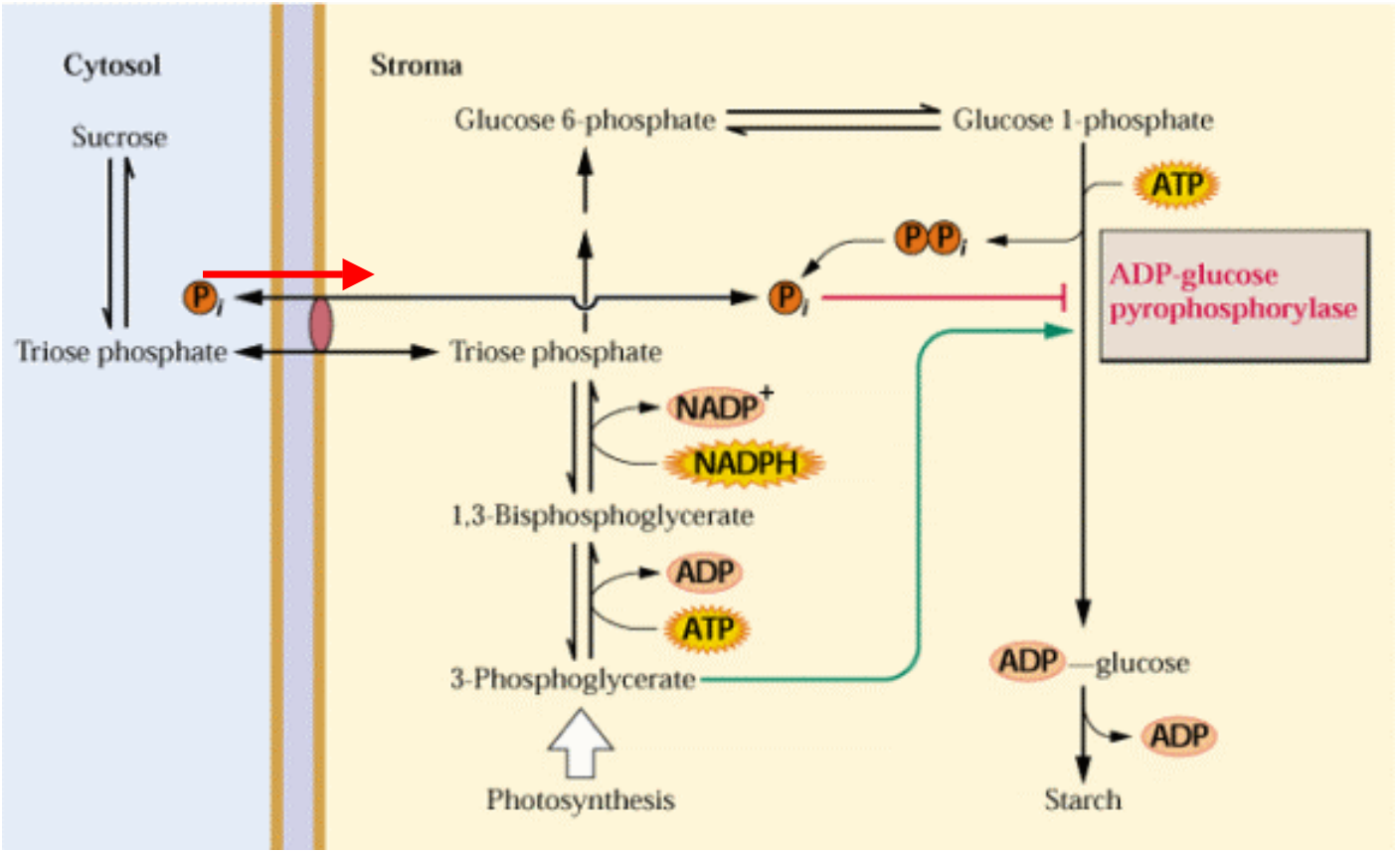

Je-li 3-fosfoglycerátu (přímý produkt reakce CO2 s RuBP) mnoho, je stimulována syntéza škorbu; klesne-li „pool“ fosforylovaných cukrů zvýší se rel. konc. anorg. fosfátu, který inhibuje syntézu škrobu.

Vysoká cytoplasmatická koncentrace Pi umožňuje rychlou výměnu za triosa-fosfáty a tedy jejich efektivní transport do cytoplasmy.

V nezelených částech rostliny (př.kořeny), je škrob syntetizována z importovaného glukosa-6-fosfátu (výměnou za Pi).

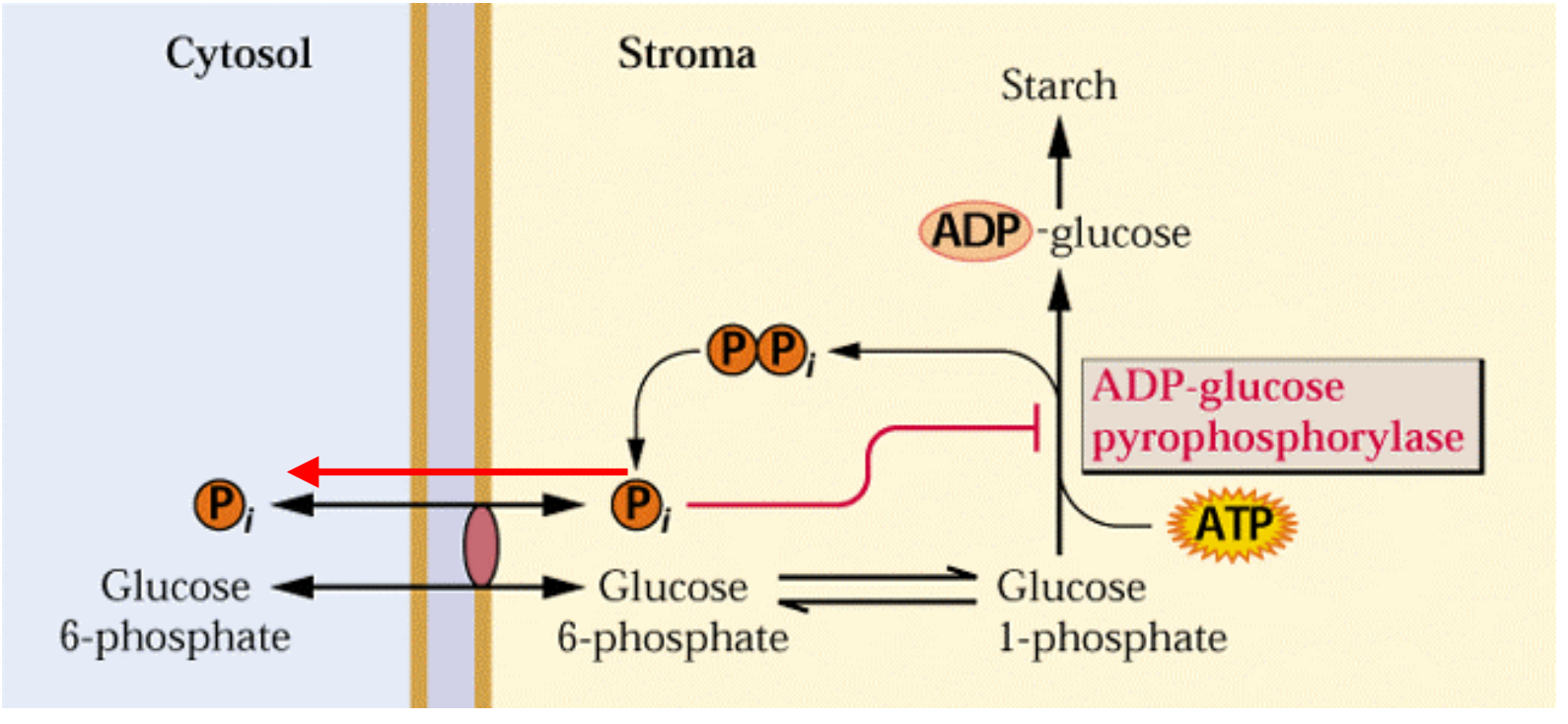

Vysoká koncentrace Pi v plastidech tedy signalizuje, že v cytoplasmě je málo cukr-fosfátů.

Import bílkovin do plastidů

Bílkoviny určené k lokalizaci do plastidu mají na N´konci jeden (příp.2) transitní peptidy (TP).

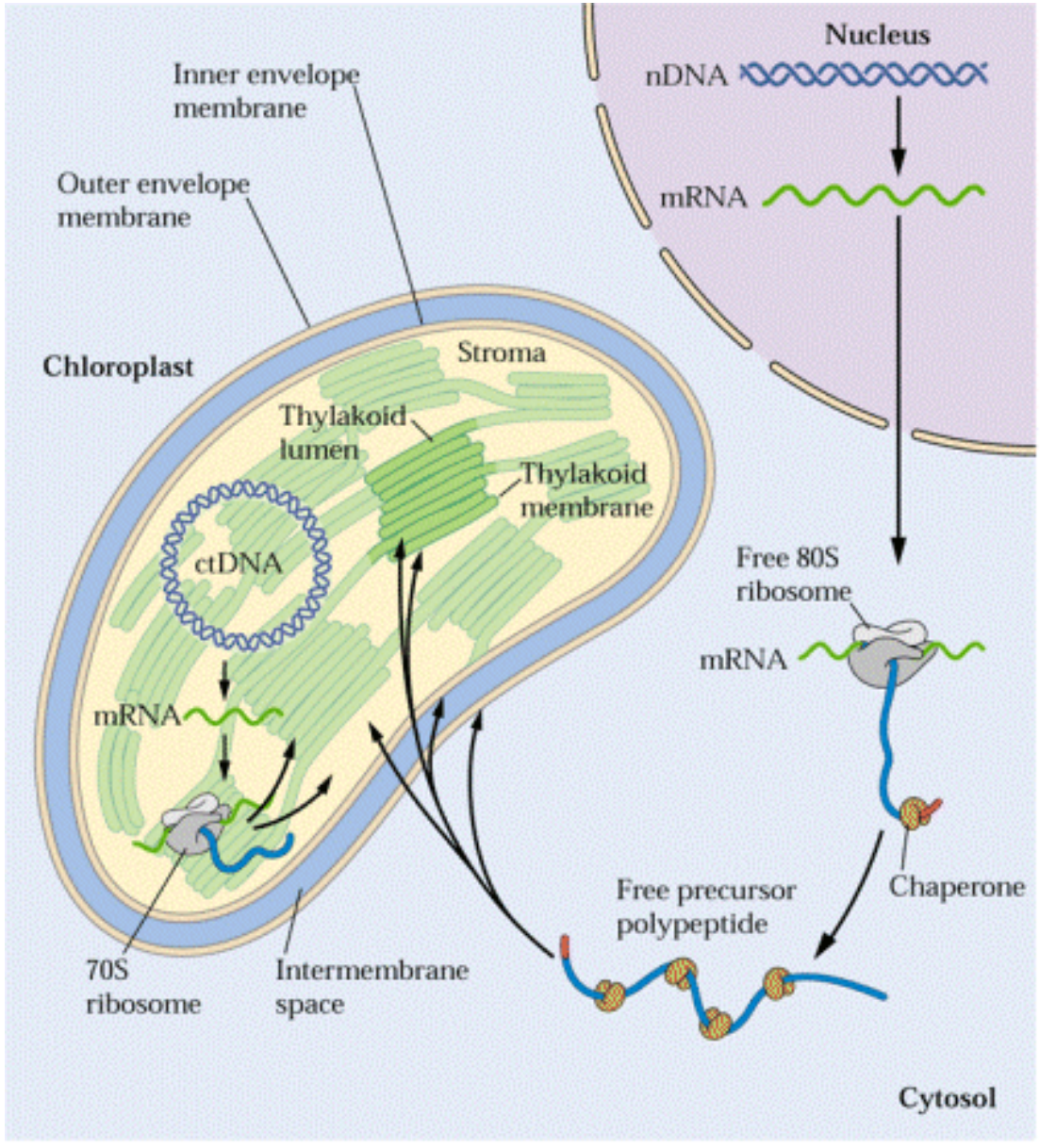

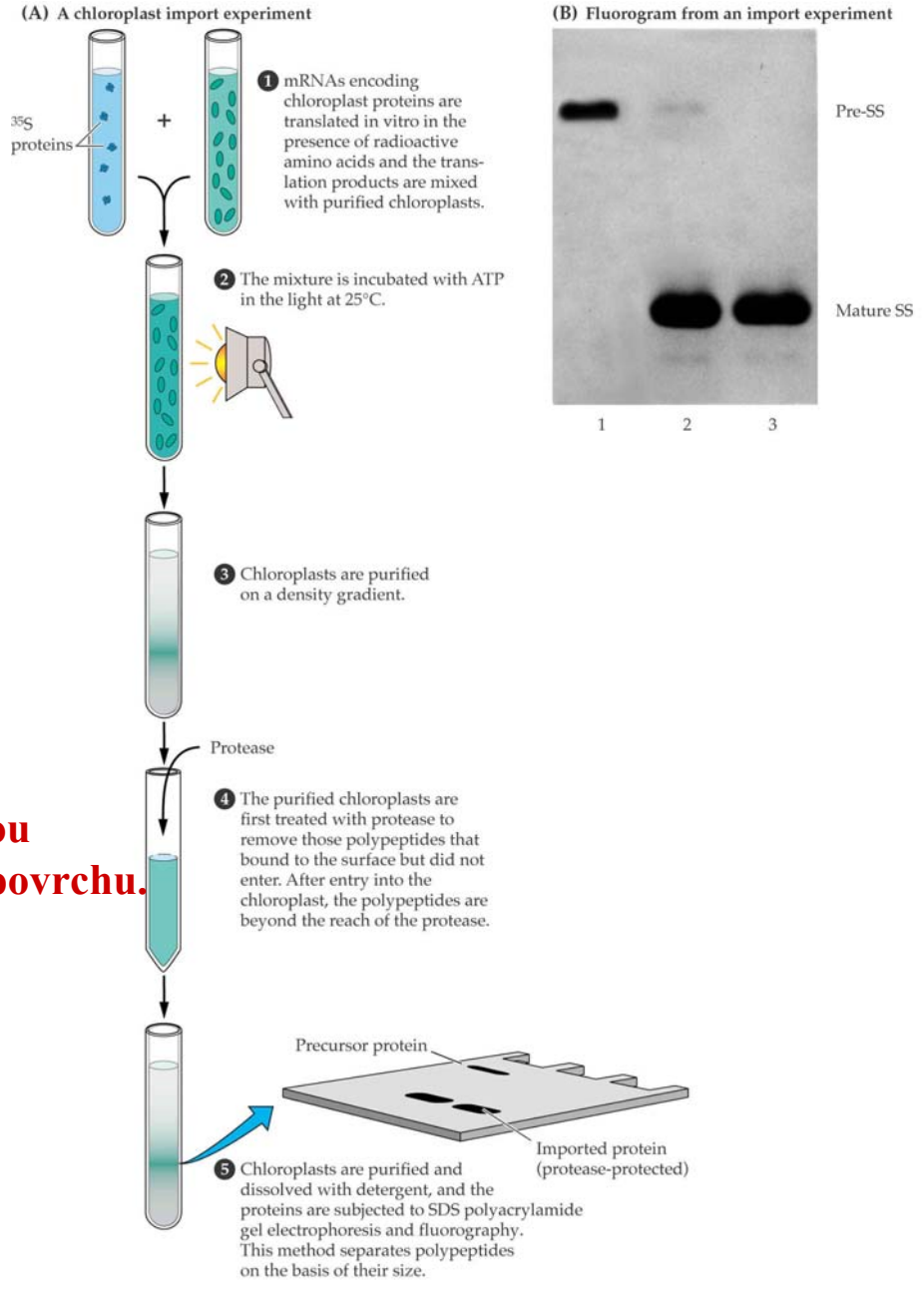

působení proteázou odstraní bílk. na povrchu.

Metody studia

Transport do stromatu

TOC = translocon of the outer membr..chlor.

TIC = dtto… inner…

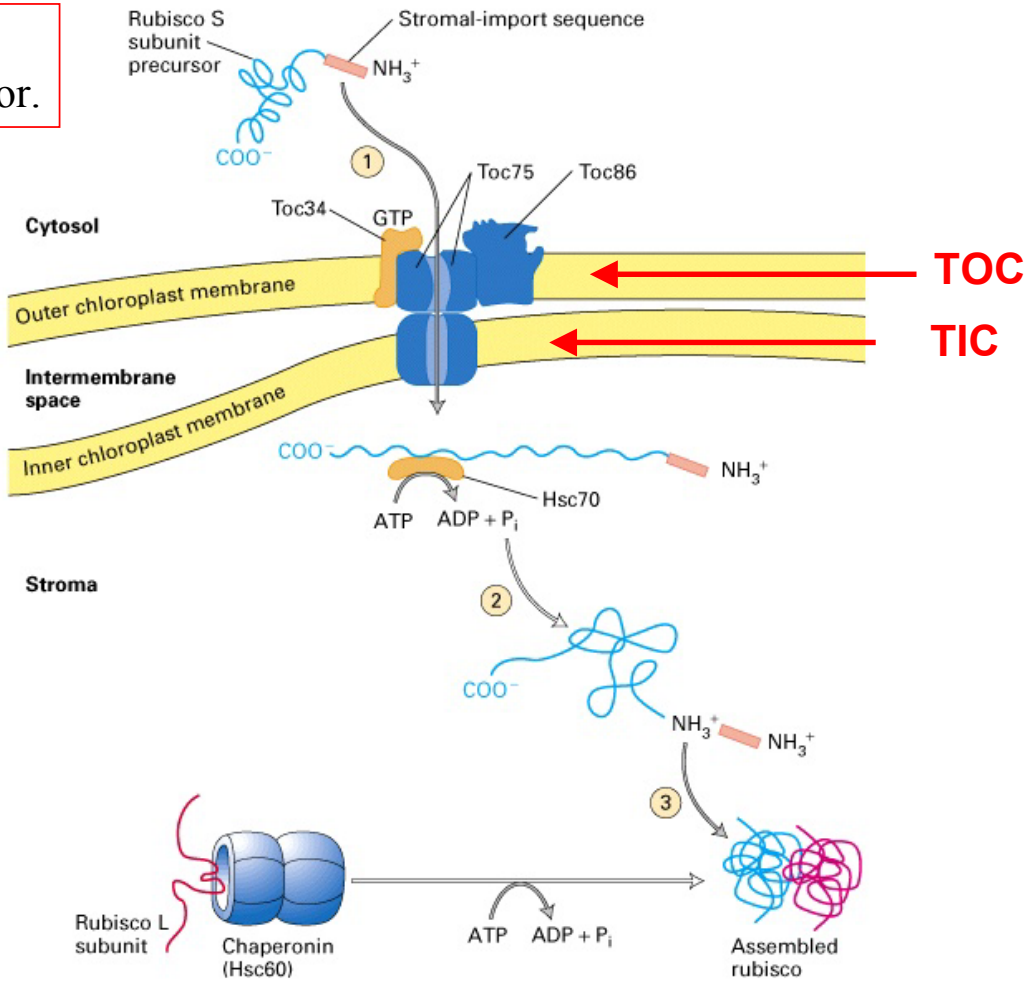

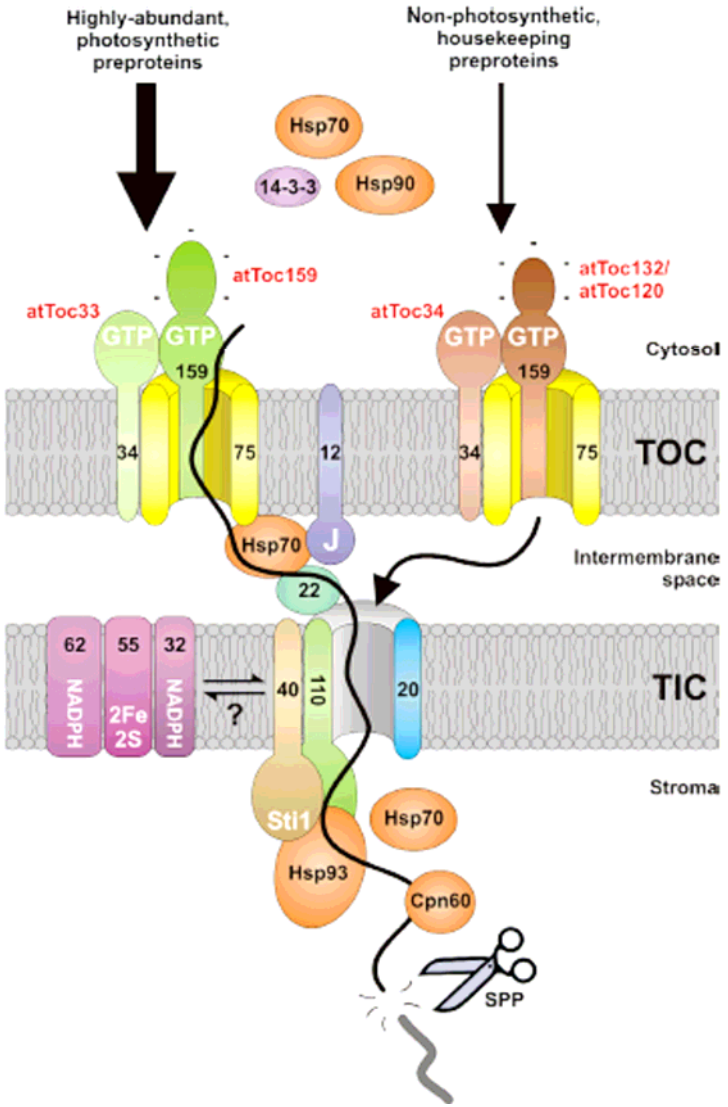
Highly-abundant, photosynthetic preproteins
Non-photosynthetic, housekeeping preproteins
Hsp70
14-3-3
Hsp90
atToc159
atToc33
atToc132/ atToc120
atToc34
GTP
GTP
159
Cytosol
34
75
12
34
75
TOC
Hsp70
J
Intermembrane space
22
62
NADPH
55
2Fe 2S
32
NADPH
?
40
110
20
TIC
Stroma
Stl1
Hsp70
Hsp93
Cpn60
SPP

Transport do thylakoidů

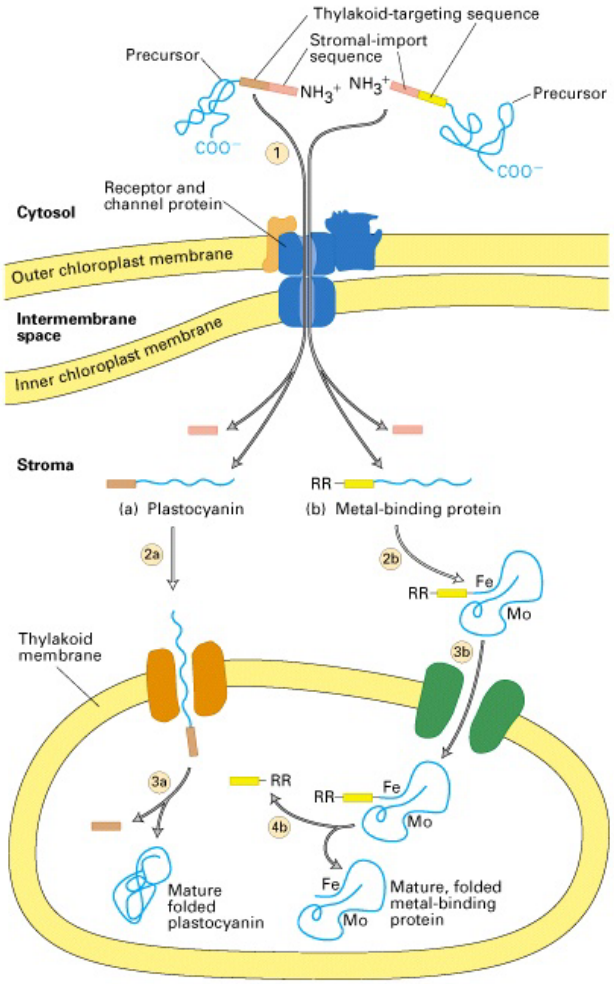

Bílkoviny zůstávají ve stromatu v rozvolněné konformaci (pomocí spec. chaperonů) a jsou transportovány dále.
Po odštěpení 1. TP je aktivován 2. TP.
Při importu do thylakoidů se uplatňují nejméně tři dráhy:
ATP-dependentní tzv .**SEC pathw**.(př. plastocyanin)
ATP-indep. tzv. **delta pH pathw**.
Pro integrální bílkoviny thylakoidů - GTP dep. dráha., také aktivovaná rozdílem pH. Protože využívá homol. SRP (signal. recog. partcle) ve stromatu říká se jí také **SRP pathw (**př. - LHCP - light harv. chloroph. bind. prot**)**

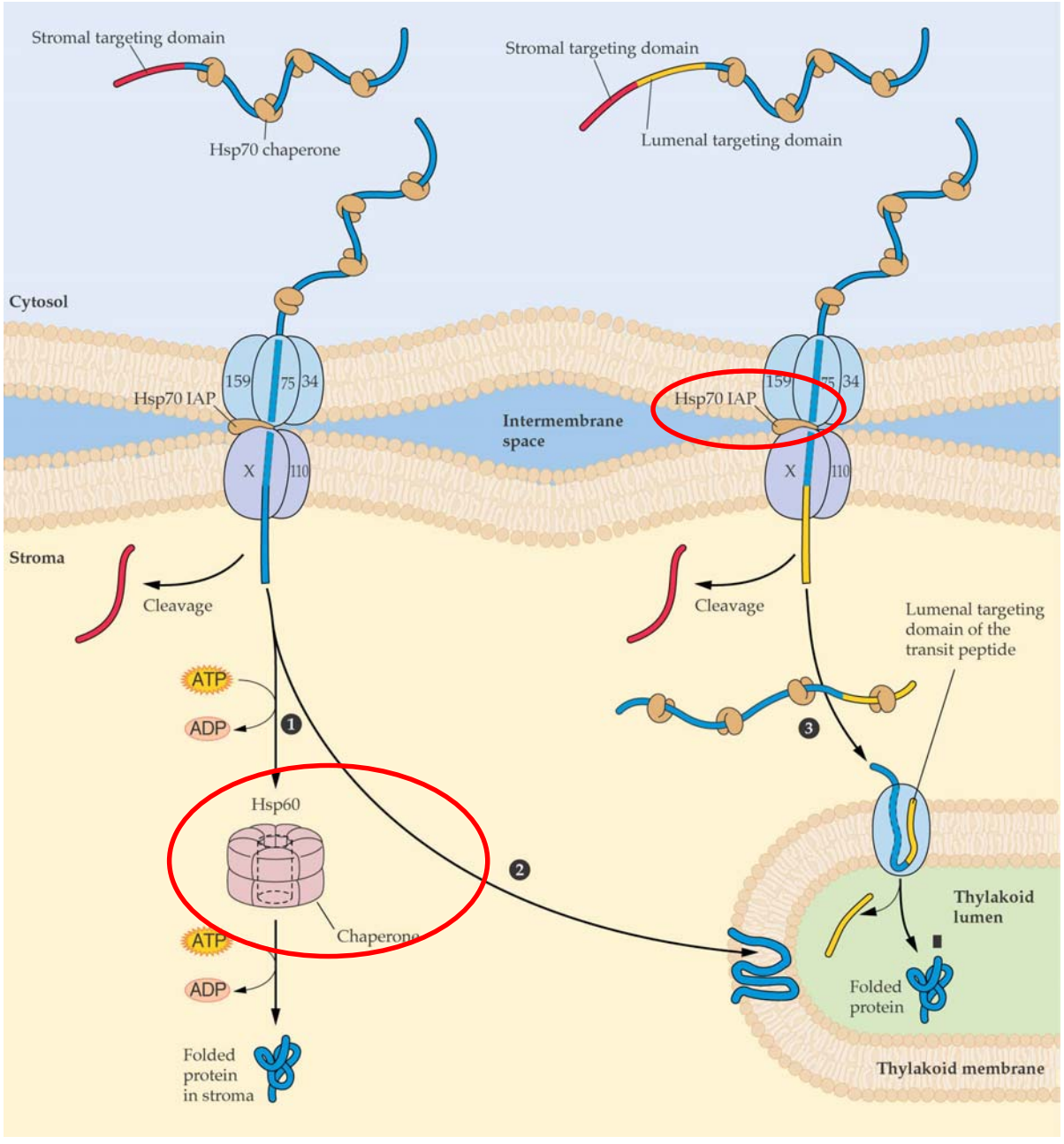

Ve všech krocích hrají důležitou roli bílkovinné chaperony - a to jak při "roz- tak zabalování bílk.

Ve stromatu je nativní konf. proteinu dosaženo pomocí HSP60

Proteiny vnější membrány jsou inkorporovány přímo z cytoplasmy.

Nedávno byla pozorována dráha importu z ER pomocí váčků.

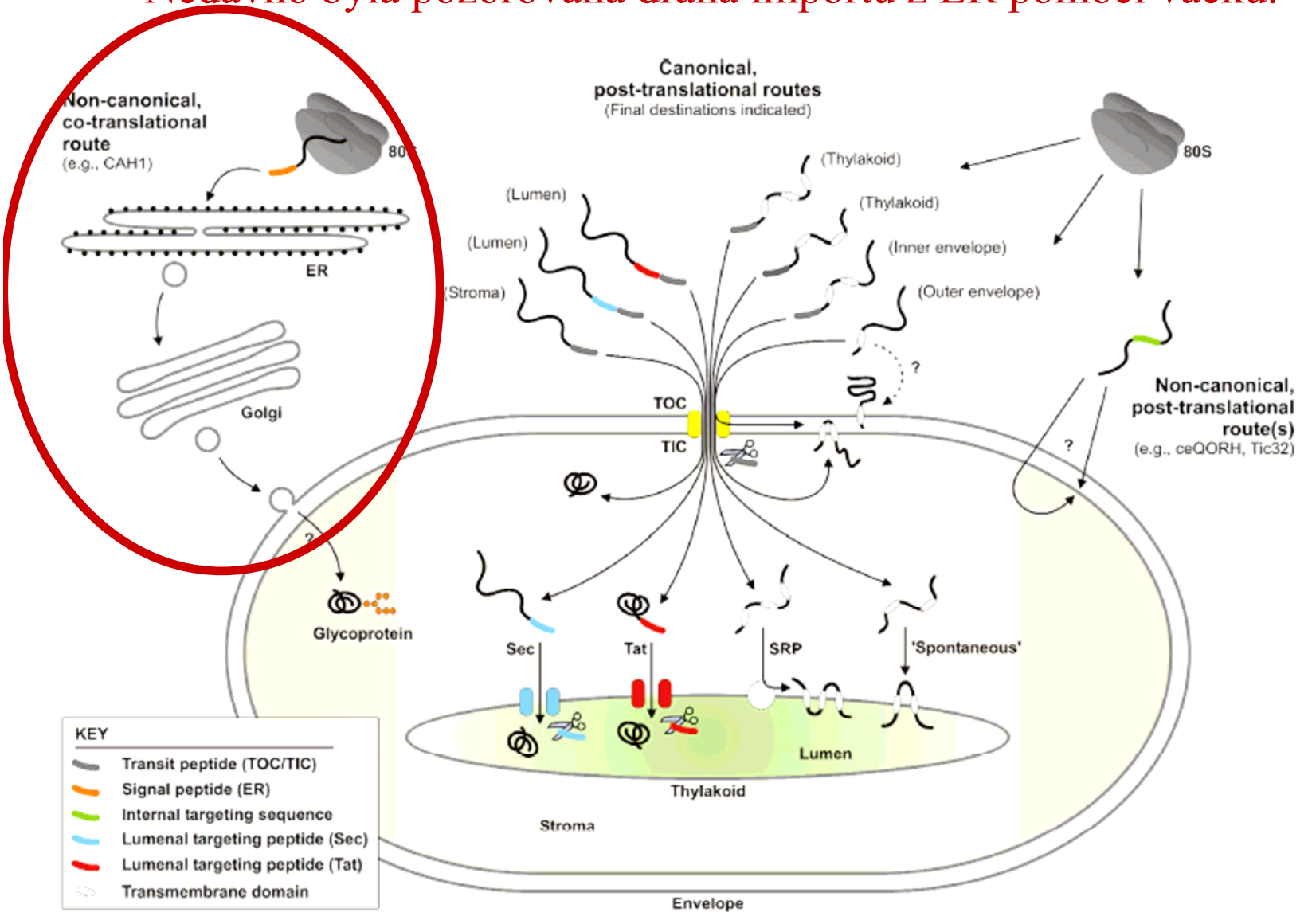

Zvyšuje se také počet bílkovin u kterých je prokázáno dvojí cílení = „dual targeting“ jak do plastidů, tak mitochondrií – př. NEP dále (a viz. příště.)

Organizace genomu plastidů suchozemských rostlin.

Physical map (e. g. restriction map or DNA sequence) indicates a **120-160 kb circular genome**

Large inverted repeat (**LIR**) commonly 20-30 kb

Divides genome into large single copy (**LSC**) region and **small single copy** (**SSC**) region

Inversion of genome segments indicates active recombination within the LIR

Expansion and contraction of LIR is the primary length polymorphism in land plants (10-76 kb)

Conifers and some legumes have no LIR

Inversion polymorphisms within single copy regions mediated by small dispersed repeats

Primary form of the plastid DNA may be multigenomic, branched linear molecules.

Př. organizace plastomu rýže.

(stejnou základní architekturu mají už játrovky) kóduje kol. 130 genů: **1. bílk. fotos. aparátu**;

2.bílk. a RNA genové expr.

plastidů

Chloroplast mezofylu může obsahovat až 200 kopií plastomu. (obvykle kol. 30).

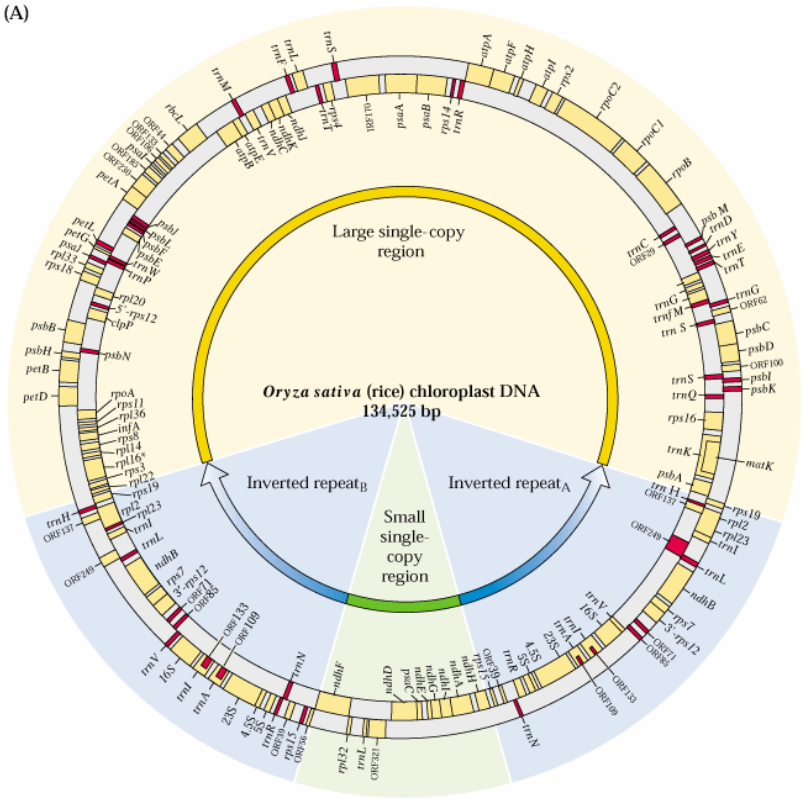

Biochemistry & Molecular

Plastidový genom je až 10x menší než mitochondriální, ale kóduje více funkcí.

Rýže

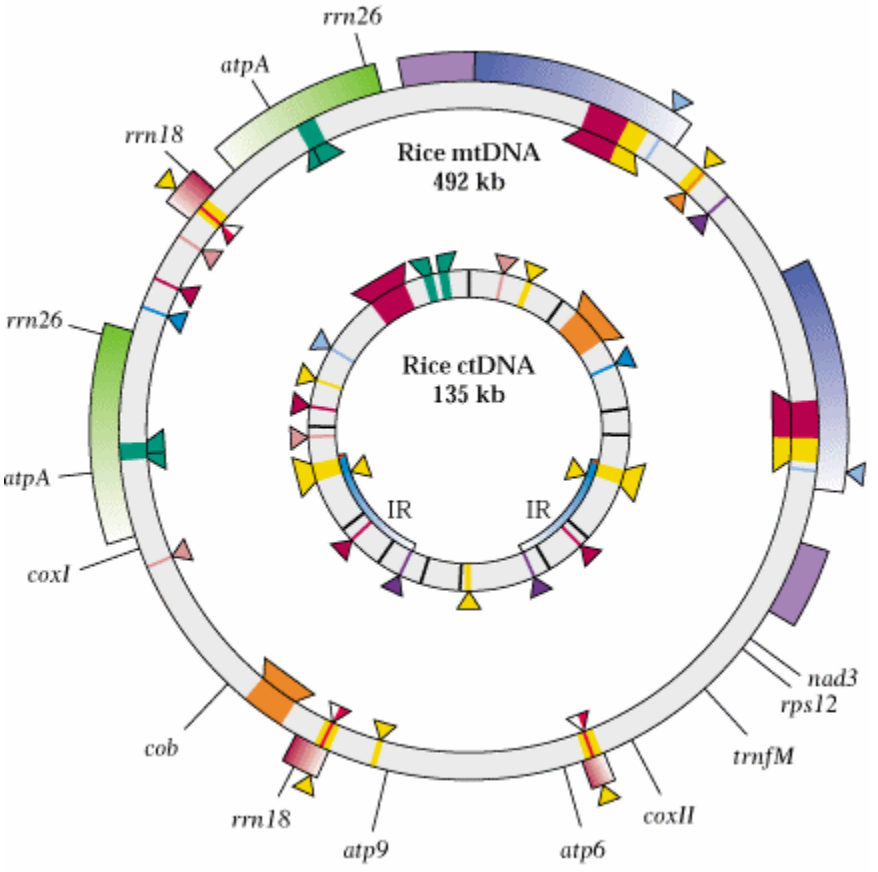

Co vše plastidový genom kóduje?

Generally conserved among land plants, more variable among algae

Genes involved in plastid gene expression
- rRNAs, tRNAs
- ribosomal proteins
- RNA polymerase

Genes involved in photosynthesis
- 28 thylakoid proteins *psa* and *psb* subunits
- RUBISCO large subunit (*rbcL*)

ATP synthase subunits (*atp*)

NADH dehydrogenase subunits (*nad*)

Cytochrome b6f subunits (*pet*)

Organized in operons; some gene orders conserved with bacteria

Rekombinace invertovaných opakování vede Ke vzniku inverzí

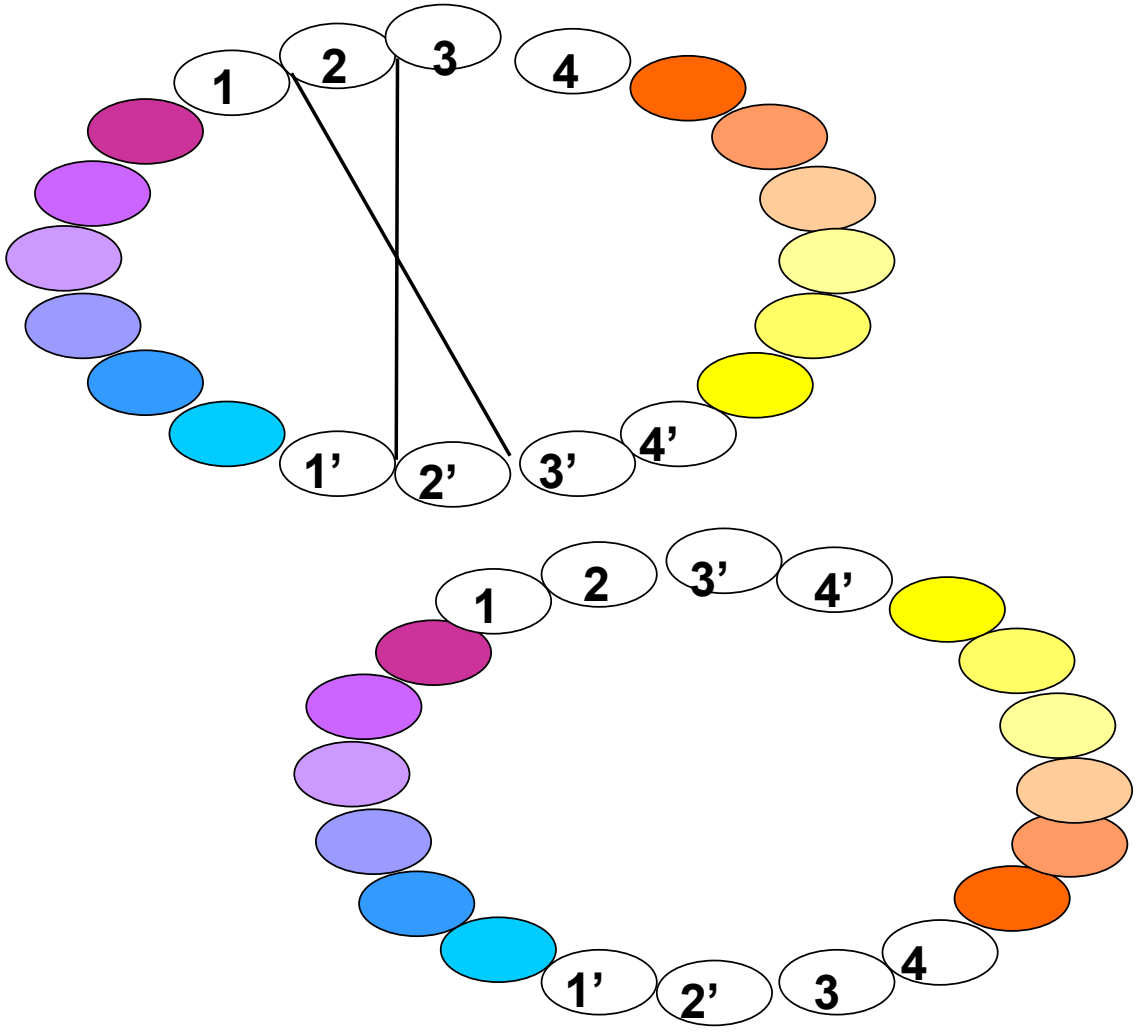

Ve skutečnosti je plastom daleko „barvitější“

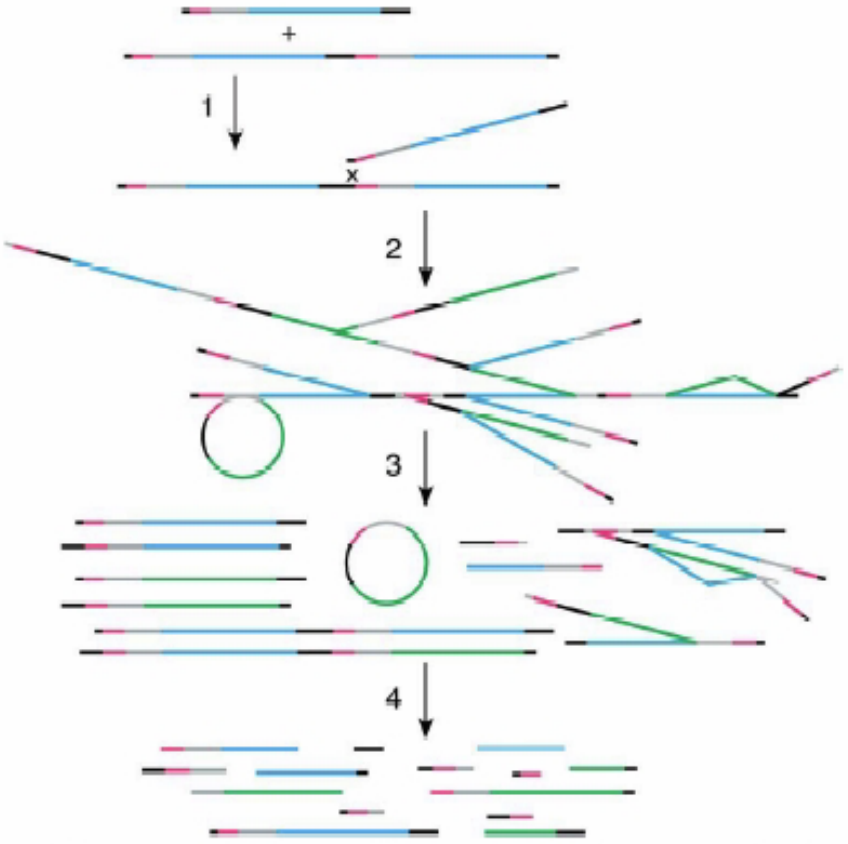

Figure 13. From multigenomic to subgenomic forms: recombination-dependent replication and degradation of chloroplast DNA. Step 1: the products of the OPaLI mechanism shown in Figure 12(c) are genome-sized linears with single-strand 3′ overhangs and an h-t dimer. The single-strand end of the monomer invades the homologous region of the dimer to initiate replication. The long single-copy region (LSC) is shown in blue, the short single-copy region is red, and the inverted repeats (IR_A and IR_B) are indicated by the grey and black lines, respectively. Step 2: continued strand invasion and replication generates a branched structure containing many genome equivalents of cpDNA. A blue or green (inverted) LSC orientation depends on whether strand invasion occurs at IR_A or IR_B.[4] Step 3: replication ceases, and smaller forms arise as forks reach the ends of their template strands and branchpoints are resolved by recombination. The four linear monomers (two with blue and two with green LSCs) and two h-t dimers that are shown (on the left) were predicted by restriction mapping.[4] Incidental recombination of direct repeat sequences (IR_A in this example) on an h-t concatemer produces a genome-sized circle. Step 4: degradation leaves most of the cpDNA as less-than-genome-sized fragments (a genome-sized molecule is shown at bottom left), perhaps by metallo-nucleases as suggested for rice cpDNA.[22] Continued degradation eliminates the DNA from most mature chloroplasts (Figure 5).

a v plastidech je mnoho rekombinované a linearizované DNA.

Plastidové geny jsou uspořádané do operonů

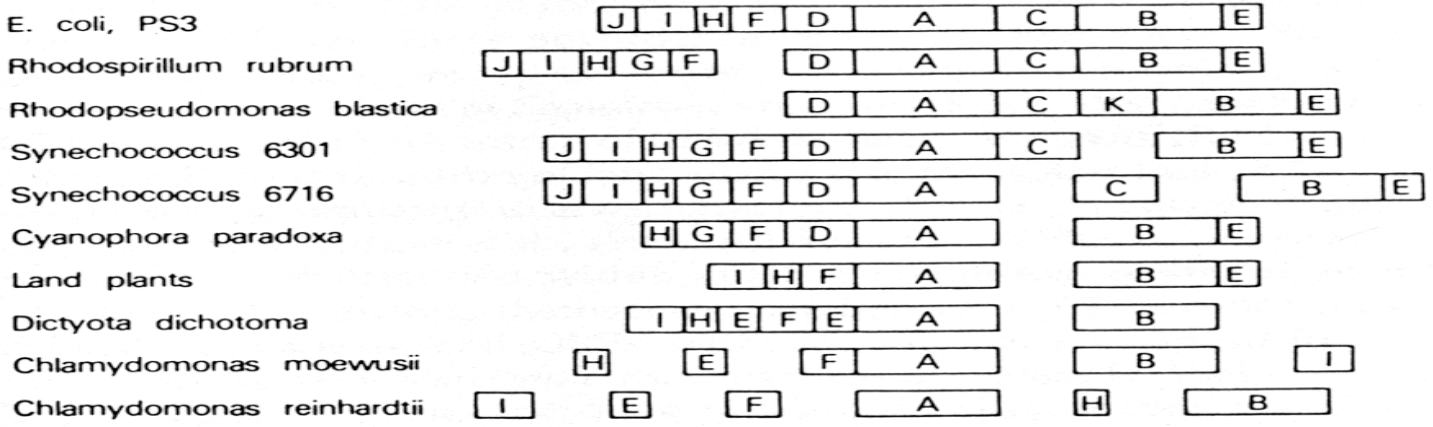

FIG. 2. Organization of ATP synthase genes in chloroplasts and bacteria. Genes drawn without any space between them are found adjacent in the indicated genome and are probably cotranscribed; genes or gene clusters that are shown separated by an open space are physically and transcriptionally unlinked. Genes are drawn proportional to coding length; introns (e.g., in *atpF* in land plants) are not shown. All genes shown have been sequenced except for *atpB* from *Dictyota;* all six genes from *C. moewusii;* and *atpA, atpF, atpH,* and *atpI* from *Chlamydomonas reinhardtii,* all of which have been mapped using heterologous gene probes. *Rhodopseudomonas blastica* has not been examined for several *atp* genes. Data are summarized from Falk and Walker (1988), six bacterial genomes; Breiteneder *et al.* (1988), Lambert *et al.* (1985), and D. Bryant (unpublished), *Cyanophora;* Sugiura (1989), land plants; Hallick and Buetow (1989) and R. Hallick (unpublished), *Euglena;* Kuhsel (1988), *Dictyota;* Turmel *et al.* (1988) and Boynton *et al.* (1991), two *Chlamydomonas* species.

(z Palmer (1991) in Cell Culture and Somatic Cell Genetics of Plants, V 7A. L Bogorad and IK Vasil eds. Academic Press, NY, pp 5-142)

Transformace plastidů

Nástroj základního výzkumu i důležitá biotechnologie.

Transformace plastidů

DNA delivery by particle bombardment or PEG precipitation

DNA incorporation by homologous recombination

Initial transformants are heteroplasmic, having a mixture of transformed and non-transformed plastids

Selection for resistance to spectinomycin (spec) and streptomycin (strep) antibiotics that inhibit plastid protein synthesis

- **Spec *or* strep resistance conferred by individual 16S rRNA mutant**
- **Spec *and* strep resistance conferred by *aadA* gene (aminoglycoside adenylyl transferase)**
- **Untransformed callus bleached; transformed callus greens and can be regenerated**
- **Multiple selection cycles may be required to obtain homoplasmy (all plastid genomes of the same type)**

Selekce plastidových transformantů

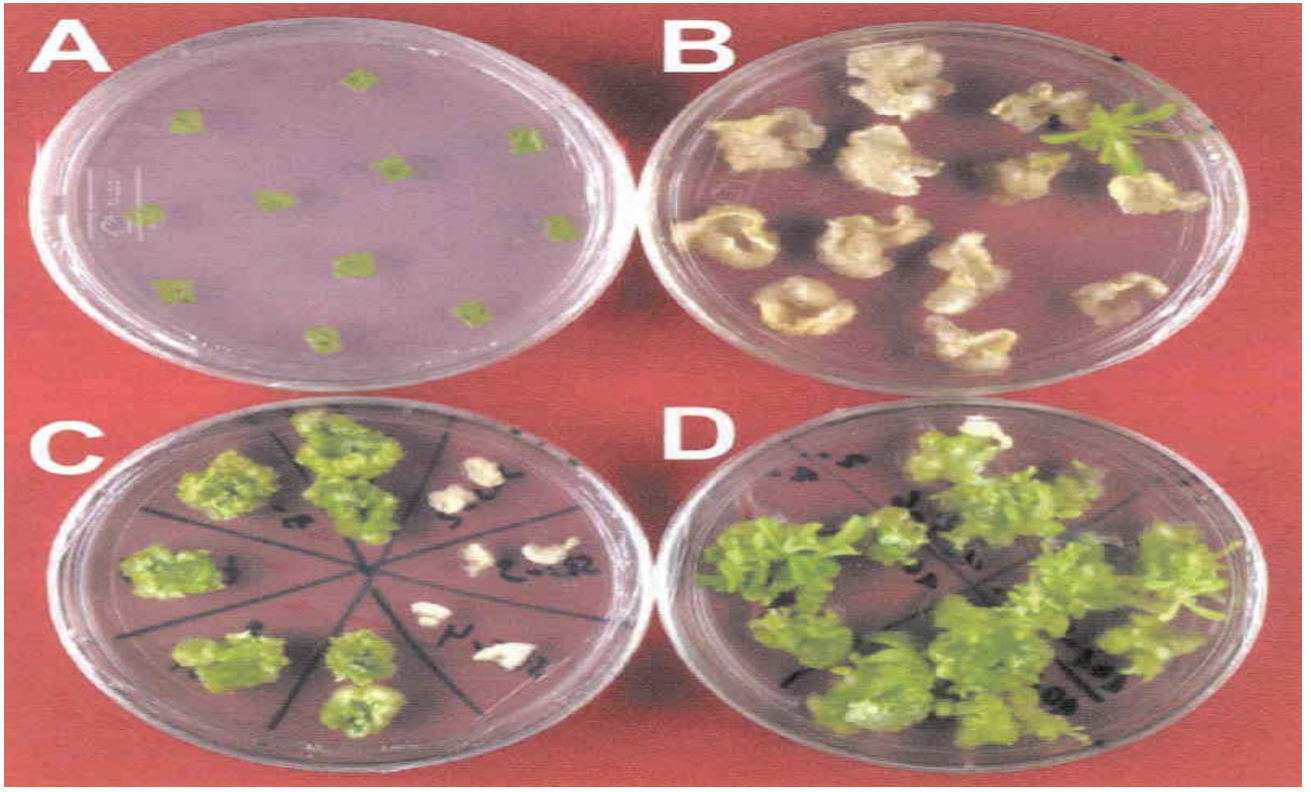

Figure 1. Generation of tobacco plants with transgenic chloroplasts A) leaf segments post bombardment with the aadA gene; B) leaf segments after selection on spectinomycin; C) transfer of transformants to spectinomycin + streptomycin to eliminate spontaneous spectinomycin resistant mutants; D) recovery of homoplasmic spec + strep resistant transformants after multiple rounds of regeneration on selective medium Bock (2001) J Mol Biol 312:425

Výhody transformace plastomu

High levels of expression

- **Plastid proteins the most abundant in the world**
- **No apparent gene silencing in plastids**

Codon preference

- **Bacterial codon preferences used in the plastid mean that bacterial genes can be expressed efficiently without re-engineering codon usage**
  - **antibiotic resistance, herbicide resistance, insect resistance, etc.**

Containment

- **Plastidové geny nejsou přenášeny pylem (although plastid genomes may be present in some species); eliminates pollen toxicity**

- **Plastid genomes are not transmitted through the pollen of many plant species; eliminates pollen transmission of transgenes to neighboring wild or cultivated plants**

Important research tool

- **Precise gene targeting by homologous recombination**

Transformace plastidů v buněčné suspenzi a somatická embryogeneze.

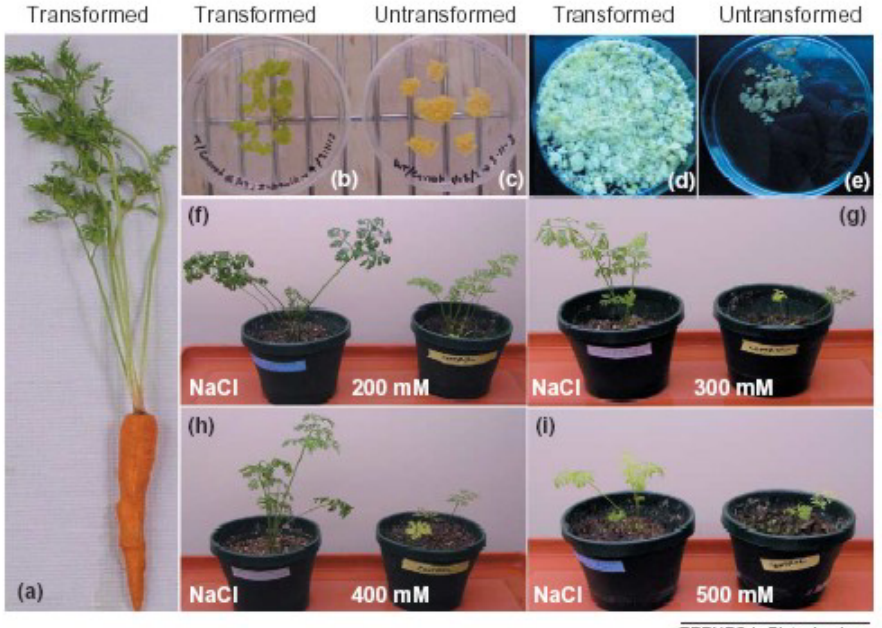

Figure 1. Transformation of the carrot plastid genome. **(a)** Complete transgenic carrot plant with orange color of root (edible part) and green shoots. The expression of betaine aldehyde dehydrogenase in carrot cells promoted the green color in transgenic cells, which offers the visual selection of transgenic calli **(b)** versus yellow non-transgenic carrot calli **(c)**. **(d)** Transgenic carrot cells showed proliferic growth in the liquid medium supplemented with 100 mM NaCl, whereas **(e)** untransformed carrot cell culture did not grow in the presence of salt. **(f–i)** Transgenic carrot plants thrived well in soil pots irrigated with 200–500 mM sodium chloride, whereas untransformed carrot plants showed retarded growth in the presence of salt.

Vývoj speciálních plasmidových vektorů pro plastidy.
mrkev je odolnější k zasolení

Příklad experimentálního využití transformace plastidů

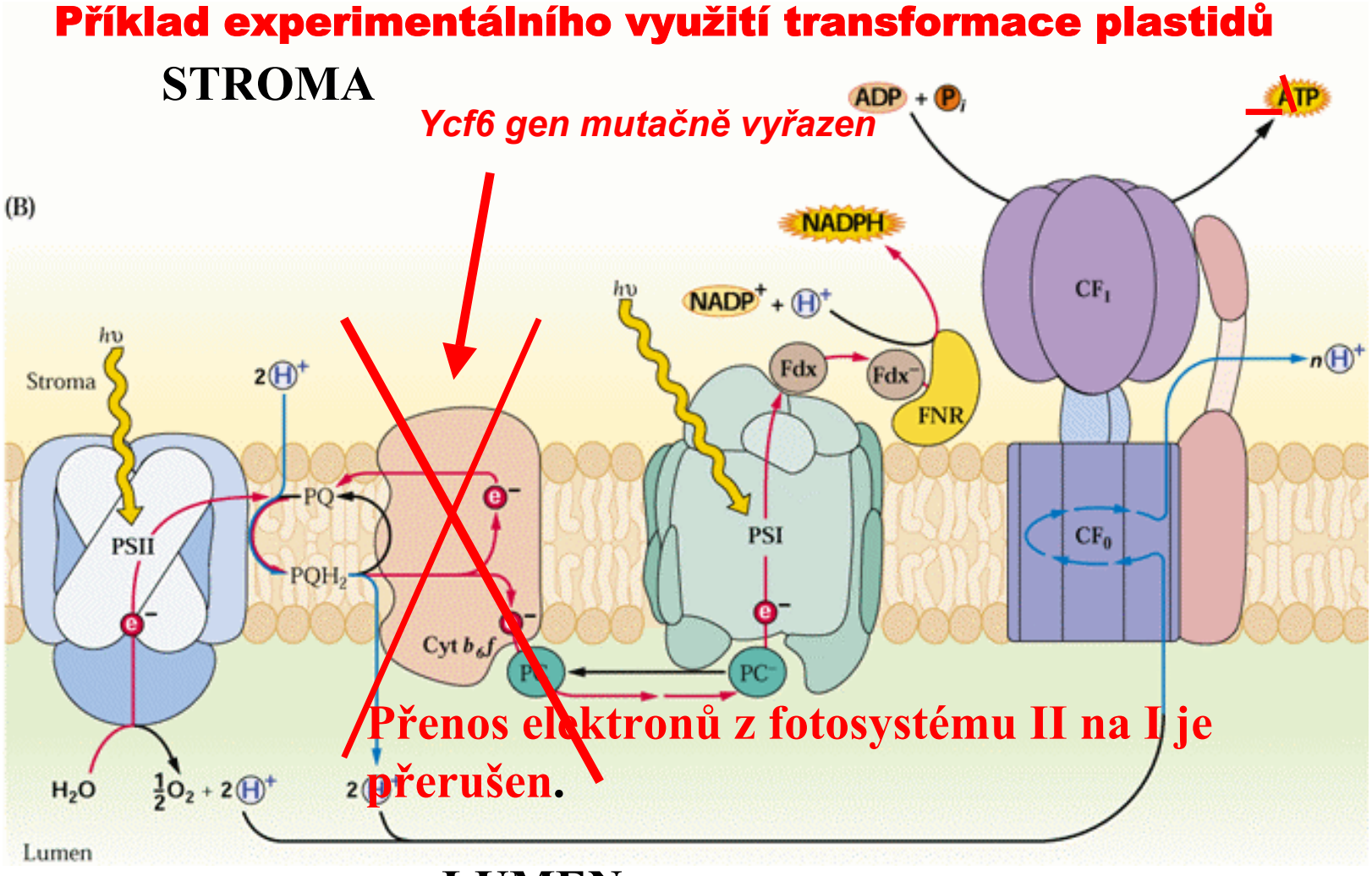

Lokus *ycf6* je nejmenší ORF (29AA)plastomu a kóduje podjednotku cytochromu b6f.

Funkční analýza plastidového lokusu *ycf6* v transgenních plastidech

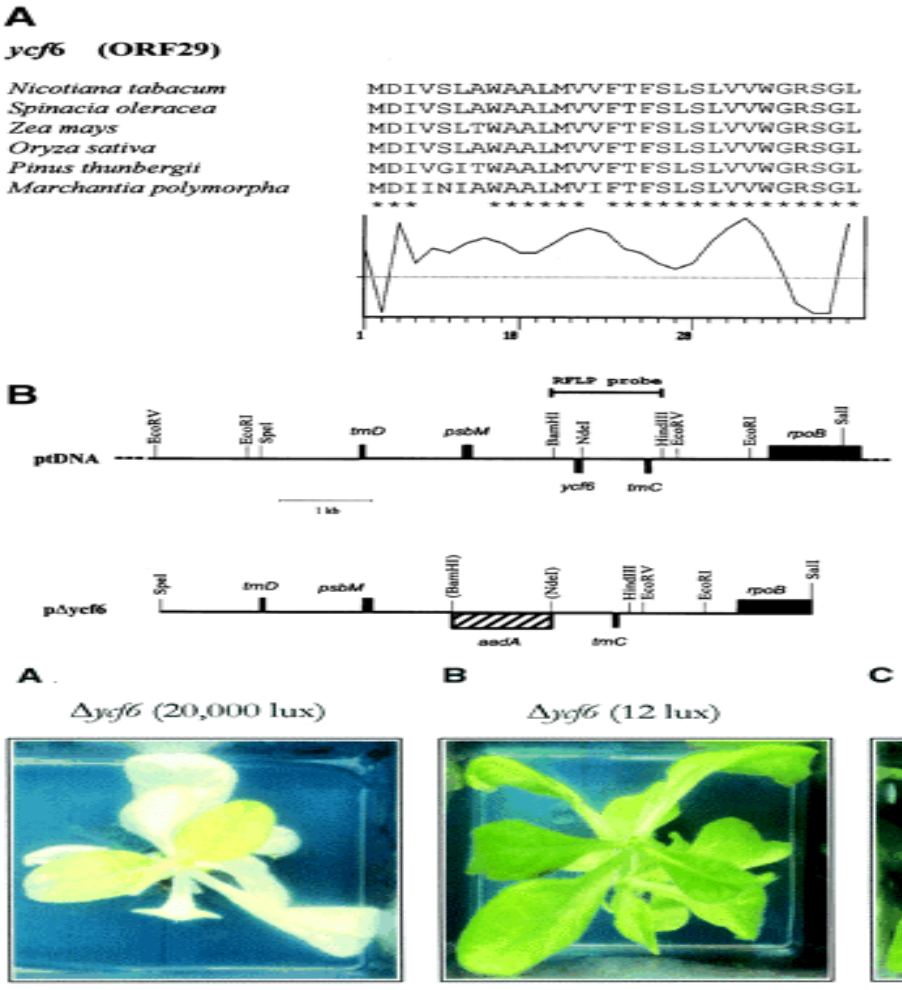

Přenos elektronů
z fotosystému II na I
je přerušen.
A – standardní (silné)
světlo působí vybělení.

from Hager et al. (1999) EMBO J 18:5834

Právě na příkladu b6f cytochromu (viz.dále) bylo také ukázáno, že je-li narušena stechiometrie komplexu výpadkem jedné podjednotky, je destabilizován celý komplex. Bílkoviny, které se nestanou součástí funkčního komplexu jsou degradovány.

To pak už souvisí s regulací GENOVÉ EXPRESE

Regulace genové exprese v plastidech

RNA pol. A PROMOTORY ORGANEL

Polymerase	Subunits	Consensus promoter
Bacterial	✂αα' and ☞70	-35/-10 GTGTTGACA/TATAATG
Plastid encoded (**PEP**)	✂αα' and (nuclear-encoded ☞)	-35/-10 TTGACA/TATAAT
T7	single core no ☞	overlaps initiation ATACGACTCACTATAGGGAGA
Nuclear encoded plastid (**NEP**)	single core and ☞-like	overlaps initiation ATAGAAT A/G AA
Nuclear encoded plant mit	single core and ☞-like	overlaps initiation CRTA G/T

Ze tří NEP u Arabidopsis je **jedna importována jak do plastidů, tak mitochondrií**; zbylé dvě jsou mitoch. a plast. specifické.

Dvě RNApol plastidů

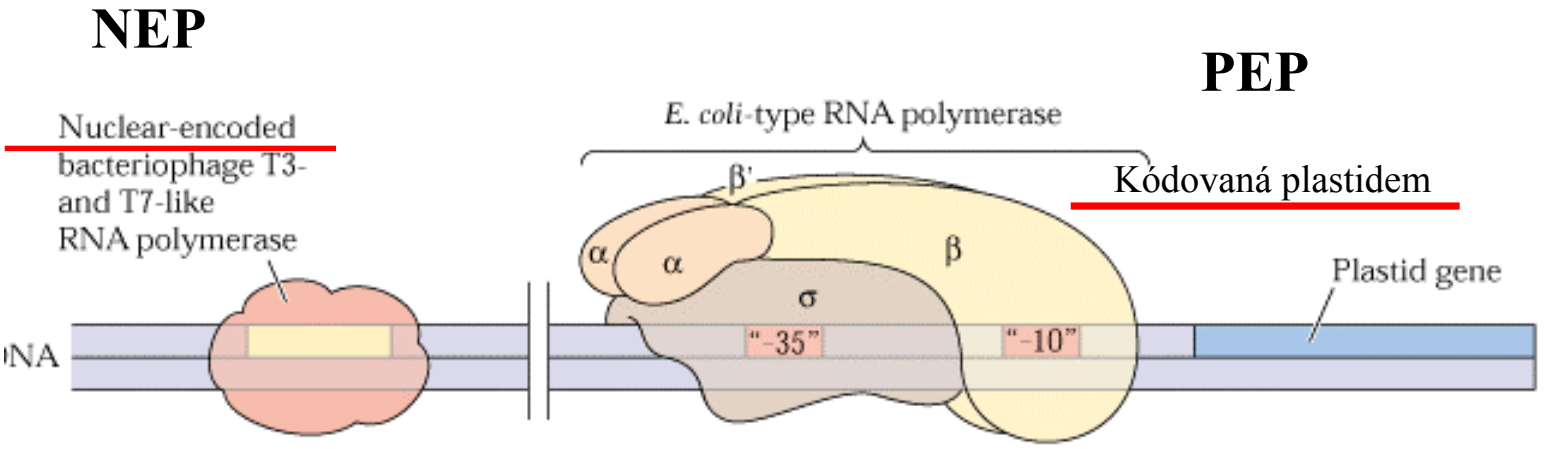

Rostlinná PEP komplementuje RNApol. mutanta E. coli.

Specifická genová exprese založená na specifickém rozpoznávání různých promotorů NEP a PEP

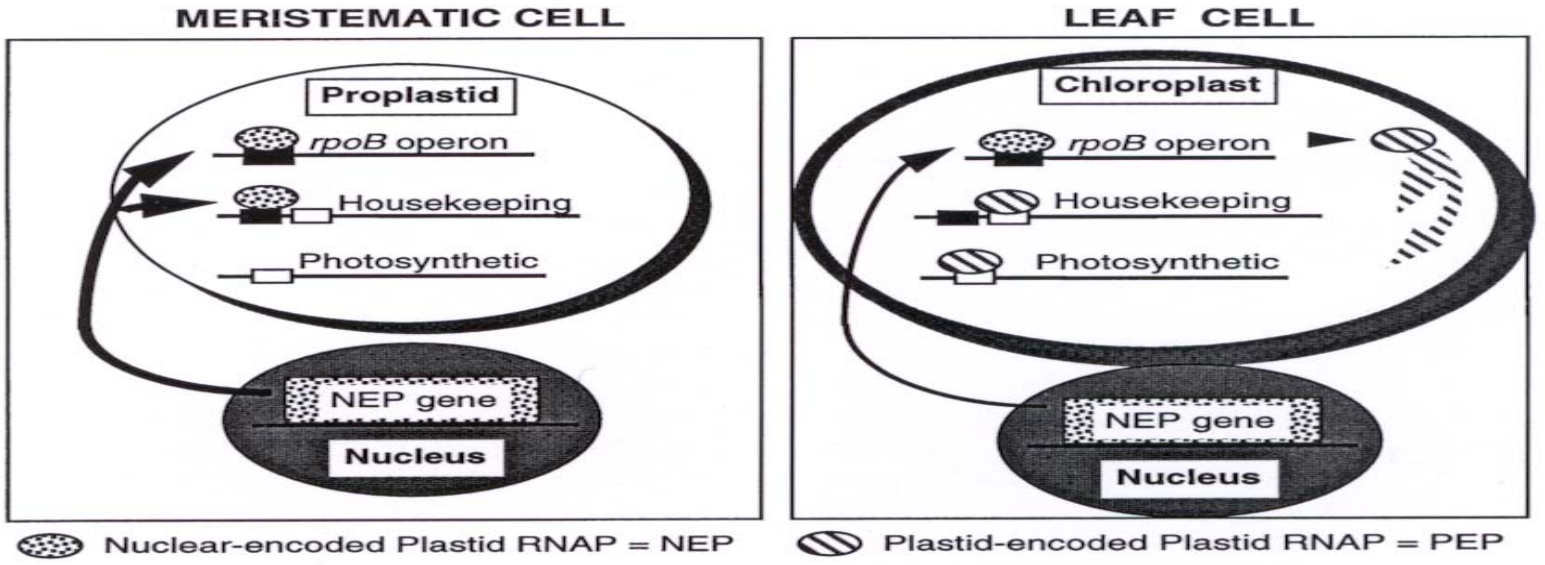

Začíná NEP

Pokračuje PEP

(z Hajdukiewicz et al. EMBO J 16:4041-4048)

Úpravy mRNA organel

Like prokaryotes, plant organelle genes are often co-transcribed as operons

In contrast to prokaryotic transcripst, plant organelle transcripts:

- Are frequently processed to di or mono-cistronic transcripts before translation
- Frequently contain introns that must be spliced prior to translation
- Must undergo an RNA editing process to restore proper amino acid coding

Introny rostlinných organel - většinou typ II

Land plant organelle introns almost exclusively Group II

Characteristic spoke-and-wheel structure necessary for splicing

Self-splicing *in vitro*

Trans-acting RNA and/or protein factors required for splicing *in vivo*

e.g. maize nuclear mutants encoding proteins required for splicing

Genome rearrangements have split introns, which then require trans-splicing

The spoke-and-wheel structure is assembled from separate transcripts

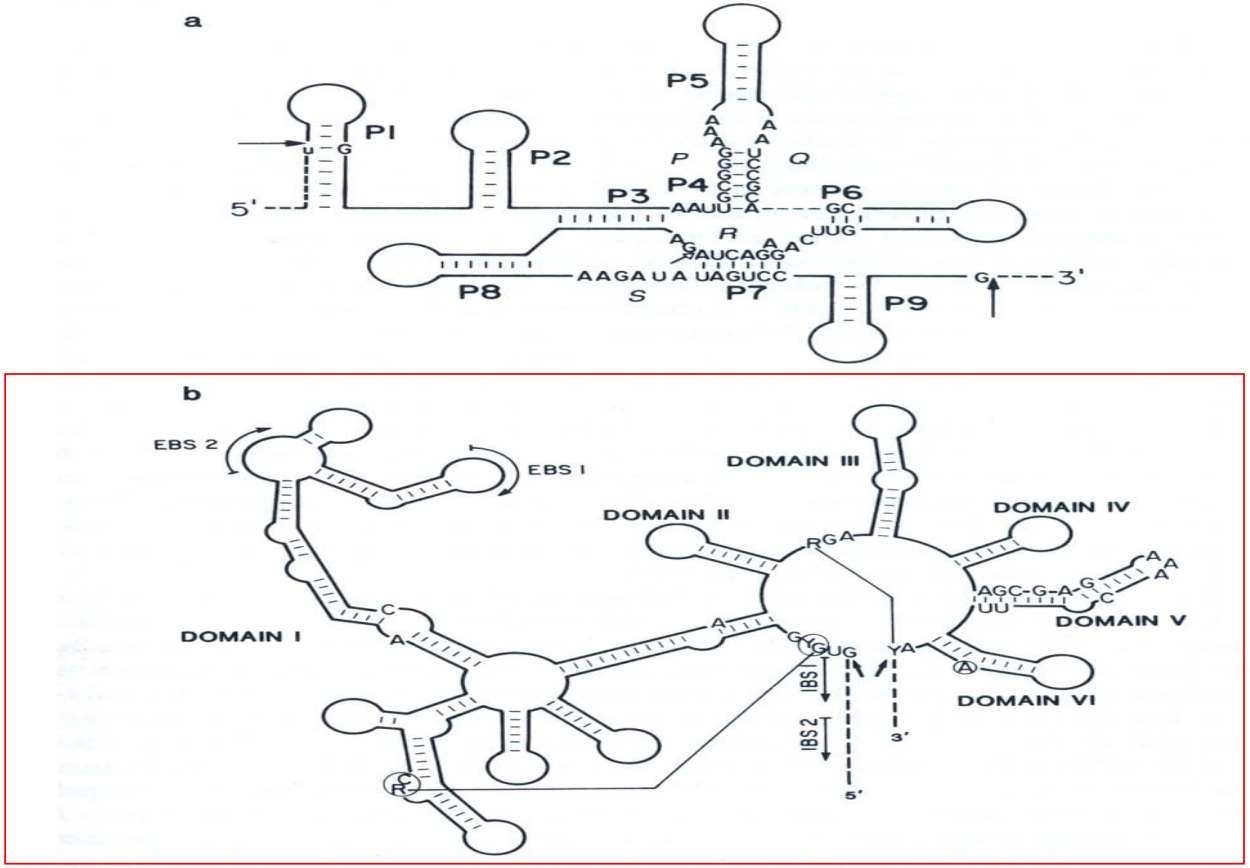

Fig. 10–2. (a) Secondary structure of group I introns as proven by comparative sequence analysis. A typical structure indicating conserved base-paired elements P1–P9. *P*, *Q*, *R*, and *S* represent conserved sequence elements and are represented by their most common nucleotide sequences. Dashed line between P4 and P6 is added to make the diagram less crowded, and does not indicate any omission of nucleotides. Filled arrow, 5′ and 3′ splice sites. Open arrow, site of insertion of extra stem–loop(s) P7.1 and P7.2 in group IA introns. From Cech (1990) with permission. (b) The core secondary structure of group II introns (see Michel and Dujon, 1983). Sections of the structure are identified as domains bounded by inverted repeat sequences. Pairing interactions have been identified involving intron-binding sites (IBS1 and IBS2) within the 5′ exon (E1) and exon-binding sites (EBS1 and EBS2) within D1 of the intron (Jacquier and Michel, 1987). A second pairing involves CR and YG where R and Y equal a purine and a pyrimidine respectively. Filled arrows, 5′ and 3′ splice sites. Dashed lines at the 3′ and 5′ ends in A and B represent exon sequences. From Cech, unpublished, with permission.

z Gillham 1994 Organelle Genes and Genomes

Stabilita transkriptů v organelách

Plant organelle transcripts are stabilized by 3' stem-loop structures

Removal of the stem loop (by endonuclease cleavage) makes the 3' end accessible for polyA addition

In contrast to nuclear transcripts, plant organelle transcripts are destabilized by the addition of 3' poly A tracts

3' polyA is also a de-stabilizing feature of bacterial transcripts

3' polyA enhances susceptibility of transcript to degradation by exonucleases

Model "metabolismu" plastidové mRNA (turn-over)

(z Monde et al. Biochimie 82:573)

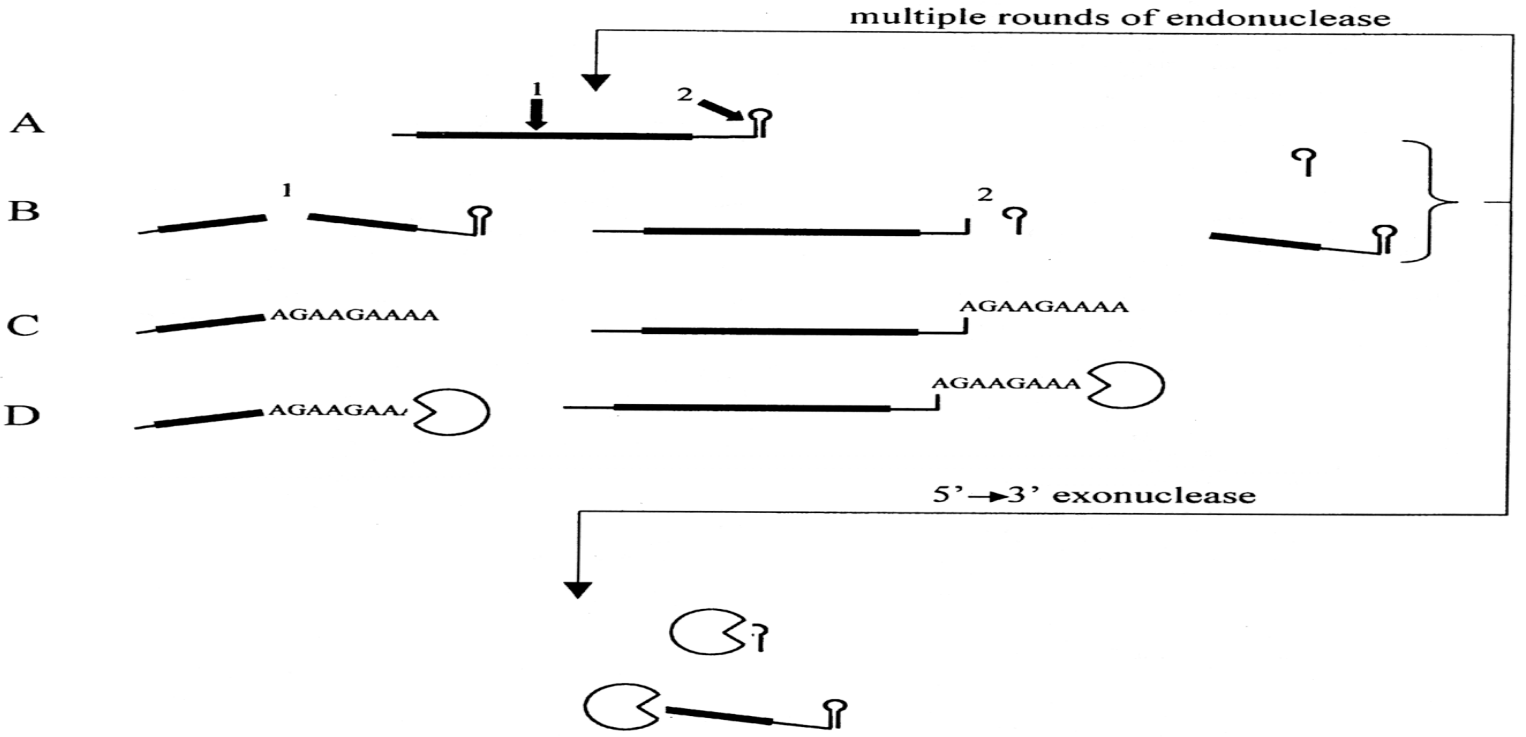

Figure 1. A working model for chloroplast mRNA degradation. The scheme is shown for a typical chloroplast mRNA with a 3' IR, such as spinach *psbA* or *Chlamydomonas atpB*. The thick portion represents the coding region. **A.** Initially, endonuclease attack occurs within the coding region (1) or the 3' IR (2), catalyzed by enzymes such as those discussed in the text. **B.** This cleavage yields proximal and distal products. The distal products are subject to further rounds of endonucleolytic cleavage (upper arrow), or may be degraded by a 5' to 3' exonuclease activity (lower arrow). **C.** The proximal products are efficiently polyadenylated with a tail up to several hundred nucleotides in length, either containing some proportion of guanosine (as in spinach) or without guanosine (as in *Chlamydomonas*). **D.** The polyadenylated RNA molecule is rapidly degraded by exonuclease(s), such as PNP.

Editování mRNA v plastidech a mitochondriích

Typické znaky editování

Post transcriptional C > U and less frequently U > C

genomic coding strand	5' ACG.....
unedited RNA	5' ACG.....
edited RNA	5' AUG....
edited cDNA	5' ATG.....

Occurs by enzymatic de/trans-amination

Occurs in plastids and plant mitochondria (more frequently in mitochondria)

Occurs primarily in coding sequences and improves overall conservation of predicted protein products

Creates initiation codons	ACG > AUG
Creates termination codons	CGA > UGA
Removes termination codons	UGA > CGA
Changes amino acid coding	CCA > CUA (P > L)
Silent edits	ATC > ATU

Edit sites within the same gene vary among species. An edit site in one species may be "pre-edited" (ie correctly encoded) in the genomic sequence of another species

eg. plastid *psbL* gene:

maize	ATGACA.....
tobacco	ACGACA.....

RNA editing zachovává konzervovanost bílkovin.

(z Mulligan and Maliga 1998)

Table 1. Evolutionary Conserved Amino Acid Residues Changed by C-to-U Editing in Ribosomal Protein S12 (RPS12) of Plant Mitochondria

Amino acid residues encoded by unedited and edited maize mitochondrial transcripts are compared to amino acid residues in RPS12 polypeptides from other taxa.

	Amino Acid Residue No.					
	24	66	73	90	95	97
Maize mito (unedited RNA)	S	H	S	S	S	R
Maize mito (edited RNA)	L	Y	L	L	F	C
Acanthamoeba mito	L	Y	L	L	Y	L
Drosophila mito	L	Y	L	V	L	A
Maize plastid	L	Y	L	L	Y	I
Tobacco plastid	L	Y	L	L	Y	I
Chlamydomonas plastid	L	Y	L	L	Y	I
Marchantia plastid	L	Y	L	L	Y	I
Escherichia coli	L	Y	L	L	Y	T

RNA editování probíhá v organelách rostlin převážně enzymatickou deaminací

z Rajasekhar and Mulligan Plant Cell 5:1843

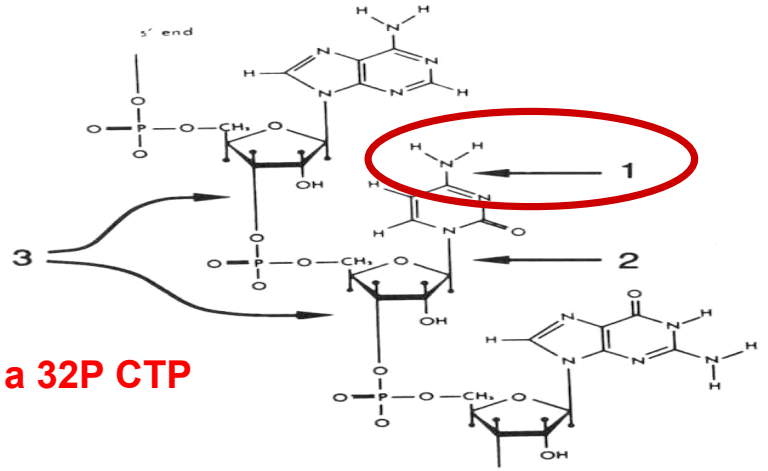

Figure 1. RNA Editing Mechanisms Potentially Responsible for C-to-U Conversion.

The bonds cleaved by various RNA editing mechanisms are indicated by the numbered arrows. Mechanism 1 involves deamination (or transamination) of the C-4 amide of cytosine to convert the base to uracil. Mechanism 2 involves transglycosylation of the ribosyl moiety to replace the base. Mechanism 3 involves deletion and insertion of a new nucleoside monophosphate.

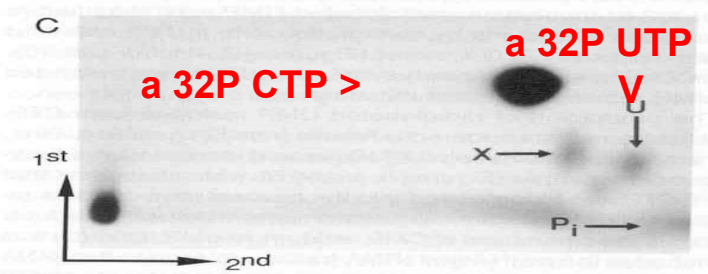

Figure 5. Two-Dimensional Fractionation of NMPs from Petunia Mitochondrial Transcripts.

Petunia mitochondrial transcripts were radiolabeled with CTP and extracted after 10 min or 2 hr of incubation. RNA was digested to NMPs and fractionated by two-dimensional chromatography on thin-layer cellulose plates by method 1 **([A]** and **[B])** or method 2 **[C].** The arrows at lower left indicate the directions of the first and second dimensions of TLC. The arrows on the autoradiogram indicate the migration of uridine monophosphate (U), inorganic phosphate (Pi), and an unknown product (X).
(A) and **(B)** Mitochondria were labeled and incubated for 10 min or 2 hr, respectively, and NMPs were fractionated by TLC method 1.
(C) Mitochondria were labeled and incubated for 2 hr and NMPs were fractionated by TLC method 2.

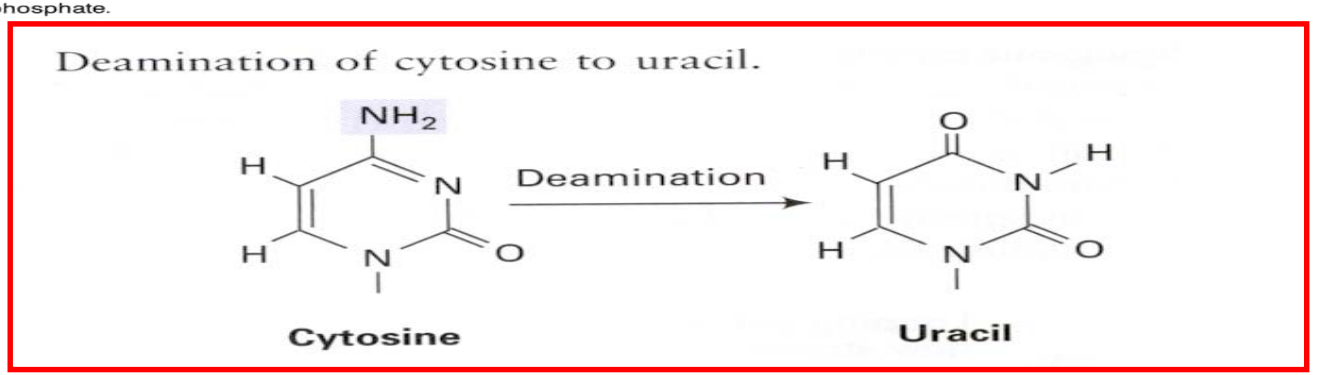

from Russell, 1995, Genetics

RNA editování

Evidence for the importance of cis-guiding sequences in plant mitochondrial RNA editing

Editing of recombinant or rearranged mitochondrial genes

- Recombination breakpoint immediately 3' to an editing site in rice *atp6* did ***not*** abolish editing
- Recombination breakpoint seven nucleotides 5' to an editing site in maize *rps12* did abolish editing
- Recombination breakpoint 21 nucleotides 5' to an editing site in maize *rps12* did ***not*** abolish editing

Electroporation of genes into isolated mitochondria, followed by isolation of mitochondrial cDNA

- Editing of mutated *coxII* gene demonstrated sequences from –16 to +6 required for editing

Podobná analýza u plastidů - pro editování důležité okolí -14 až +5.

RNA editování

Důkaz o důležitosti „trans“ faktoru – kompetice o vazbu s homol. oligo-RNA.

Plastid *in vitro* RNA editing system demonstrates competition among oligoribonucleotides for editing factors
and proteins that specifically bind competing oligonucleotides

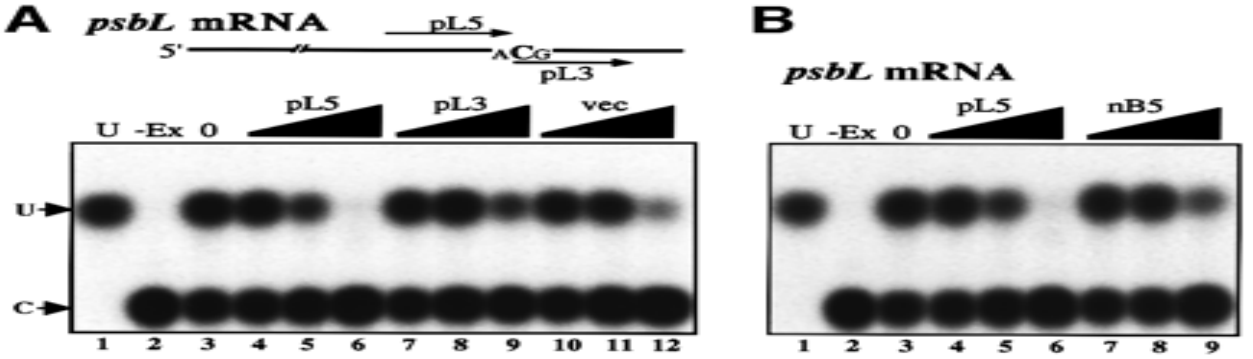

Fig. 3. Competition analysis of *in vitro* RNA editing. (**A**) Increasing amounts of upstream (pL5 and nB5), downstream (pL3 and nB3) and vector (vec) oligoribonucleotides were added to *in vitro* editing reactions with *psbL* and *ndhB* mRNAs. pL5, pL3 and vec oligos of 1 µmol (lanes 4, 7 and 10), 10 µmol (lanes 5, 8 and 11) and 100 µmol (lanes 6, 9 and 12) were added. nB5, nB3 and vec oligos of 0.25 µmol (lanes 4, 7 and 10), 2.5 µmol (lanes 5, 8 and 11) and 25 µmol (lanes 6, 9 and 12) were added. U, authentic pU; –Ex, no chloroplast extract; 0, no competitor. (**B**) Analysis with heterologous competitors. nB5 (1, 10 and 100 µmol, lanes 7, 8 and 9, respectively) was added for *psbL* mRNA. pL5 (0.25, 2.5 and 25 µmol, lanes 7, 8 and 9, respectively) was used for *ndhB* mRNA.

z Hirose and Sugiura EMBOJ 5:1144

Při kompetičních experimentech je obvykle narušeno také editování dalších nehomologních cílových sekvencí.

Editování se účastní PPR bílkoviny jako specifické „adaptory“ pro editování.

Pentatricopeptide repeat proteins (PPR) are characterised by tandem repeats of a degenerate 35 amino acid motif

Arabidopsis thaliana ***crr4*** mutant is defective with respect to RNA editing for creating the translational initial codon of the plastid *ndhD* gene (the ndhD-1 site). CRR4 contains 11 pentatricopeptide repeat motifs but does not contain any domains that are likely to be involved in the editing activity

Pentatricopeptide repeat (PPR) proteins are characterised by tandem repeats of a degenerate 35 amino acid motif [1]. Most of PPR proteins have roles in mitochondria or plastid [2]. PPR repeats were discovered while screening Arabidopsis proteins for those predicted to be targeted to mitochondria or chloroplast [1, 3]. Some of these proteins have been shown to play a role in post-transcriptional processes within organelles and they are thought to be sequence-specific RNA-binding proteins [4, 5, 6]. Plant genomes have between one hundred to five hundred PPR genes per genome whereas non-plant genomes encode two to six PPR proteins.

Translace v plastidech

Translation machinery is bacteria-like:

- Ribosomes:
  -70S (composed of L (50S) and S (30S) subunits)
  -contain 23S (L), 16S (S), and 5S (L) rRNAs
  -each subunit (L and S) contains ~30 proteins
- Initiation factors: if1, if2, if3
- Elongation factors: ef-Tu, ef-Ts, and G
- Translation is initiated with *fmet* (formylated Met.)

Translace mRNA plastidů (organel) je nejdůležitějším regulovaným parametrem plastidové genové exprese.

A significant regulatory process in plastid gene expression

light-regulated chloroplast protein accumulation increases 50-100 fold w/out changes in mRNA accumulation

5’ UTR is key in regulating translation

about ½ of plastid genes have a “Shine-Delgarno” sequence (GGAG) homologous to small subunit rRNA in this region

nuclear-encoded translation factors bind 5’ untranslated region (UTR) (and in some cases also the 3’ UTR)

Při zelenání plastidů stoupá obsah řady plastidových bílkovin až 100x aniž by se měnila hladina mRNA.

Jak je mRNA "vybrána" k translaci?

- many cp mRNAs contain Shine-Dalgarno region preceding the first codon: base-pairs to the 3'-end of 16S rRNA

```
        S-D            start
5'----GGAGG-------AUG-----3'      mRNA
      I I I  I I
 3'----CCUCC--------5'             16S rRNA
```

Function: helps position mRNA in ribosome.

Plastid mRNA recognition by the **Shine-Dalgarno** sequence in plastid mRNAs

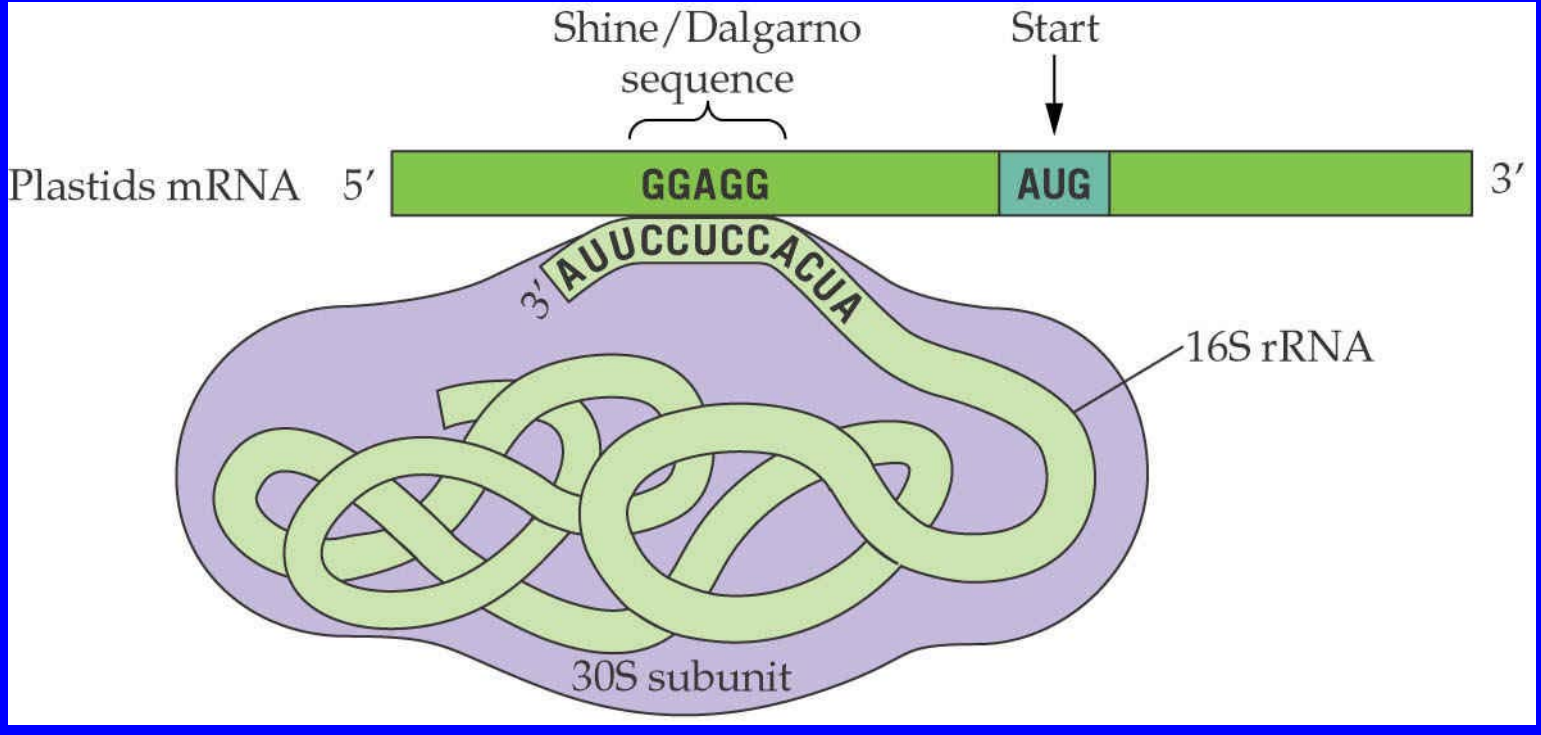

Fig. 9.17

Jádrem kódované bílkoviny kontrolují expresi řady plastidem kódovaných bílkovin na úrovni translace.

REDOXNÍ REGULACE TRANSLACE PLATIDOVÉ GENOVÉ EXPRESE

Translace mRNA organel - př. D1 bílkovina (psbA) PSII

Regulation of plastid gene translation by light
(mediated by ◑pH, ADP, redox signals)

Best-studied example is the translation of PSII D1 (PSBA) protein in **Chlamydomonas**

Accumulation of PSBA increased in light by post-transcriptional regulation (ie no change in steady-state level of mRNA)

Site-directed mutagenesis of *psbA* 5' UTR identified an SD sequence and a stem-loop region as requirements for translation

A set of 4 major 5'UTR binding proteins was identified
Binding increased 10X in the light
Protein reduction by thioredoxin required for binding; binding abolished by oxidation of the binding proteins

(Similar complex seen in Arabidopsis)

Binding to the 5' UTR was decreased following ADP-dependent phosphorylation
ADP accumulates in the dark

U Arabidopsis to funguje podobně

psbA encodes ~32-35 kDa **D1 polypeptide** of PSII

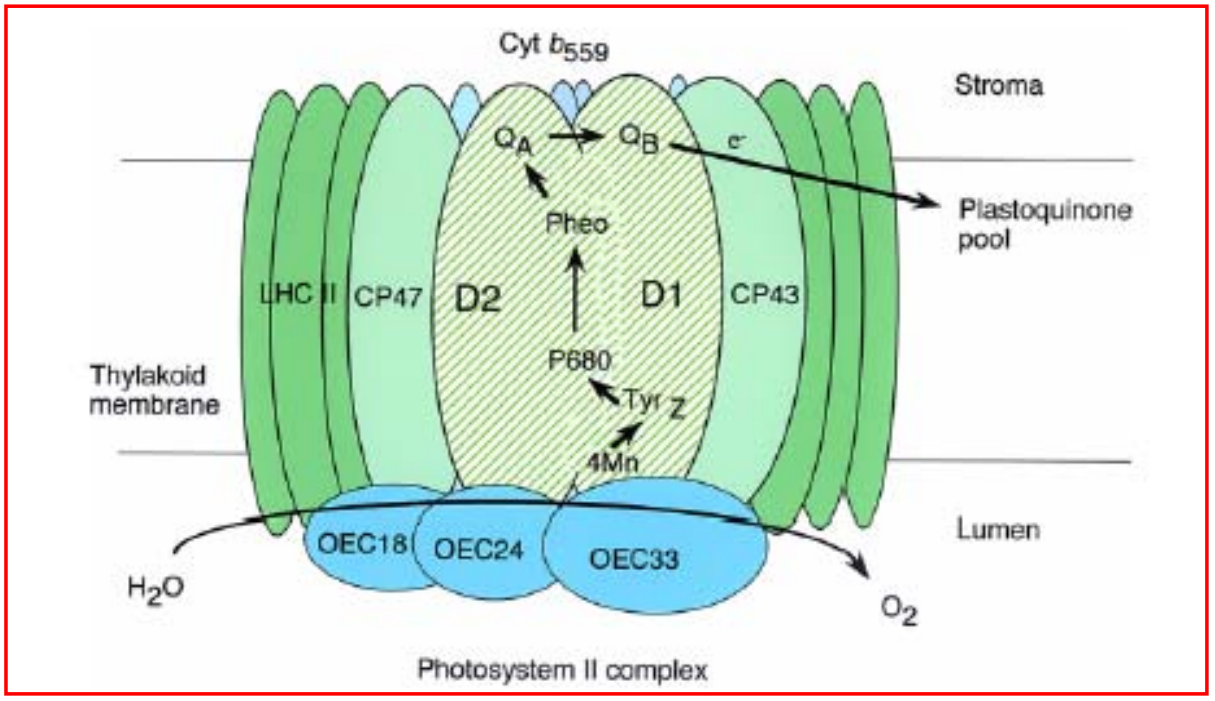

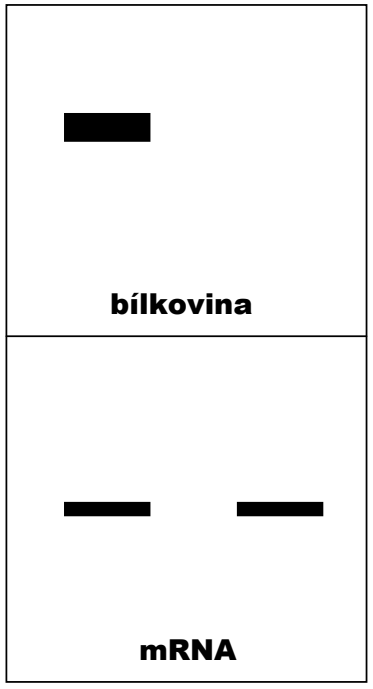

Yamamoto, *Plant Cell Physiol*. 2001

D1 protein turns over rapidly because it becomes damaged in the light.

Světlem aktivovaná translace *psbA* mRNA (koduje D1 bílk. Světlosb. Kompl.)

- Complex of proteins that bind to the 5' UTR of *psbA* mRNA in the light

- D+prot. demonstrate with gel-shift assay.

Interakce mRNA s bílk. kompl. analyzovaná pomocí "gel-shift" assaye.

Lane 1 – control (no protein extract)
Lane 2 - extract from light-grown cells
Lane 3 - extract from dark-grown cells

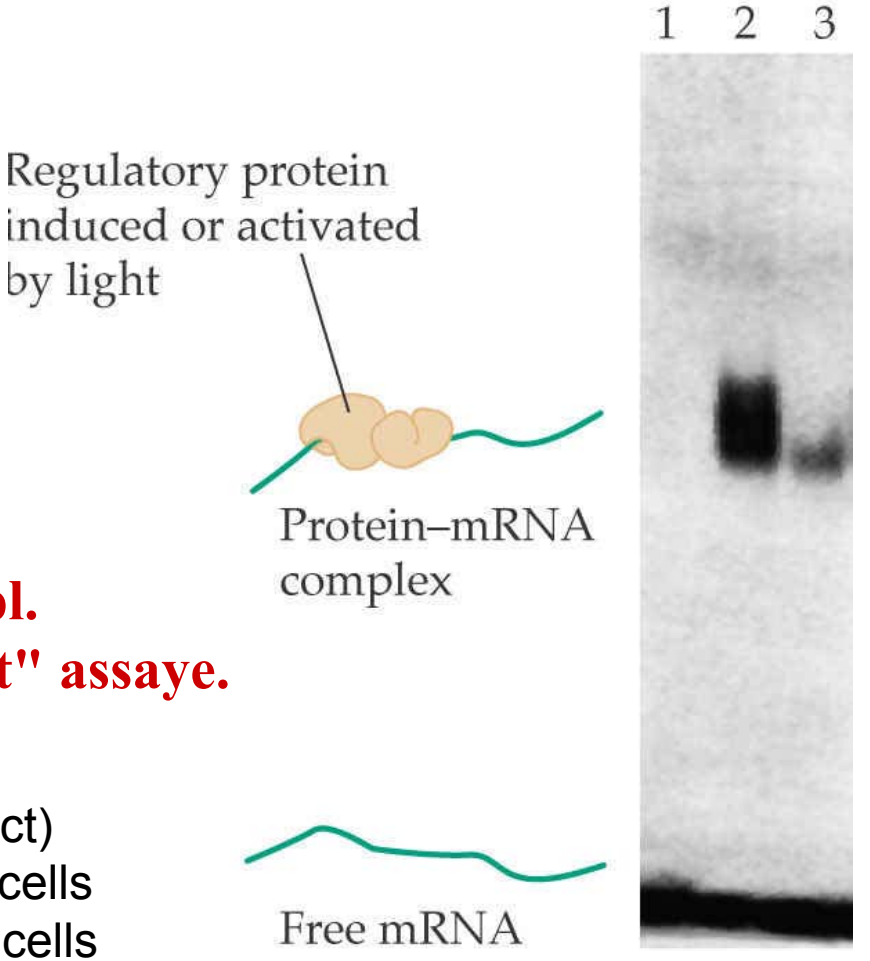

Model for Activation of *psbA* translation by Light via photosynthesis.

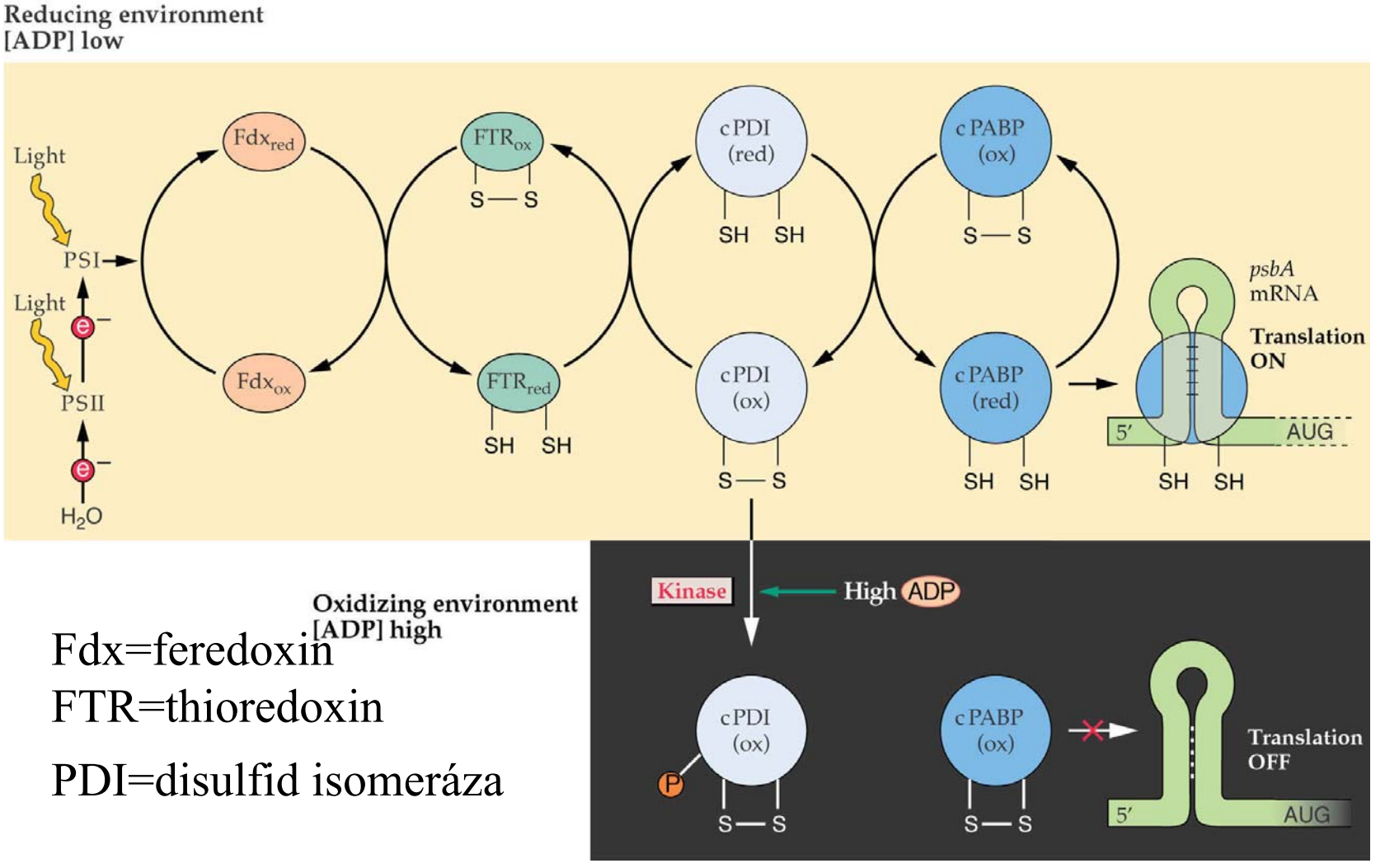

Fdx=feredoxin

FTR=thioredoxin

PDI=disulfid isomeráza

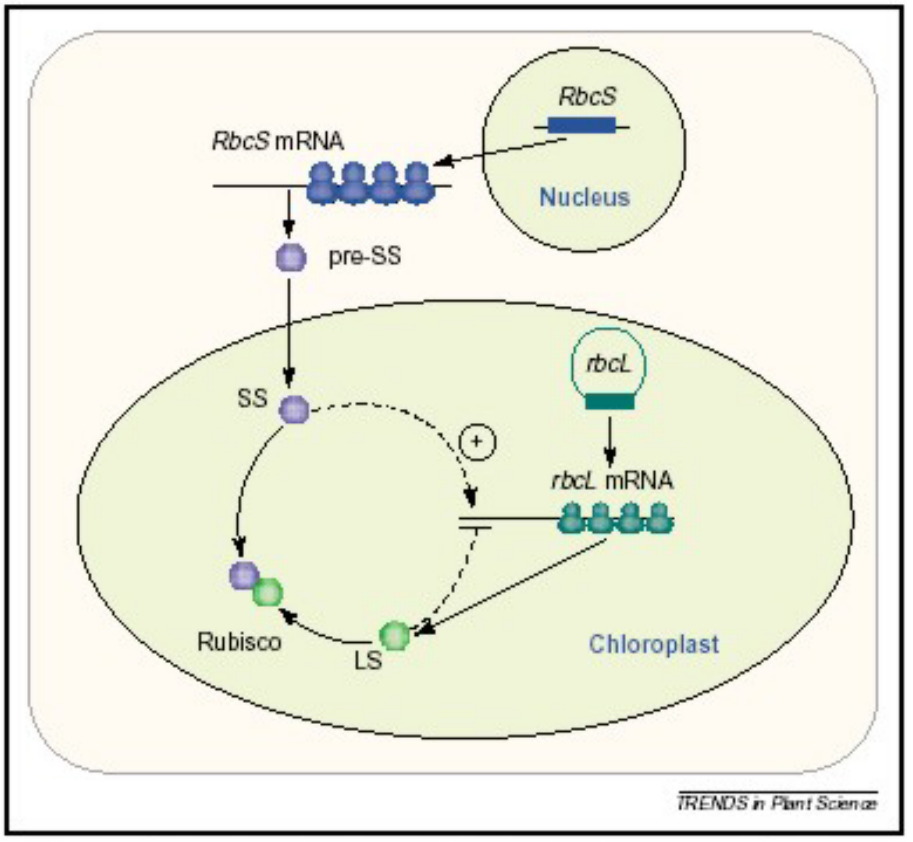

Fig. 1. Control of Rubisco biosynthesis by subunit abundance. Rubisco is composed of eight small subunits (SSs) and eight large subunits (LSs). The SSs are encoded by a small multigene family (*RbcS*) in the nucleus, translated as precursors on 80S ribosomes in the cytosol and imported into the plastid post-translationally. The LSs are encoded by single (*rbcL*) genes on the multicopy chloroplast chromosome and translated on 70S ribosomes. The SSs and LSs assemble in a chaperonin-mediated reaction. Under conditions of SS limitation (such as in *RbcS* antisense DNA mutants), *rbcL* mRNAs accumulate normally, but stoichiometric amounts of the LSs and SSs are produced[6]. LS protein accumulation is reduced in the mutants because of a restriction at the level of *rbcL* mRNA translation initiation. One possibility is that SS protein levels positively influence the recruitment of ribosomes onto *rbcL* mRNAs (positive regulation, broken line). Another possibility is that translation is inhibited by negative feedback in response to unassembled LS (negative regulation, broken line). (Adapted from Ref. 6.)

Importovaná malá podjednotka Rubiska pozitivně působí na translaci velké na ribozom. plastidů.

Metabolický stav plastidů
také
ovšem zpětně reguluje
genovou expresi v jádře.

Regulace jaderné genové exprese plastidem.

Plastidy regulují expresi genů v jádře m.j. **meziprodukty syntézy tetrapyrrolů**.

gun (***genome uncoupled***) genes **SCREEN - METODA**

(lab of Joan Chory)

gun mutant selection:

nuclear ***lhcb*** **promoter down-regulated** when plastid development is disrupted with **norflurazon** - působí fotooxidační poškození chloroplastů inhibicí
syntézy karotenoidů..

To identify mutants in which this plastid-to-nucleus signal was disrupted, Arabidopsis carrying two transgenes was used:

lhcb promoter / gus
lchb promoter / hygromycin resistance

Following mutagenesis, screened for hygromycin resistance and gus expression in the presence of norflurazon

Identified 5 loci, 4 have been cloned and all encode proteins that function in tetrapyrrole metabolism, strongly implicating tetrapyrroles in plastid-to-nucleus signaling

Pathway leads to chlorophyll, heme, and phytochrome chromophore

A

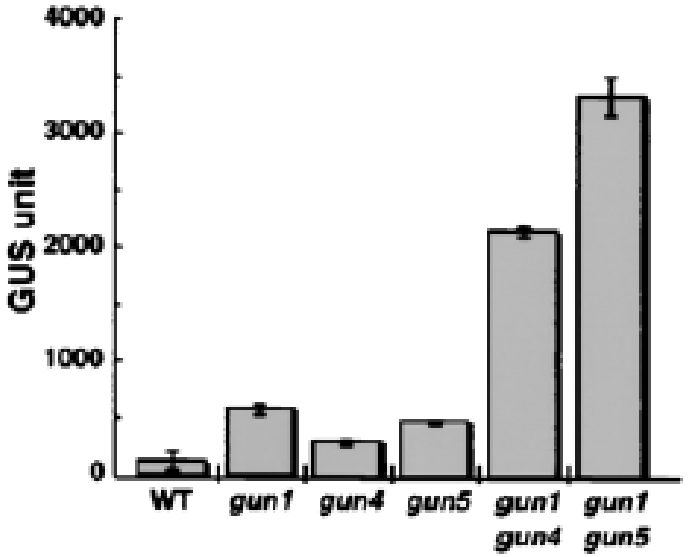

gun mutants show more gus activity;

B

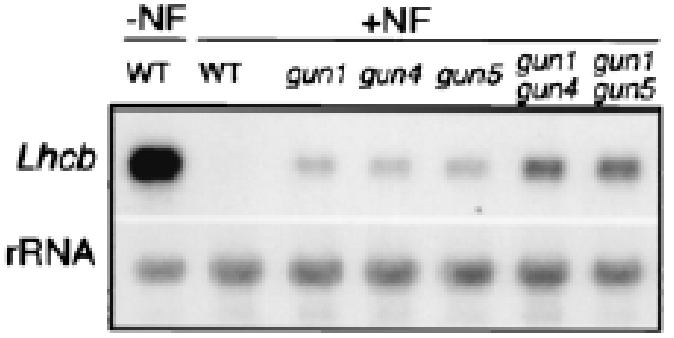

…and accumulate *Lhcb* RNA in the presence of NF

(Mochizuki et al., 2001)

TETRAPYROLOVÁ DRÁHA

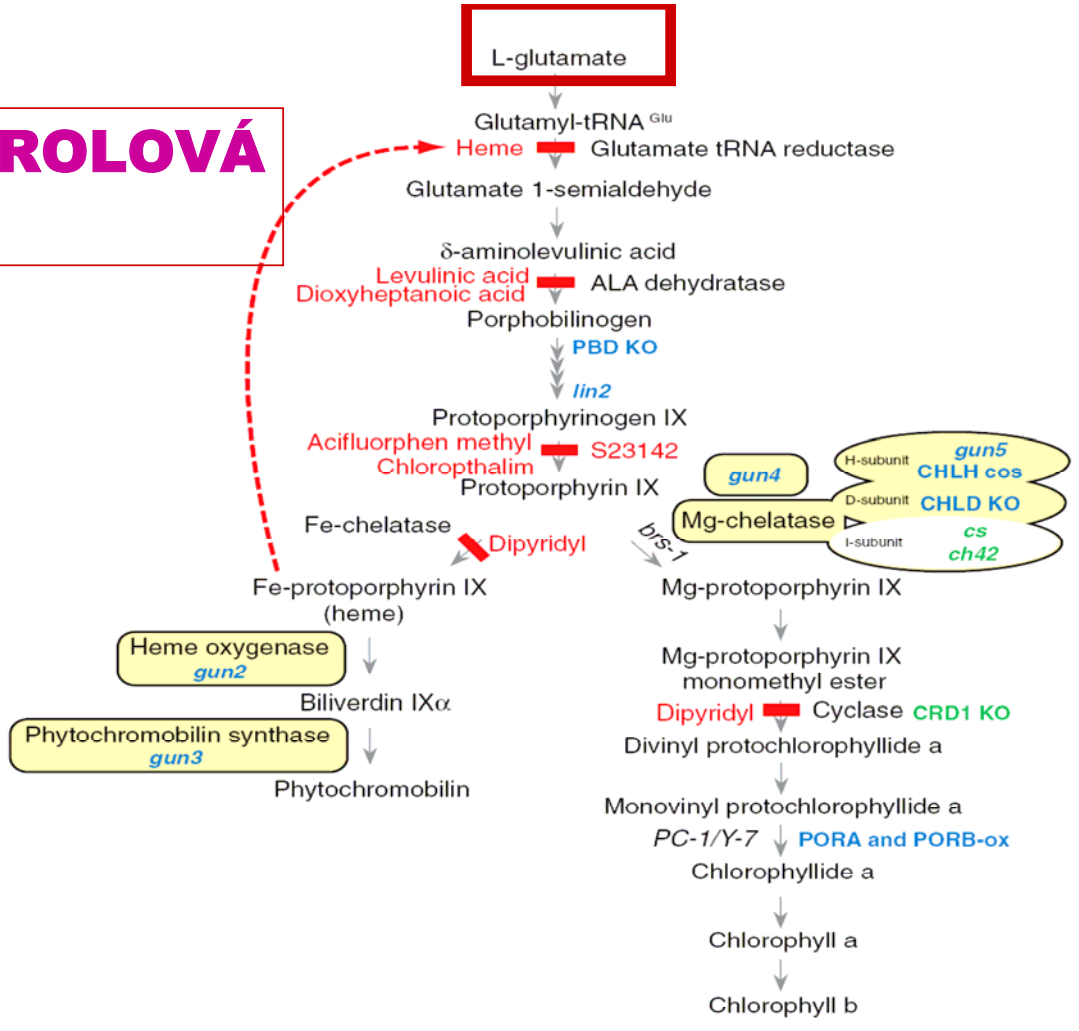

Figure 1

Tetrapyrrole biosynthetic pathway. Steps inhibited by specific inhibitors are indicated in red. Mutants with a *gun* phenotype are shown in blue, and mutants that do not show a *gun* phenotype are indicated in green. *brs-1* and *PC-1/Y-7* are *C. reinhardtii* mutants. PBD KO, T-DNA knockout of porphobilinogen deaminase; *lin2*, lesion in coproporphyrinogen oxidase; CHLD KO, T-DNA knockout of D-subunit of Mg-Chelatase; CHLH cos, cosuppression lines for H-subunit of Mg-Chelatase; CRD KO, T-DNA knockout of one subunit of the cyclase complex. *cs* and *ch42* are alleles of the I-subunit of Mg-Chelatase. PORA-ox and PORB-ox indicate overexpression of Protochlorophyllide oxidoreductase A and B, respectively.

Protoporfyrinogen (Protogen) je částečně exportován do cytoplasmy (mitochondrií) jako prekursor haemu.

(Fytochromobilin je také exportován z plastidů jako prekursor fytochromu)

Na membránách plastidu je Protogen oxidován na protoporfyrin IX (Proto). Odtud je importován ABC transporterem LAF6 (long after far red) do stromatu, kde jeho pool je nutný pro syntézu tetrapyrolů chlorofylu.

Klíčovou signální roli hraje **Mg-protoporfyrin IX (Mg-Proto),** který vzniká působením multiproteinové Mg chelatázy lokalizované do obalových membrán plastidu, kde patrně její podjednotka ChlH (GUN5) působí spolu s GUN4 (aktivátor Mg chelatázy)jako senzor, či regulátor exportu Mg-Proto.

TETRAPYROLOVÁ DRÁHA

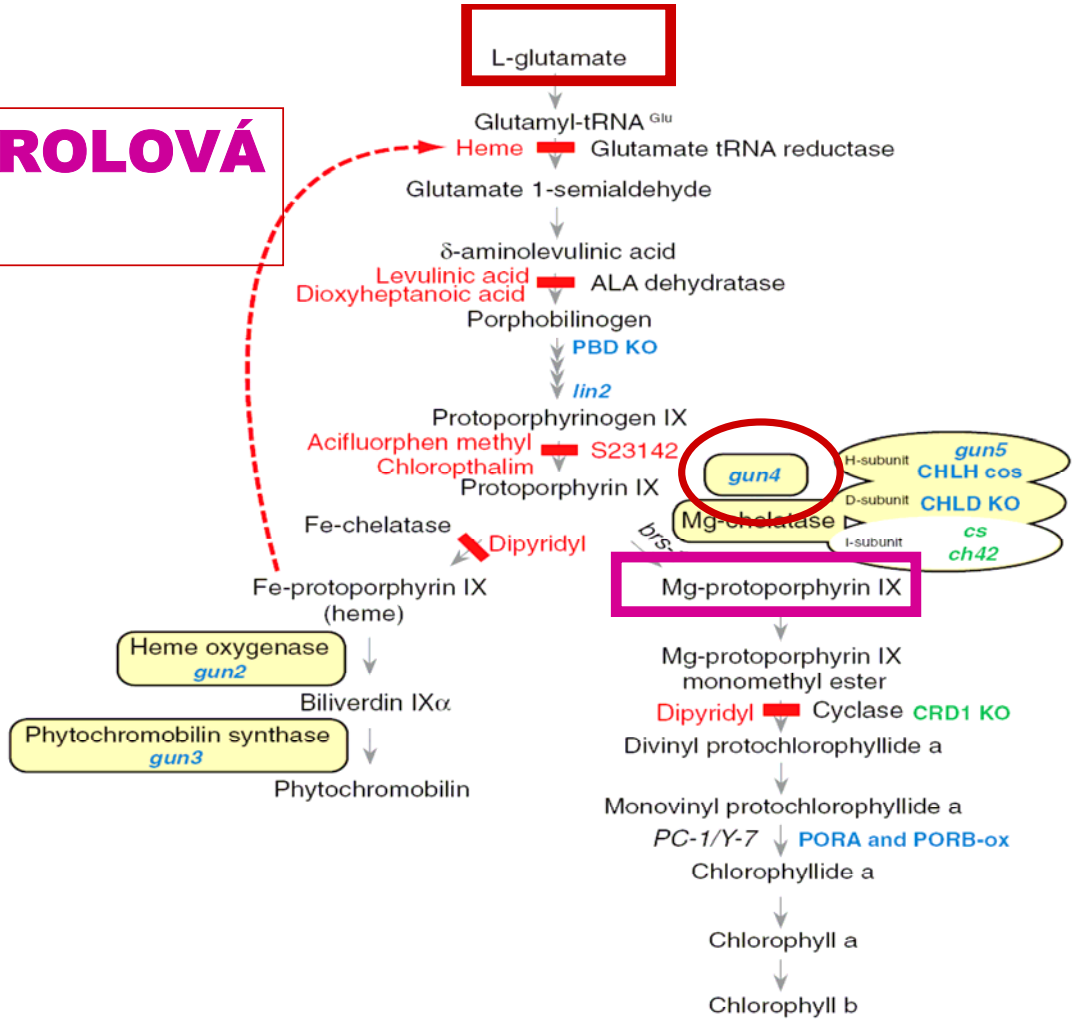

Figure 1

Tetrapyrrole biosynthetic pathway. Steps inhibited by specific inhibitors are indicated in red. Mutants with a *gun* phenotype are shown in blue, and mutants that do not show a *gun* phenotype are indicated in green. *brs-1* and *PC-1/Y-7* are *C. reinhardtii* mutants. PBD KO, T-DNA knockout of porphobilinogen deaminase; *lin2*, lesion in coproporphyrinogen oxidase; CHLD KO, T-DNA knockout of D-subunit of Mg-Chelatase; CHLH cos, cosuppression lines for H-subunit of Mg-Chelatase; CRD KO, T-DNA knockout of one subunit of the cyclase complex. *cs* and *ch42* are alleles of the I-subunit of Mg-Chelatase. PORA-ox and PORB-ox indicate overexpression of Protochlorophyllide oxidoreductase A and B, respectively.

But how is this a signal?

Strand et al. (2003) demonstrate that Mg-proto is both necessary and sufficient to drive the expression of photosynthesis-related nuclear genes.

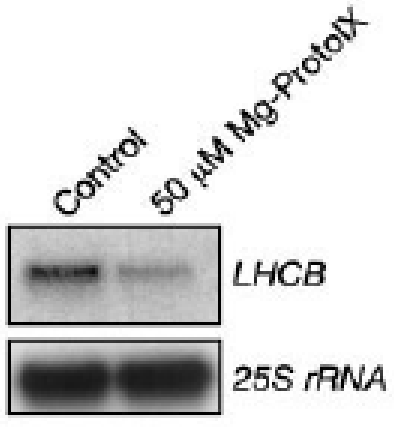

Treatment with Mg-Proto can repress *Lhcb* transcript accumulation **v protoplastech.**

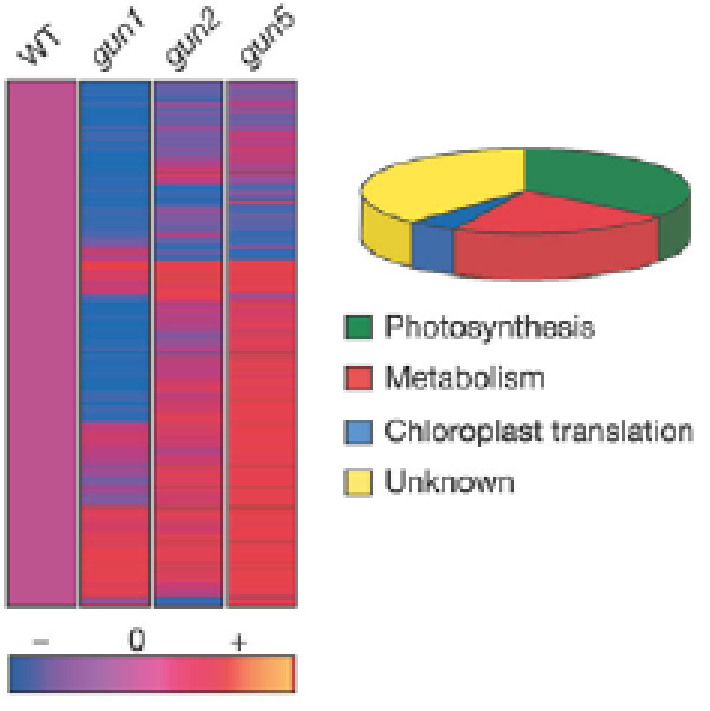

Norflurazon treatment similarly causes large-scale changes in transcript accumulation.

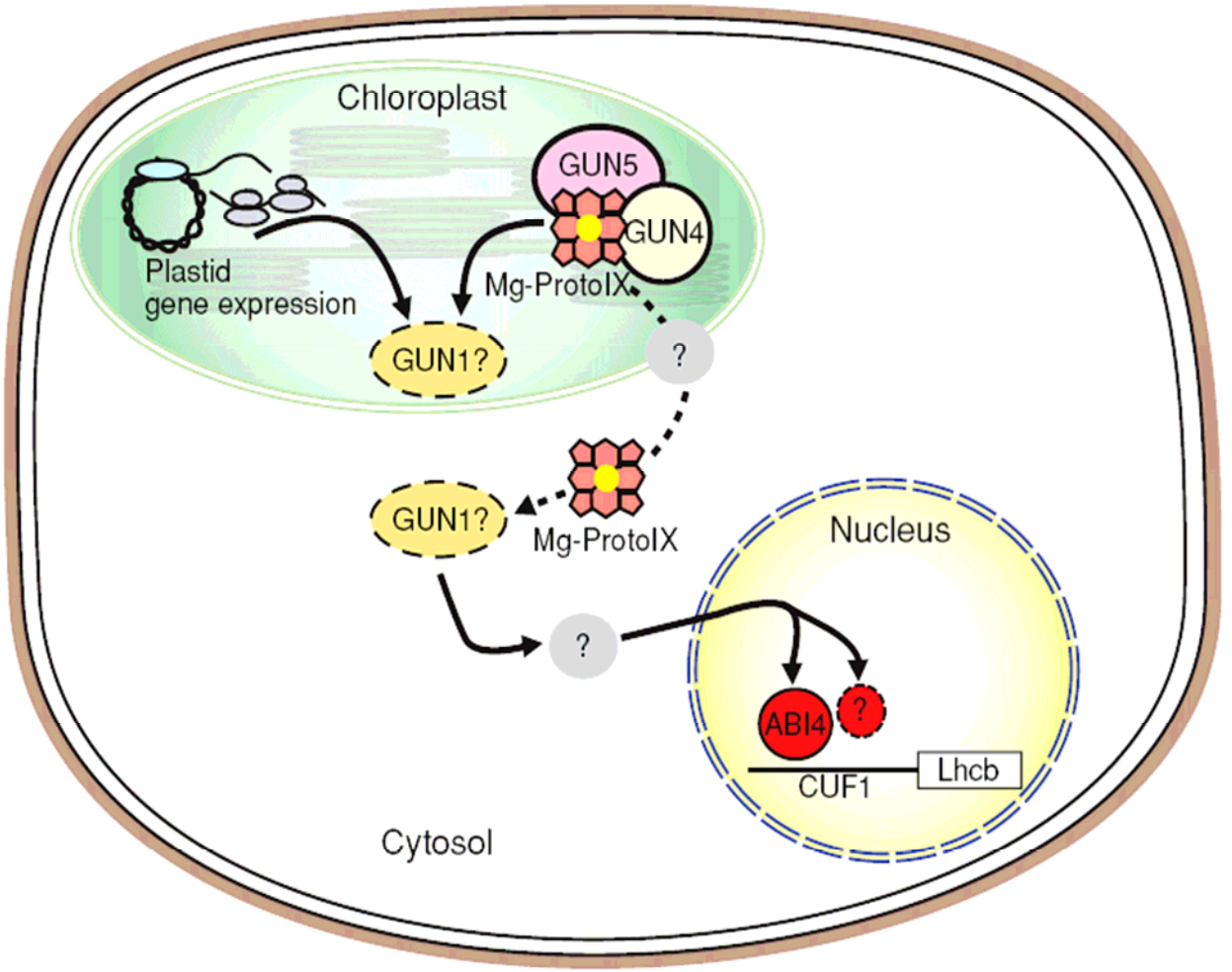

Figure 2

gun mutants in retrograde signaling. Because the identity of GUN1 is not yet known, its localization is depicted to be either in the plastid or the cytosol. GUN4 is found in stroma, thylakoid, and envelope fractions of chloroplasts. Other unidentified cytosolic components may also be involved in the signaling pathway.

Redoxní regulace jaderné genové exprese chloroplasty.

Box 1. Redox potential of photosynthetic components and 'dangerous' byproducts of photosynthesis redox chemistry

The redox potential E of an electron- or hydrogen-transferring component is described in general by the Nernst equation (Fig. Ia) and depends on the component-specific mid-point potential (E_m), the number of transferred electrons (n) and the concentration ratio of oxidized [ox] to reduced [red] forms of the component. Environmental factors that influence or participate in the electrochemistry of the component will result in a change of its respective redox potential. Because most redox-active components exhibit proper function only in a relatively small range of its redox potential, organisms have several mechanisms to keep the redox potential stable. However, reactive oxygen species are unavoidable side products of oxygenic photosynthesis [a].

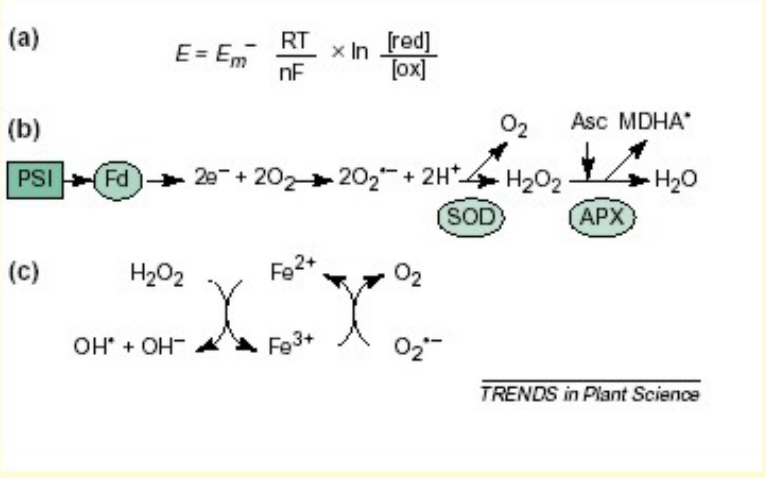

Fig. I.

In the Mehler reaction (Fig. Ib), superoxide is mainly formed at photosystem I (PSI), either directly or via ferredoxin, and is rapidly detoxified by superoxide dismutases (SODs), which produce hydrogen peroxide. Ascorbate peroxidases (APXs) then reduce hydrogen peroxide to water via the oxidation of ascorbate (Asc) to monodehydroascorbate radicals (MDHA$^\bullet$), which are reduced back to ascorbate via glutathione.

Under various stress conditions, the cellular concentration of ROS increases and can overcome the antioxidant-defence mechanisms. In the Fenton reaction (Fig. Ic), hydrogen peroxide can then be transformed into highly reactive hydroxyl radicals using divalent iron ions as catalysts. These radicals cause oxidative damage by oxidizing fatty acids or amino acids, which can impair membrane structure or proper protein function.

Reference

a Baier, M. and Dietz, K.J. (1999) The costs and benefits of oxygen for photosynthesizing plant cells. *Prog. Bot.* 60, 282–314

STROMA

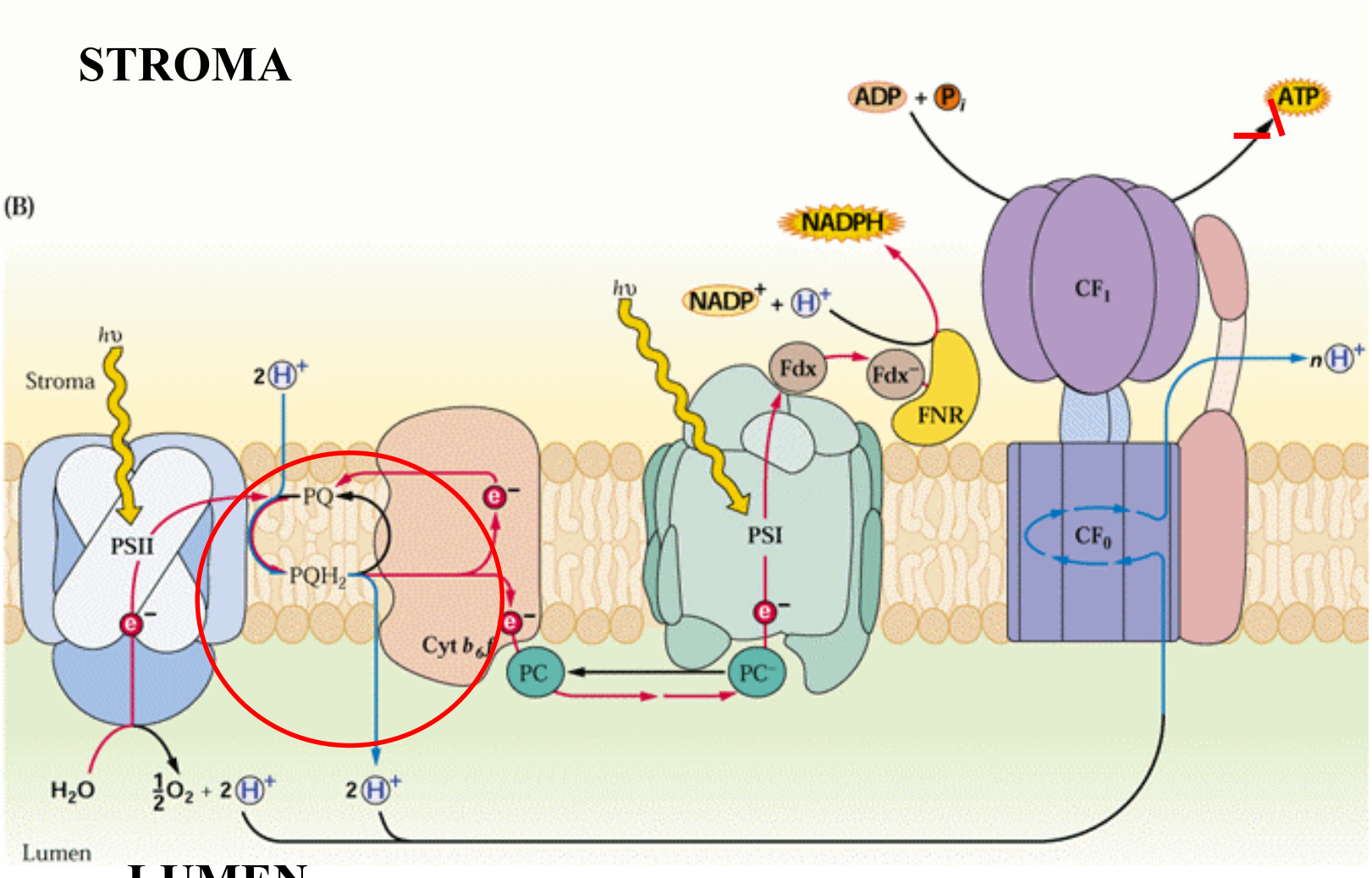

LUMEN

PQ vs. PQH2 je dominantní zdroj regulačních redoxních signálů.

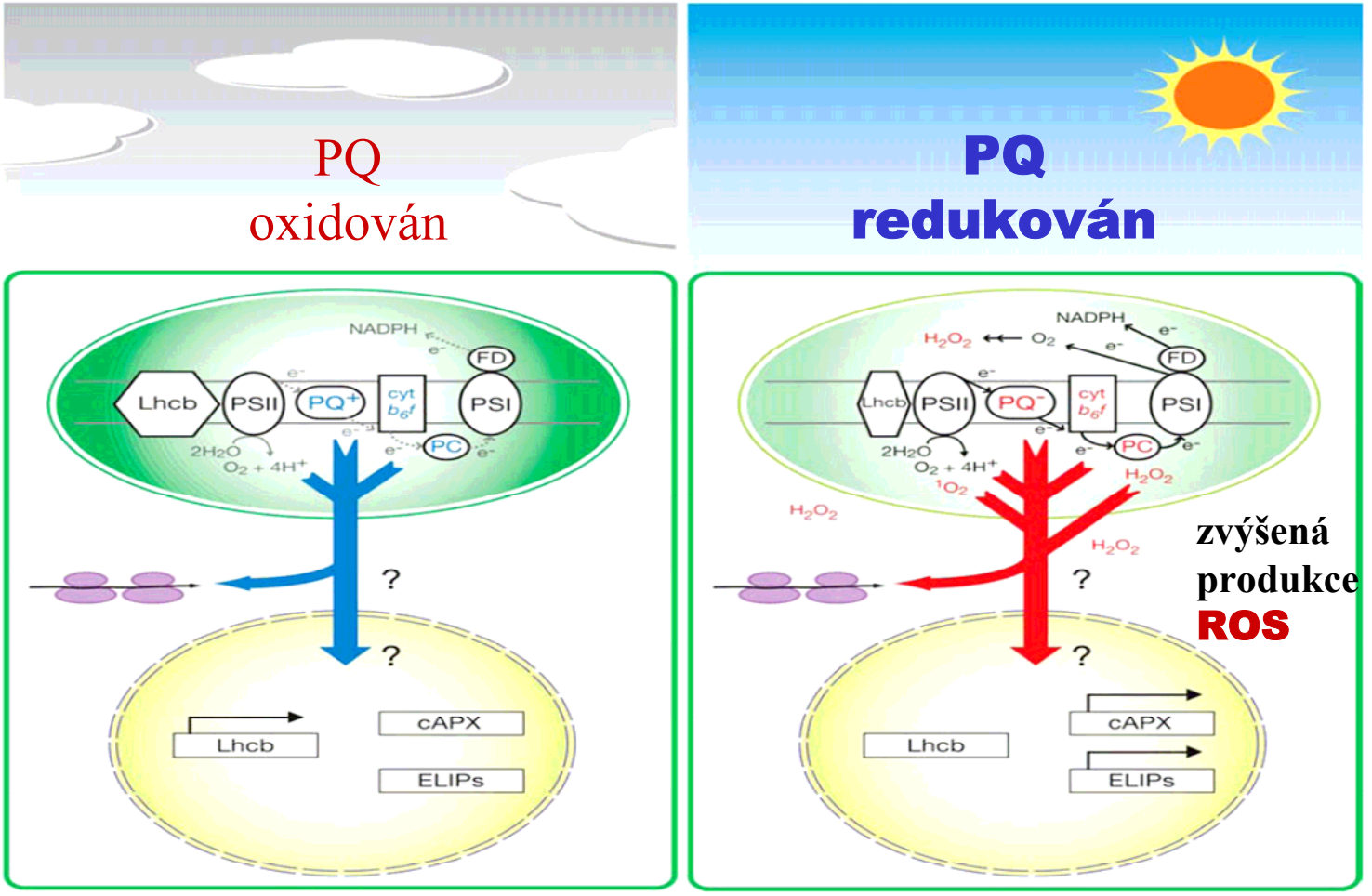

Figure 3

Under low light (*lefthand figure*), the rate of photosynthetic electron transport (PET) is low and most PET components are in oxidized states, e.g., the plastoquinone (PQ) pool is in an oxidized state (PQ^+). In contrast, in high-light conditions (*righthand figure*), due to higher excitation pressure, PET components are generally in reduced states, e.g., the PQ pool is in a reduced state (PQ^-). In addition to PET components, changes in cellular redox states are caused by different levels of reactive oxygen species (ROS) such as $O_2^{\bullet -}$ and H_2O_2 (34). Under low light (*lefthand figure*), ROS are seldom generated and, even if they are generated, most of them are detoxified by antioxidant systems (6). Under high light, however, much more ROS are generated than the antioxidant systems can deal with. These redox states may report the functional states of chloroplasts to the nucleus.

A regulatory network of nuclear and chloroplast gene expression.

zjednodušený sumář

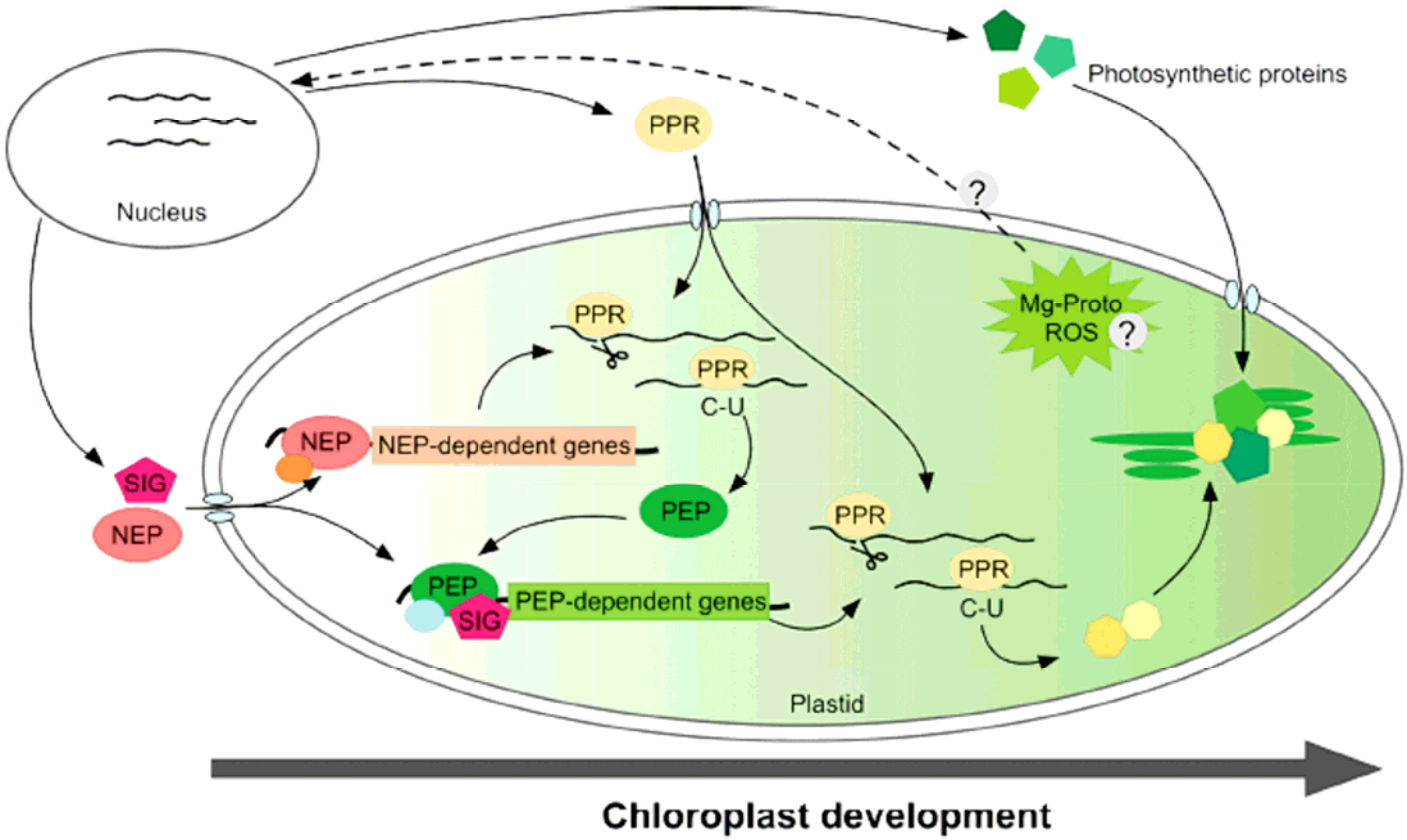

Dělení plastidů

U řady chlorofyt včetně suchozemských rostlin je **"odpojeno"** od buněčného dělení.

Dělení etioplastu zaškrcením

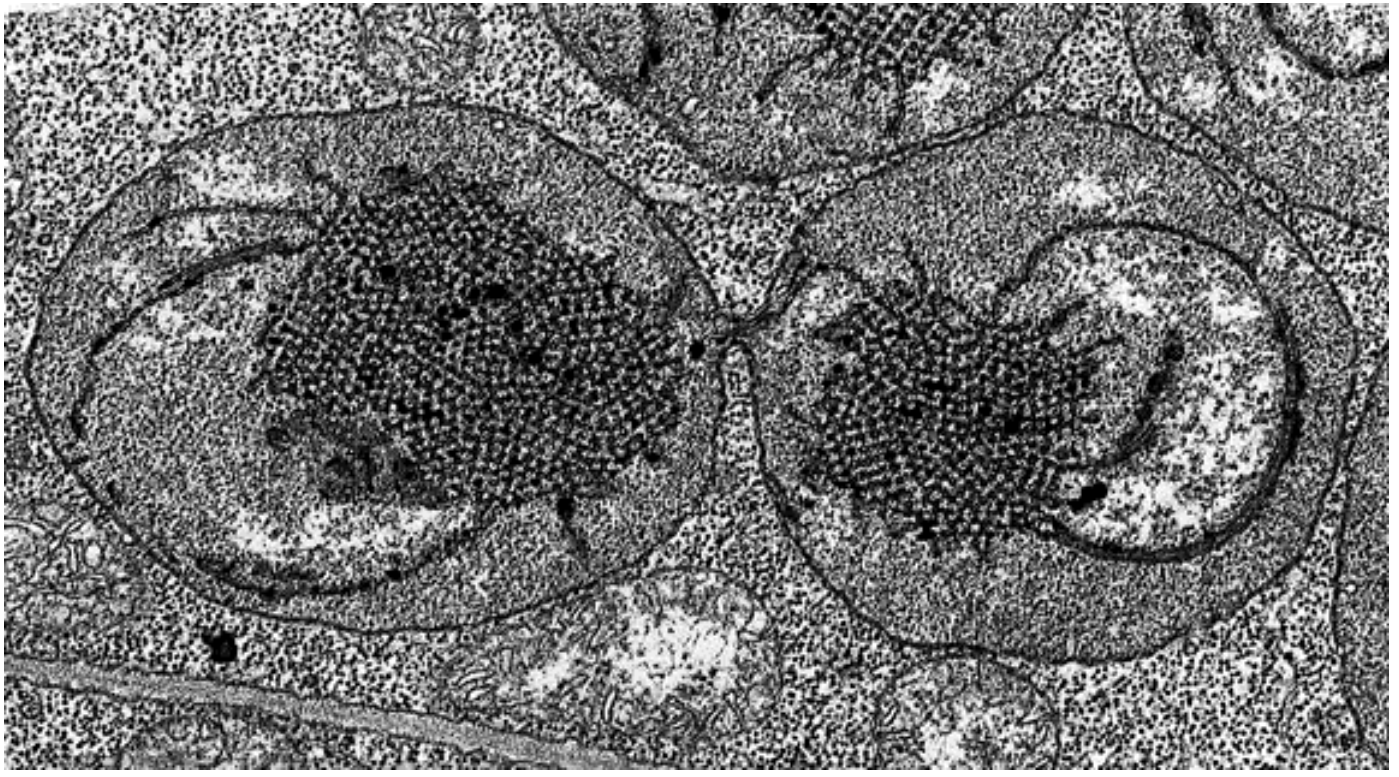

Vnitřní prstýnek - FtsZ1 a 2 (vzdál. příb. tubulinu GTPdep. polymerace) a spol. **Vnější prstýnek** - dynamin (ARC5).

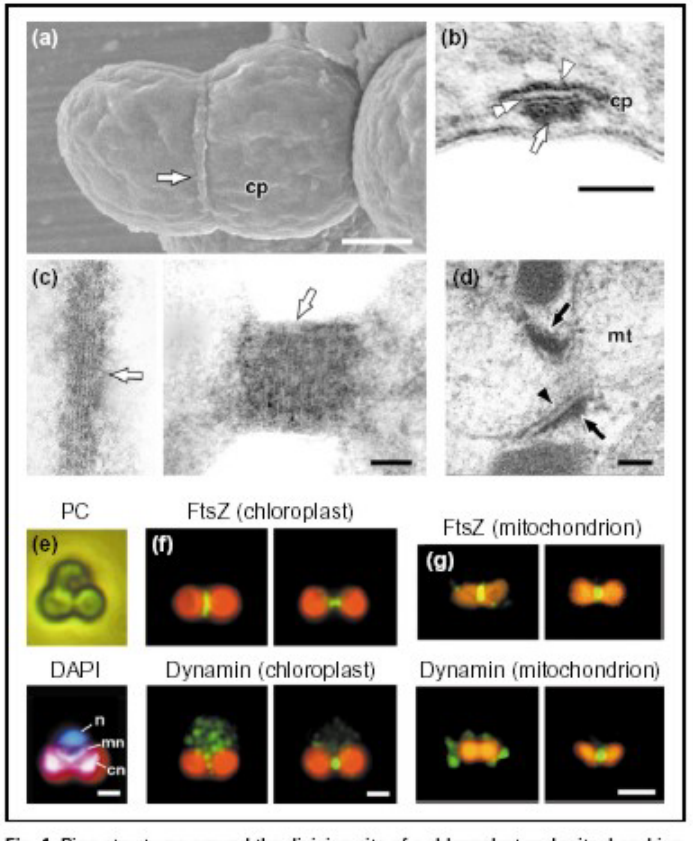

Fig. 1. Ring structures around the division site of a chloroplast and mitochondrion in the red alga *Cyanidioschyzon*. (a) A scanning electron micrograph of an isolated dividing chloroplast. (b) Magnified cross-section of the plastid-dividing (PD) ring obtained by transmission electron microscopy. The PD ring is composed of an outer ring (on the cytosolic side of the outer envelope), a middle ring (in the intermembrane space), and an inner ring (on the stromal side of the inner envelope) [24,25]. (c) Electron micrographs of the outer PD ring obtained by treating isolated

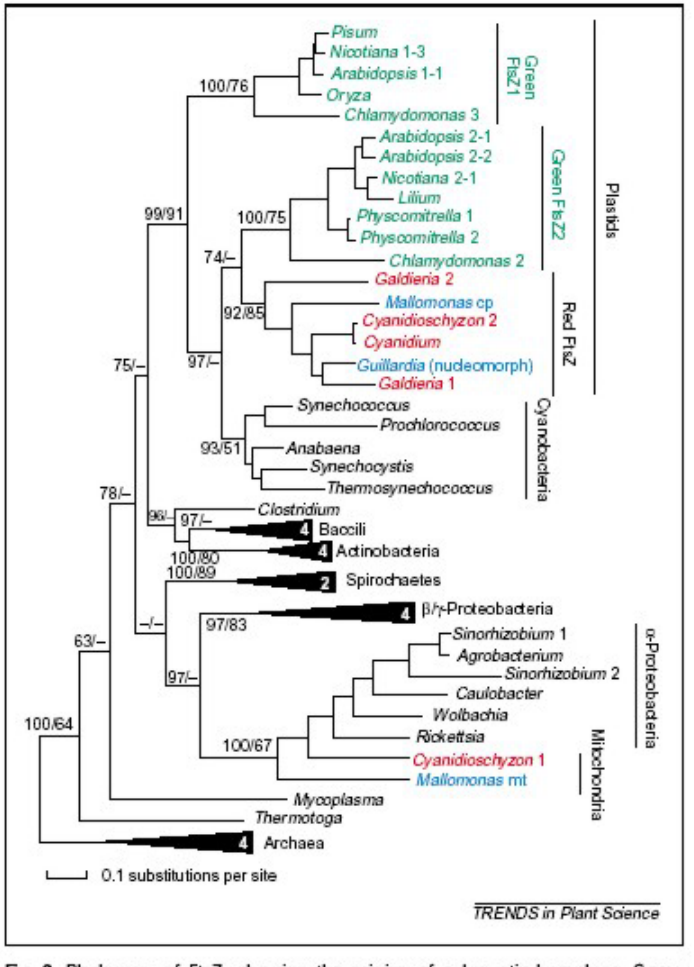

Fig. 2. Phylogeny of FtsZ, showing the origins of eukaryotic homologs. Some

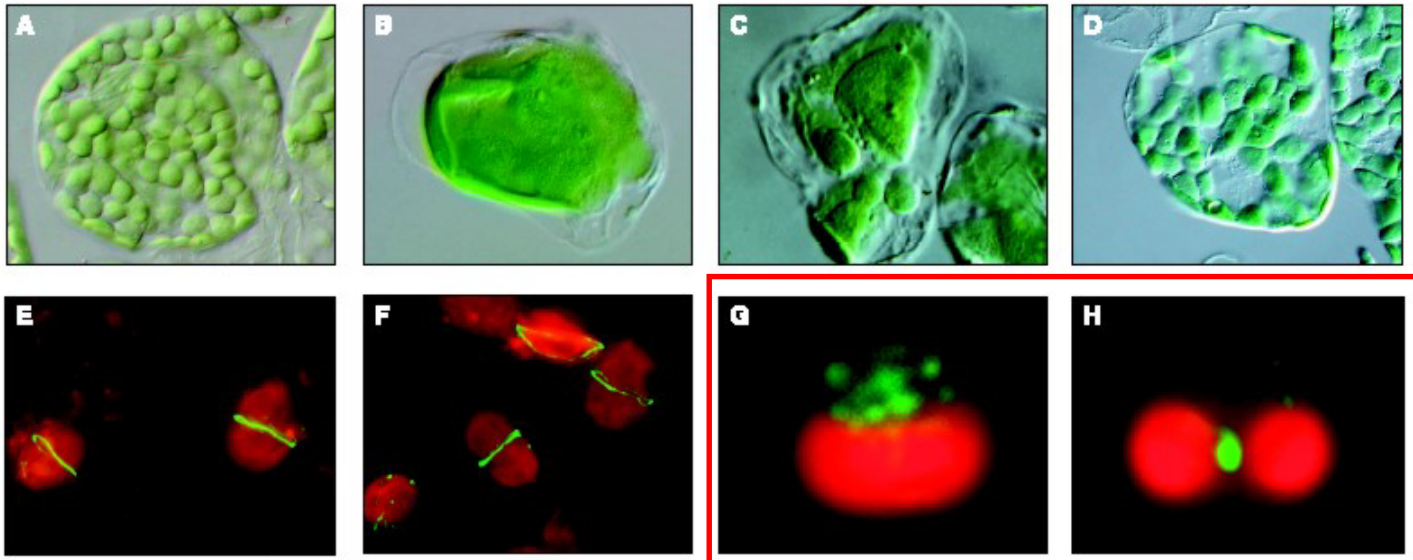

Fig. 2. Chloroplast morphology and division component organization and dynamics. (**A** to **D**) Chloroplasts in *A. thaliana* leaf cells from wild-type plants (A) and plants expressing antisense transgenes for FtsZ2 (B), MinD (C), or the DRP ARC5 (D). The chloroplasts in FtsZ1 antisense and ARC6 mutant plants look similar to those in FtsZ2 antisense plants. Magnifications, ×350 to ×370. (**E** to **H**) Visualization of chloroplast division components. (E and F) Immunofluorescence detection of FtsZ1 (E) and FtsZ2 (F) rings in *A. thaliana*. Images were processed as described (*53*). ARC6-GFP and ARC5-GFP (GFP, green fluorescent protein) are also detected at the division site. (G and H) Immunofluorescence detection of the DRP CmDnm2 in the unicellular red alga *C. merolae* (*36*). CmDnm2 localizes to cytosolic patches after constriction of the single *C. merolae* chloroplast commences (G). Subsequently, it is recruited to the division site (H). In all panels, red chlorophyll autofluorescence reveals the shape of the chloroplast. Magnifications, ×1000 to ×7000.

G a H *Cyanidioschyzon merolae* - "primitivní" ruducha - dynamin je napřed shluknut na jednom konci plastidu, teprve po začátku tvoření konstrikce je "rekrutován" do tohoto místa. Podobně je tomu i u krytosemenných r.

Při analýze dělícího aparátu plastidu Arabidopsis významě pomohla analýza ***arc*** mutantů Arabidopsis.

Accumulation and replicationof chloroplasts

arc11 mutant Arabidopsis

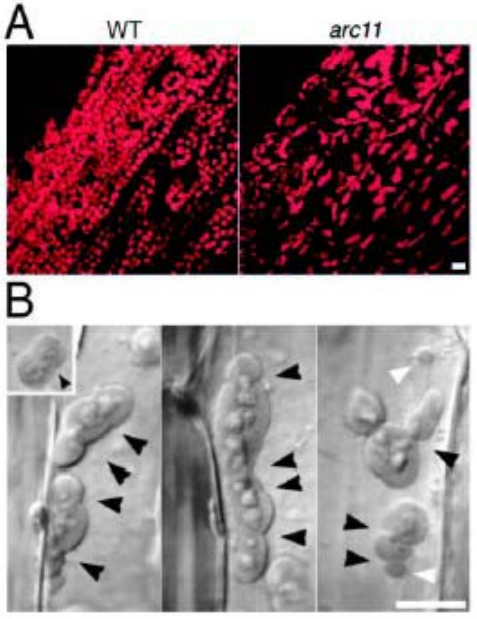

Fig. 1. The elongated and multiple-arrayed dividing chloroplasts in developing seedlings of *Arabidopsis arc11*. Chloroplasts in primary leaf petioles of 7-day light-grown wild-type (WT, L*er*) and *arc11* seedlings were observed by CLSM. (A) Imaging of chlorophyll autofluorescence of WT and the *arc11*. (B) Differential interference contrast (DIC)-single optical sections of dividing chloroplasts in WT (inset) and *arc11*. Membrane constriction sites of dividing chloroplasts are indicated by black arrowheads. Mini-chloroplasts (~2 μm in diameter) in a population of expanding and dividing chloroplasts in *arc11* are indicated by white arrowheads. Bars, 10 μm.

Accumulation and replicationof chloroplasts

ARC11 lokus kóduje AtMinD1

stromatální ATPázu, která spolu s MinE určuje polohu dělení

Komplementace expresí WT AtMinD1

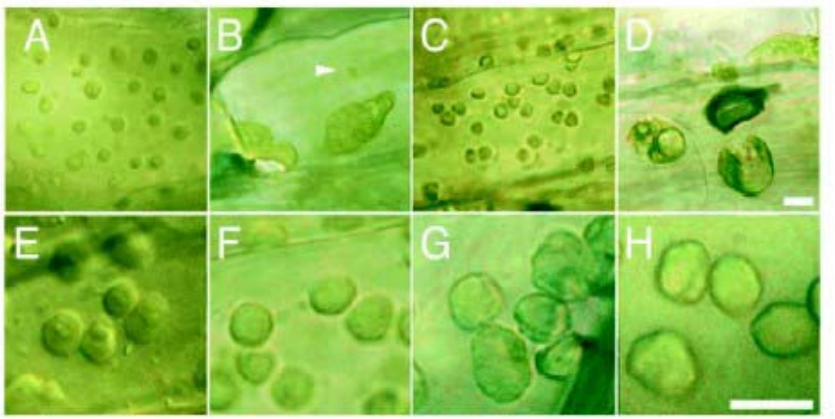

Fig. 4. Complementation of the *arc11* mutant with appropriate expression of wild-type *AtMinD1-dHA*. Chloroplasts in leaf petioles of 15-day seedlings were microscopically observed. (A) WT. (B) *arc11* mutant. A mini-chloroplast is indicated by an arrowhead. (C) Complemented *arc11* transgenic plant (11HA38, T_4 generation, see Fig. 3). (D) Division-inhibited *arc11* transgenic plant (11HA2, T_4 generation, see Fig. 3). (E-H) Partially complemented transgenic *arc11* plants containing slightly expanded and surface-rugged chloroplasts compared to WT and complemented plants. (E) WT. (F) Complemented plant (11HA38, identical to (C)). (G) A segregated plant of 11HA38 in the T_2 generation showing a partially complemented phenotype. (H) Partially complemented plant (11HA44, T_4 generation, see Fig. 3). Bars, 10 µm.

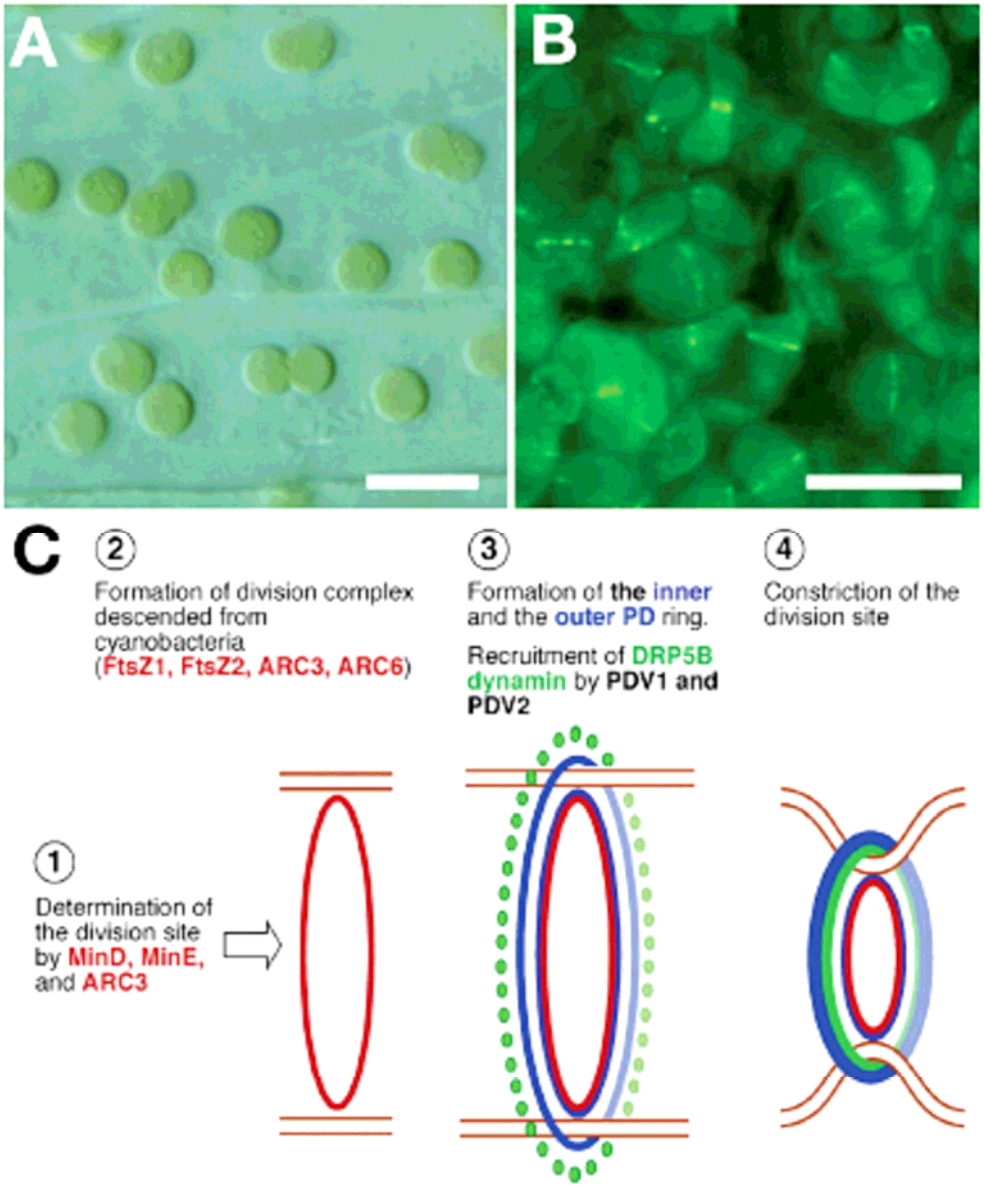

(A) Chloroplasts dividing in Arabidopsis hypocotyl cells.
(B) Localization of GFP-tagged DRP5B dynamin protein at the cytosolic side of the division site in Arabidopsis mesophyll cell chloroplasts.
(C) Schematic representation of the plastid division machinery. A 'bacterial' division complex based on FtsZ forms first at the division site. This is then followed by the formation of the inner and outer PD rings, and finally the recruitment of DRP5B dynamin. Constriction at the vision site then initiates. Scale bars in (A) and (B), 10 μm.

„Ko-Evoluční“ přenos genů z organel do jádra.

Non-functional and also functional transfer

- Large segments of DNA
  - e.g. A complete copy of the arabidopsis mitochondrial genome on chromosome 2

Functional gene transfer

- Gene by gene
- Likely occurs via RNA intermediates
- Requires acquisition of a nuclear promoter and (often) a mitochondrial targeting pre-sequence
- Evidence for frequent and recent transfers in plant lineage
- Results in coding content differences among plant organelle genomes

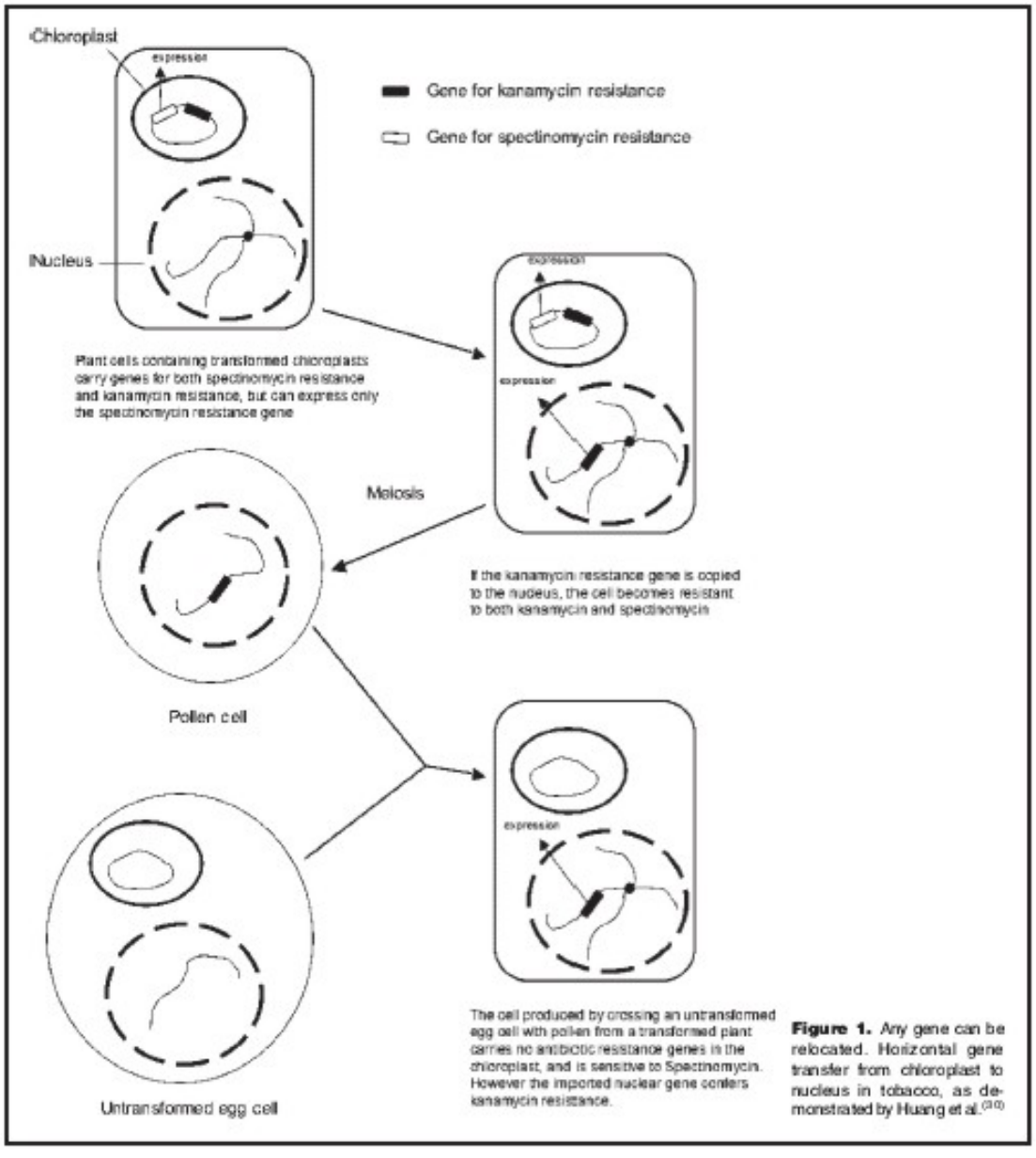

Figure 1. Any gene can be relocated. Horizontal gene transfer from chloroplast to nucleus in tobacco, as demonstrated by Huang et al.[310]

9710–9715 | PNAS | June 29, 2004 | vol. 101 | no. 26

Simple and complex nuclear loci created by newly transferred chloroplast DNA in tobacco

Chun Y. Huang*†, Michael A. Ayliffe‡, and Jeremy N. Timmis*§

*School of Molecular and Biomedical Science, University of Adelaide, Adelaide SA 5005, Australia; and ‡CSIRO Plant Industry, G.P.O. Box 1600, Canberra ACT 2601, Australia

Edited by W. Ford Doolittle, Dalhousie University, Halifax, Canada, and approved May 21, 2004 (received for review February 6, 2004)

Transfer of organelle DNA into the nuclear genome has been significant in eukaryotic evolution, because it appears to be the origin of many nuclear genes. Most studies on organelle DNA transfer have been restricted to evolutionary events but experimental systems recently became available to monitor the process in real time. We designed an experimental screen to detect plastid DNA (ptDNA) transfers to the nucleus in whole plants grown under natural conditions. The resultant genotypes facilitated investigation of the evolutionary mechanisms underlying ptDNA transfer and nuclear integration. Here we report the characterization of nuclear loci formed by integration of newly transferred ptDNA. Large, often multiple, fragments of ptDNA between 6.0 and 22.3 kb in size are incorporated into chromosomes at single Mendelian loci. The lack of chloroplast transcripts of comparable size to the ptDNA integrants suggests that DNA molecules are directly involved in the transfer process. Microhomology (2–5 bp) and rearrangements of ptDNA and nuclear DNA were frequently found near integration sites, suggesting that nonhomologous recombination plays a major role in integration. The mechanisms of ptDNA integration appear similar to those of biolistic transformation of plant cells, but no sequence preference was identified near junctions. This article provides substantial molecular analysis of real-time ptDNA transfer and integration that has resulted from natural processes with no involvement of cell injury, infection, and tissue culture. We highlight the impact of cytoplasmic organellar genome mobility on nuclear genome evolution.

terium transformation (16–18). The involvement of this mechanism also has been inferred in the nuclear integration of organelle DNA sequences (14), although the interpretation of such analyses is complicated by the presence of many preexisting organelle sequences in the nucleus and potential postintegrative rearrangement and sequence decay. With the advent of experimental systems to detect *de novo* plastid DNA (ptDNA) transfer (19, 20), direct studies of the nuclear integration mechanisms are possible for the first time.

We investigated plastid-to-nucleus DNA transfer in the progeny of a higher plant, by inserting into the tobacco plastome two marker genes: aminoglycoside 3′-adenyltransferase (*aad*A) and a neomycin phosphotransferase gene containing a nuclear intron from the potato *STLS* gene (*neoSTLS2*). Seventeen independent kanamycin-resistant (kr) plants were obtained, and each of these plants possessed the native tobacco plastome and *de novo* nupt(s) (19). Here we report the characterization of some of the *de novo* nupts, providing insight into mechanisms that promote ptDNA integration into nuclear DNA.

Materials and Methods

Plant Material. Two transplastomic lines, tp7 and tp17, and 17 kr lines containing *de novo* nupts (19) were used.

Nucleic Acid Hybridization. DNA and RNA blot analyses were performed as described in refs. 12 and 21.

Další pokusy ovšem ukazují, že se přenášejí přímo velké kusy – až 23kb - DNA, které se integrují procesem nehomologní rekombinace.

Plastidy u krytosemenných rostlin
se dědí maternálně!!
ale s nízkou frekvencí úniky i
přes pyl.

U jehličnanů jsou plastidy děděny paternálně!

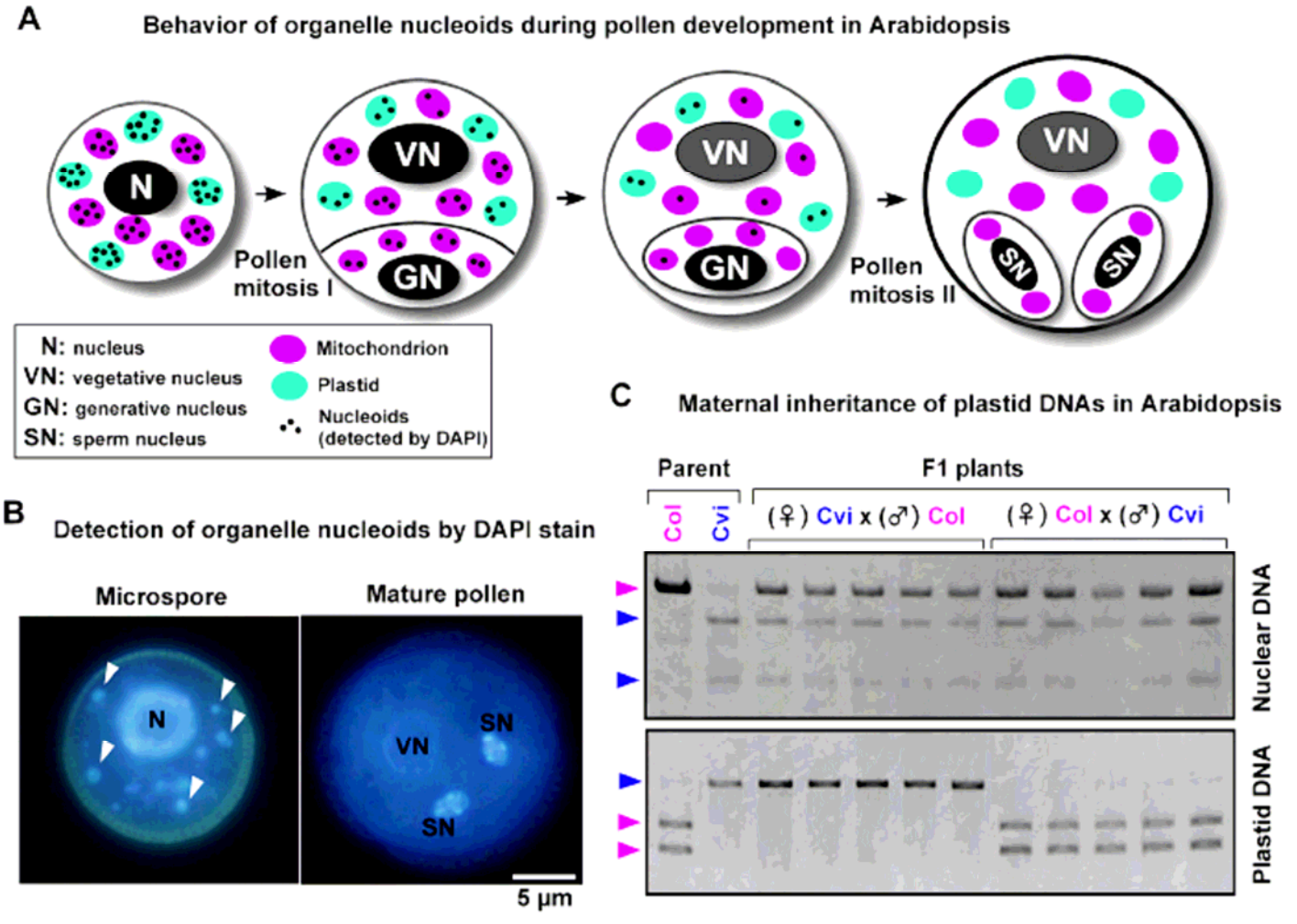
A
Behavior of organelle nucleoids during pollen development in Arabidopsis
N
VN
GN
SN
Pollen mitosis I
Pollen mitosis II
N: nucleus
VN: vegetative nucleus
GN: generative nucleus
SN: sperm nucleus
Mitochondrion
Plastid
Nucleoids (detected by DAPI)
B
Detection of organelle nucleoids by DAPI stain
Microspore
Mature pollen
5 μm
C
Maternal inheritance of plastid DNAs in Arabidopsis
Parent
F1 plants
Col
Cvi
(♀) Cvi x (♂) Col
(♀) Col x (♂) Cvi
Nuclear DNA
Plastid DNA